Cheiron school 2015 , 12th Sep. 2015, SPring-8
Hard X-ray beamline Optics

Hard X-ray Beamline Optics

～*Engineering of x-ray beamline* ～

Haruhiko Ohashi
JASRI / SPring-8

Where is "beamline" ?

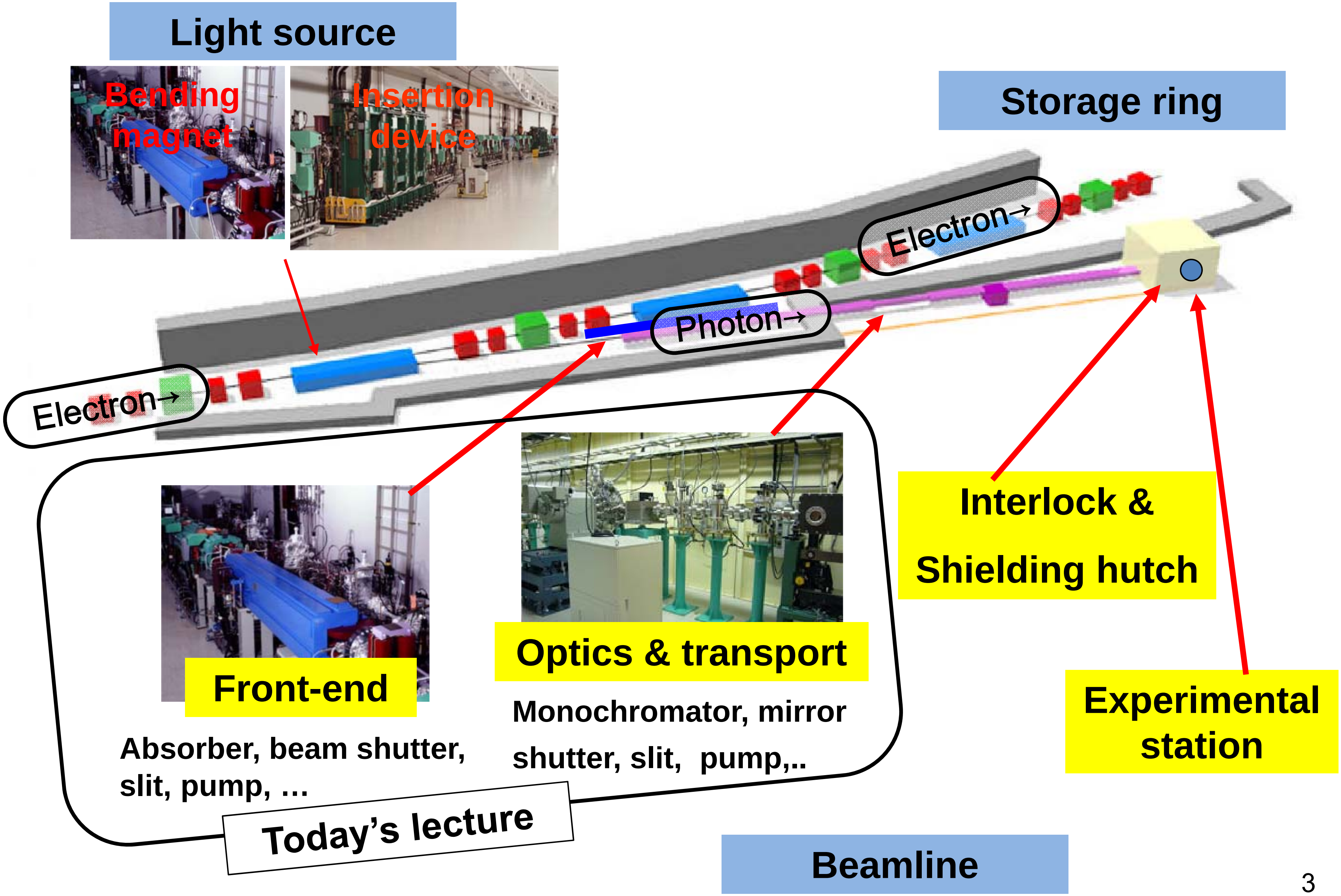

Light source

Storage ring

Front-end

Absorber, beam shutter, slit, pump, …

Optics & transport

Monochromator, mirror shutter, slit, pump,..

Interlock & Shielding hutch

Experimental station

Today's lecture

Beamline

Introduction

“X-ray beamline looks complicated?”

Storage ring

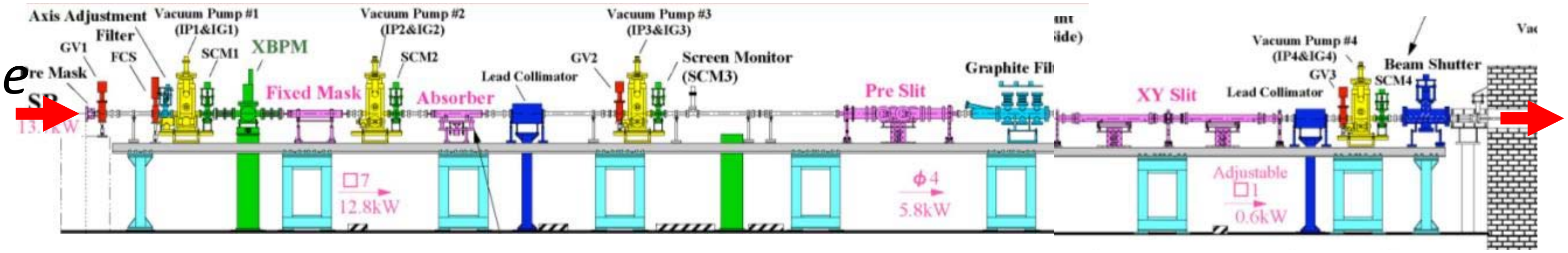

Inside shielding tunnel (front end)

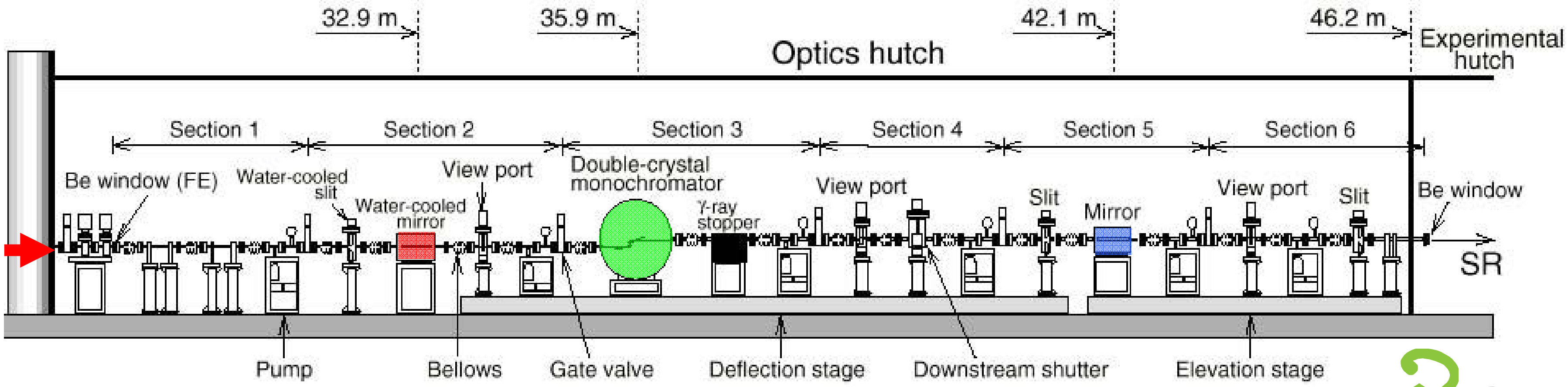

Outside shielding tunnel (optics hutch)

What function of each component ?

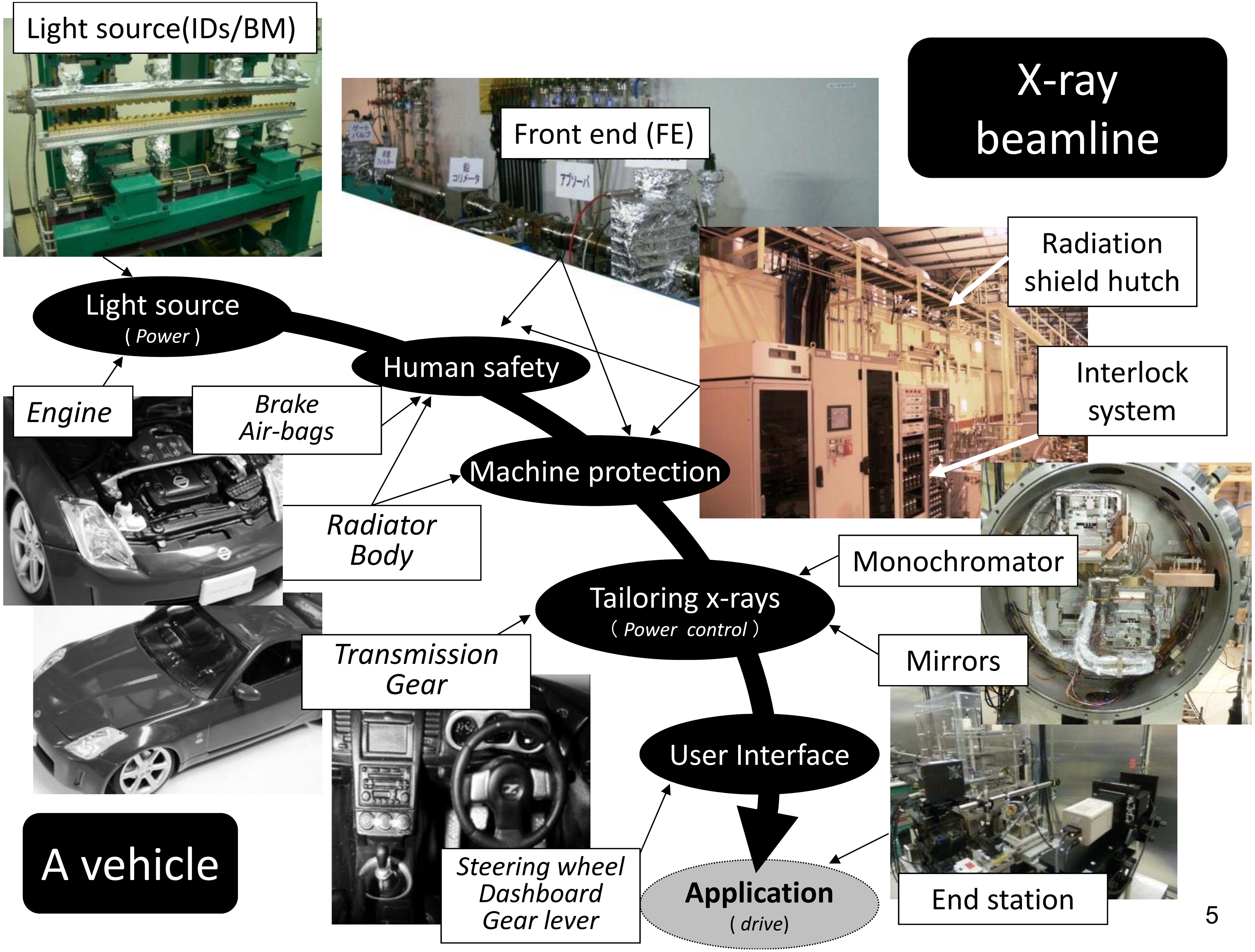

X-ray beamline

Light source(IDs/BM)

Front end (FE)

Radiation shield hutch

Interlock system

Monochromator

Mirrors

End station

Light source
(Power)

Human safety

Machine protection

Tailoring x-rays
(Power control)

User Interface

Application
(drive)

A vehicle

Engine

Brake
Air-bags

Radiator
Body

Transmission
Gear

Steering wheel
Dashboard
Gear lever

X-ray beamline

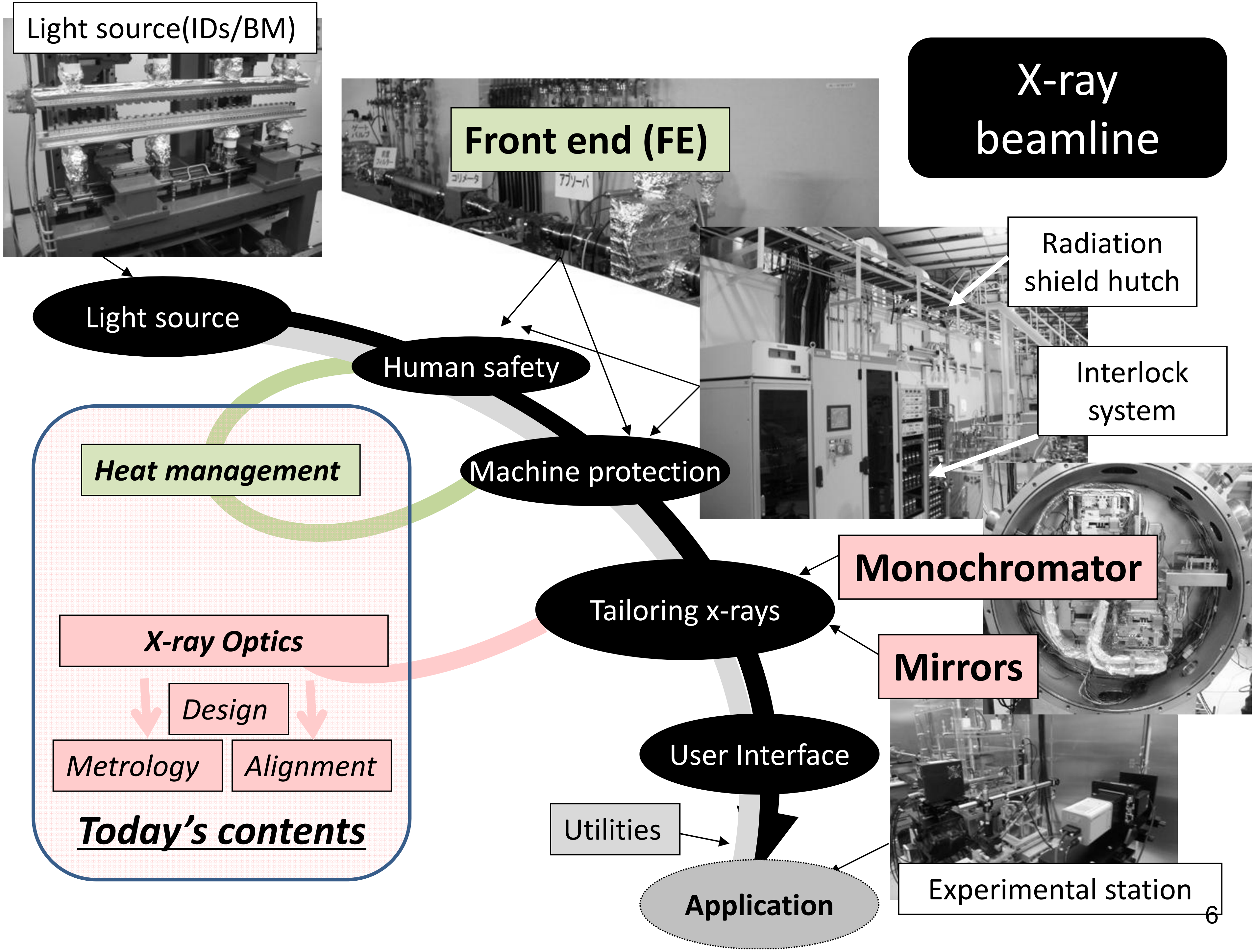

Light source(IDs/BM)

Front end (FE)

Radiation shield hutch

Interlock system

Light source

Human safety

Machine protection

Tailoring x-rays

Monochromator

Mirrors

User Interface

Utilities

Application

Experimental station

Heat management

X-ray Optics

Design

Metrology

Alignment

Today's contents

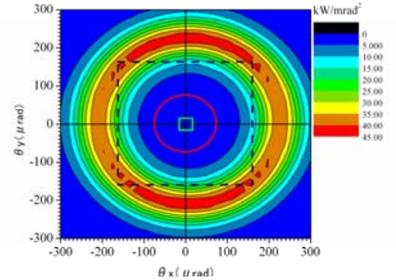

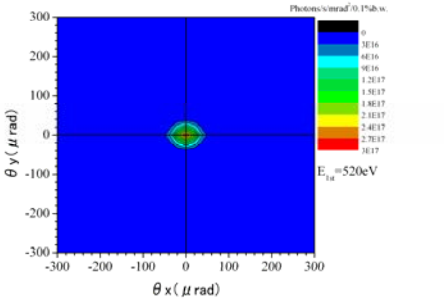

Heat management
for
human safety & machine protection

↓

<u>Front end</u>
(FE)

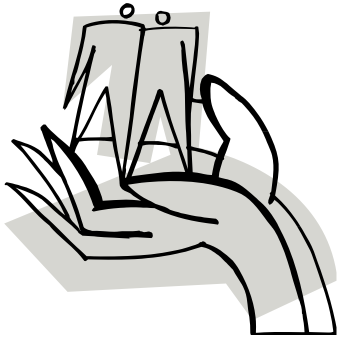

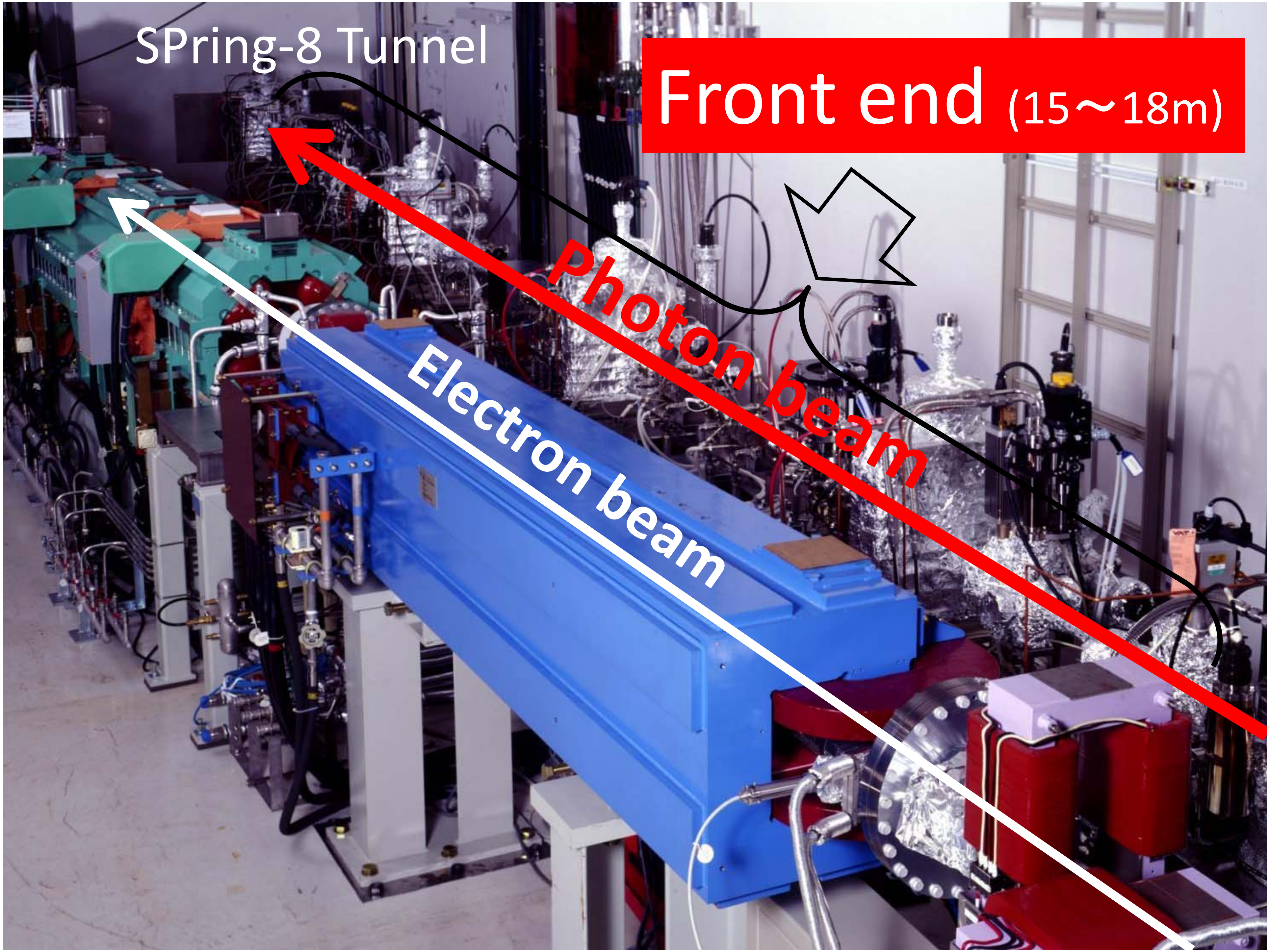

SPring-8 Tunnel

Front end (15～18m)

Photon beam

Electron beam

Schematic Layout inside the SPring-8 Tunnel

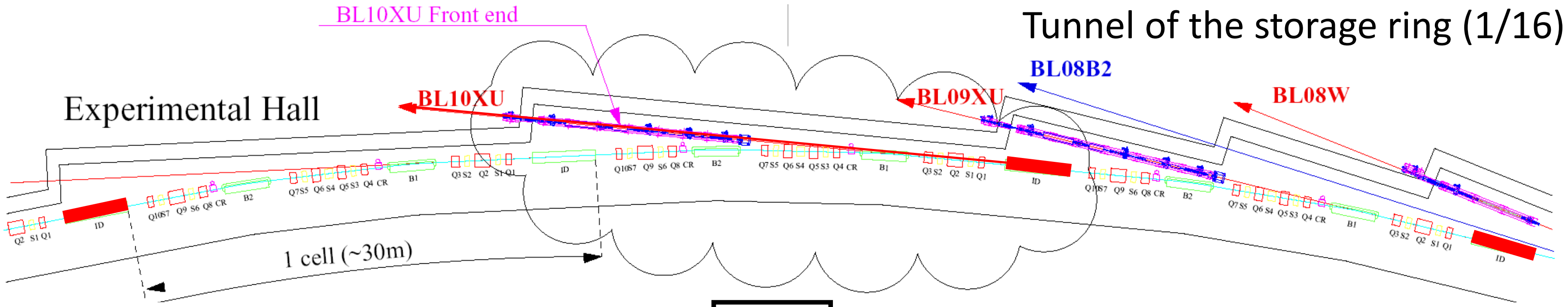

Tunnel of the storage ring (1/16)

Standard

in-vacuum undulator

Power density :

500 kW/mrad^2

Total power : 13 kW

Front end (FE)

(15〜18m)

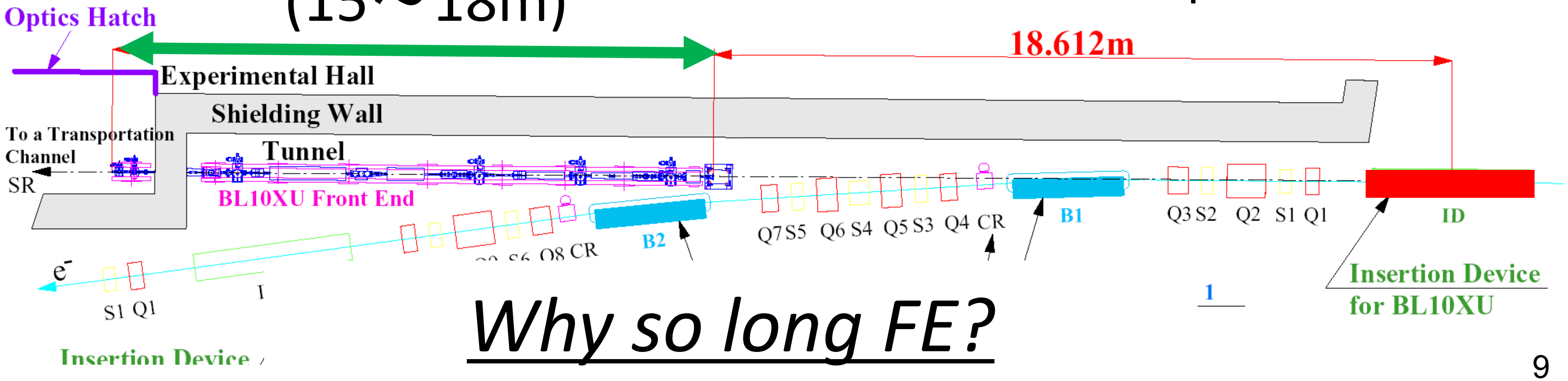

Why so long FE?

Key functions & components of FE

✓ *Shielding* ***for human safety***	**Beam shutter (BS)**, collimator
✓ *Handling high heat load* ***for safety***	**Absorber**, masks
✓ *Handling high heat load* ***for optics***	XY slit, filters
✓ *Monitoring the x-ray beam position*	XBPM (x-ray BPM), SCM (screen monitor)
✓ *Protection of the ring vacuum*	FCS (fast closing shutter), Vacuum system

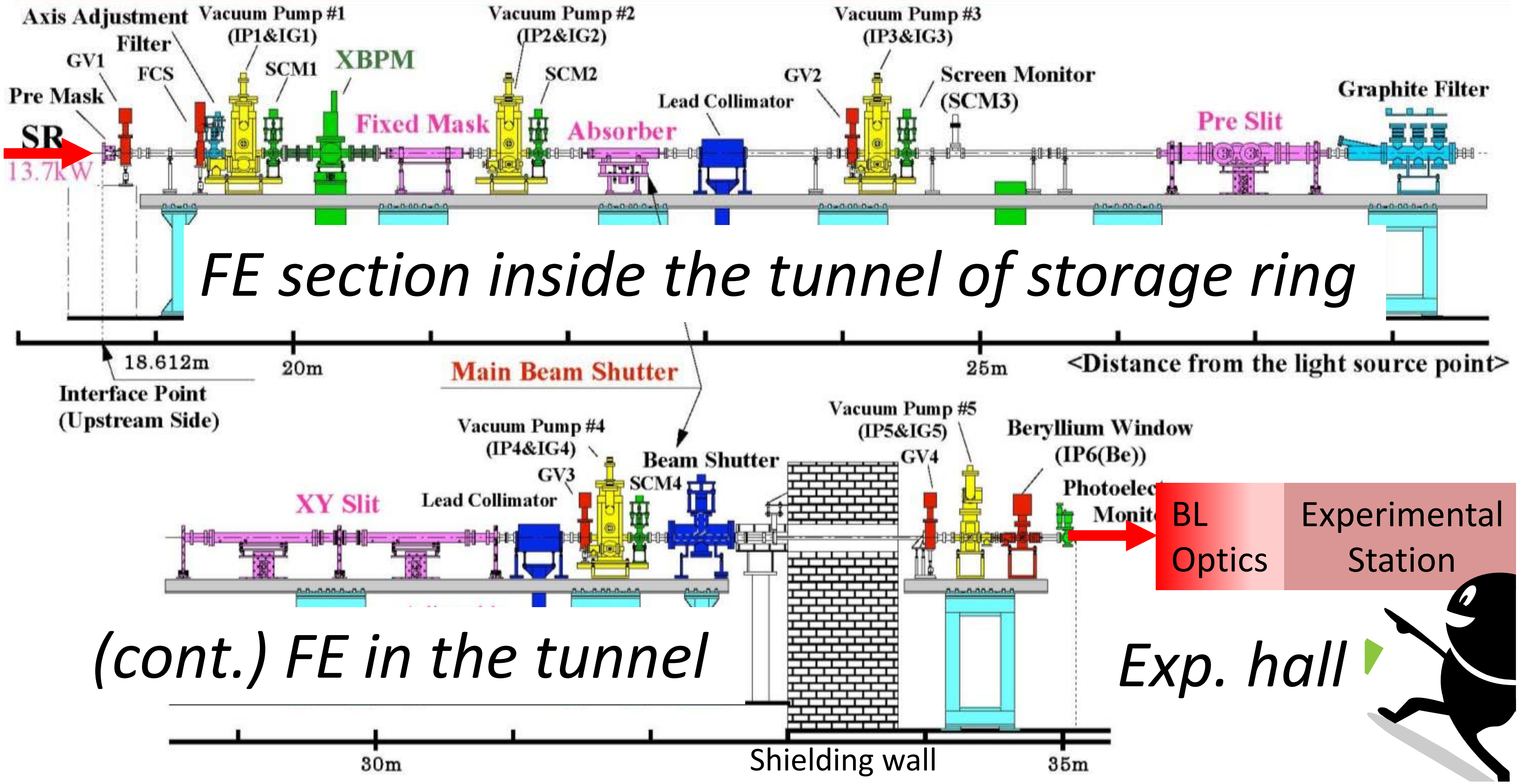

What's "*Main Beam Shutter*" ?

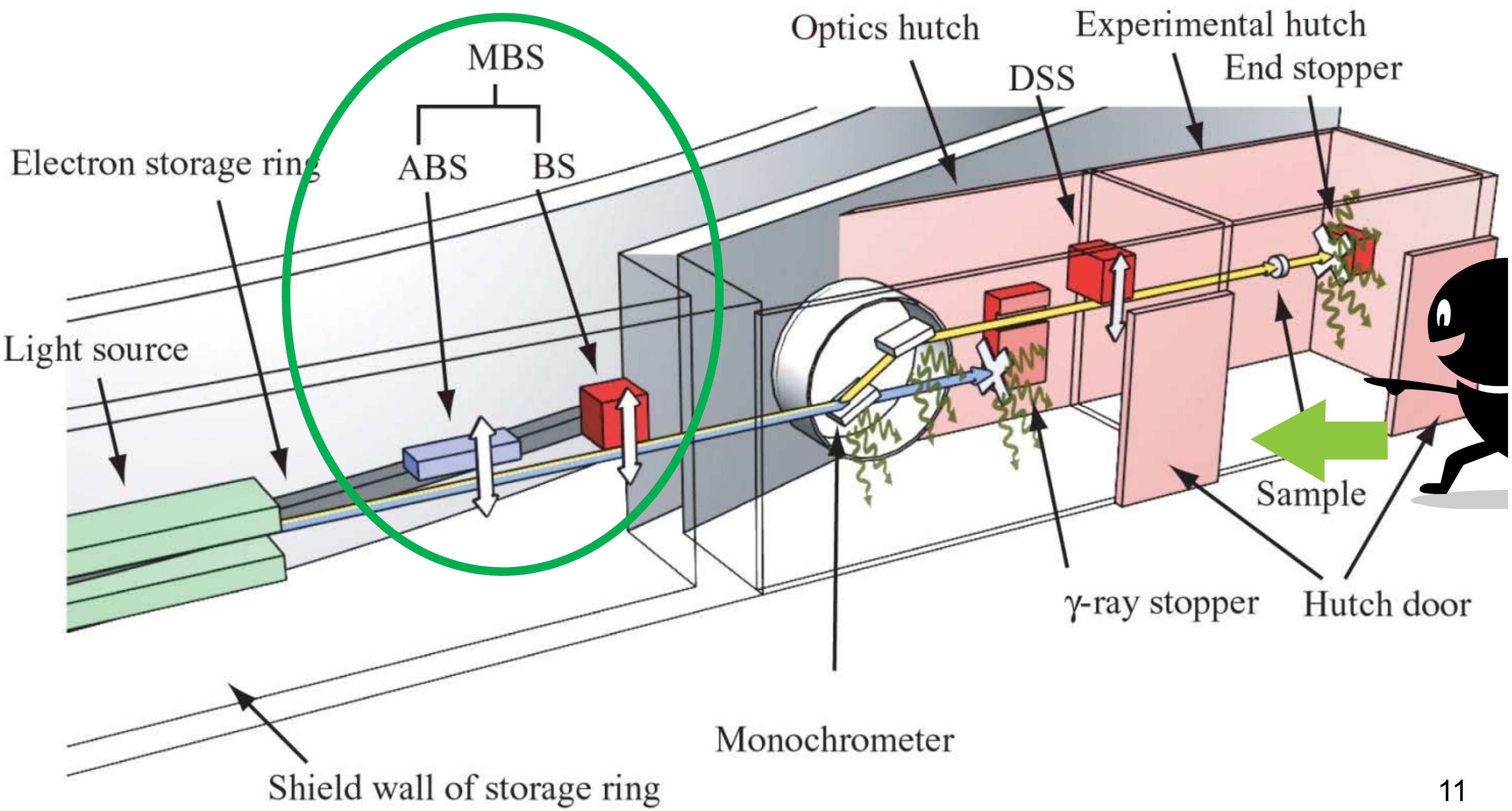

Key functions & components of FE

For safety

- ✓ *Shielding **for human safety***
- ✓ *Handling high heat load **for safety***

Beam shutter (BS), collimator

Absorber, masks

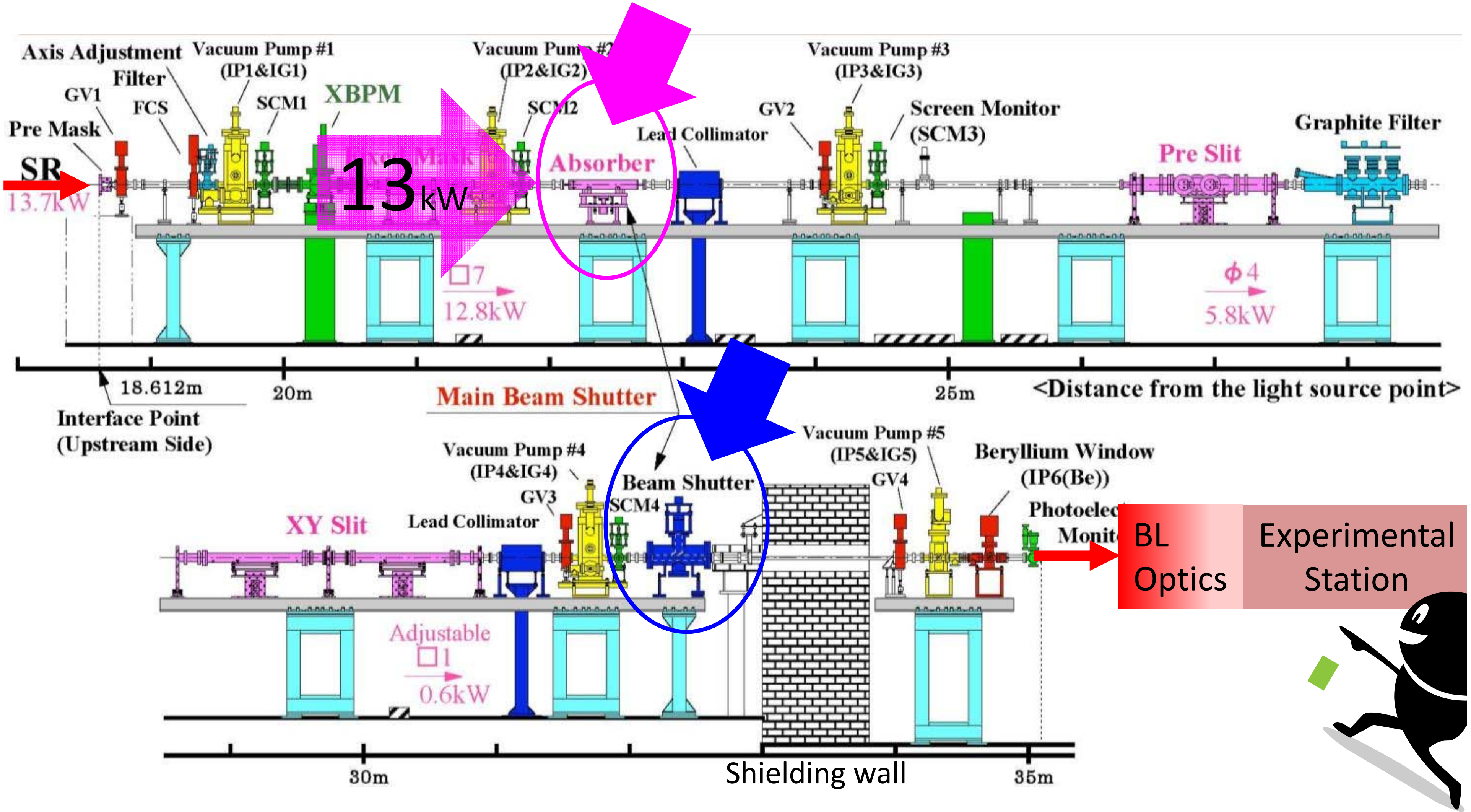

MBS (= ABS + BS) is closed → MBS accepts the incident power form ID.

For safety

When we operate a main beam shutter (MBS), what happens ?

X-ray

Absorber (Abs)

to protect BS from heat load

Beam shutter (BS)

to shield you against radiation

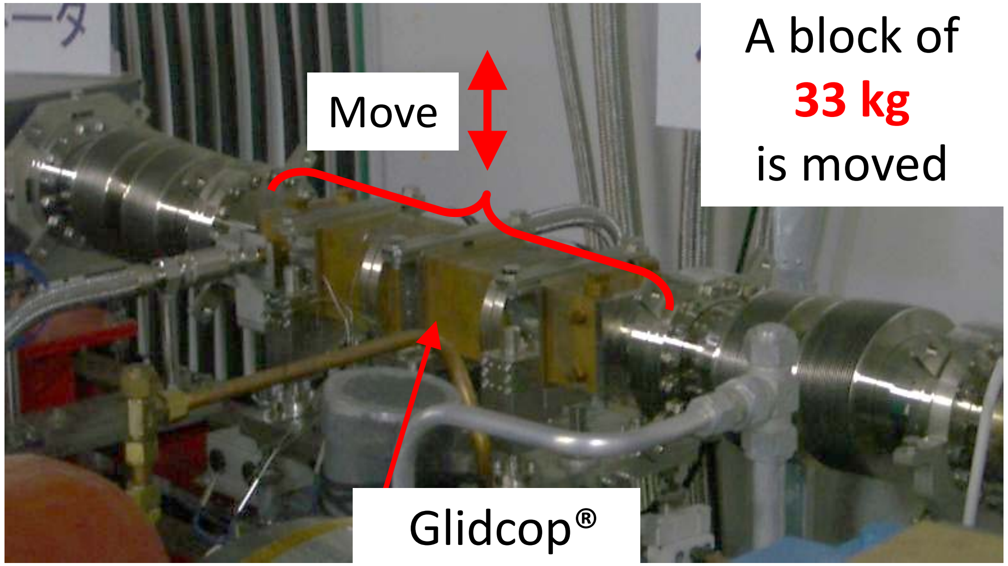

A block of **33 kg** is moved

Glidcop®

(copper that is dispersion-strengthened with ultra-fine particles of aluminum oxide)

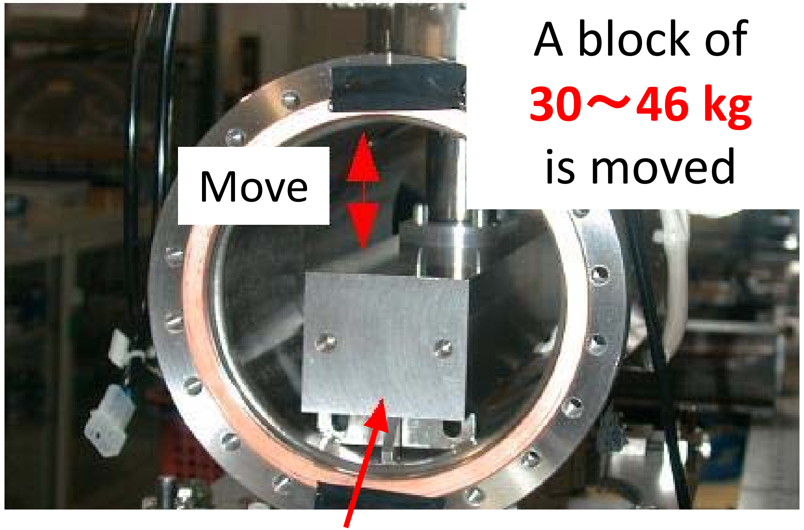

A block of **30～46 kg** is moved

Heavy metal
(alloy of tungsten)

the thermal conductivity not so high

For safety

When we operate a main beam shutter (MBS), what happens ?

X-ray → **Absorber (Abs)** → **Beam shutter (BS)**

to protect BS from heat load

to shield you against radiation

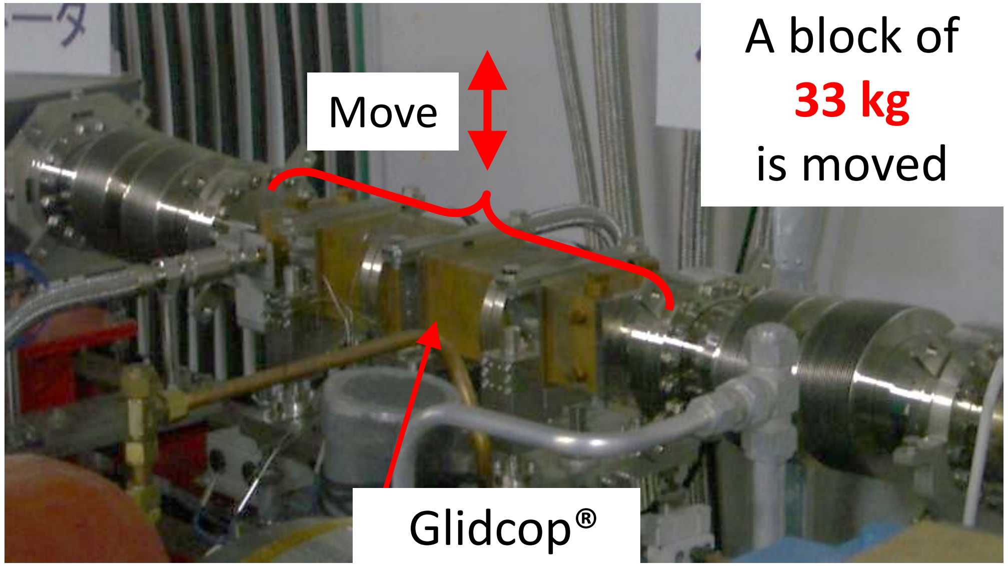

A block of **33 kg** is moved

(copper that is dispersion-strengthened with ultra-fine particles of aluminum oxide)

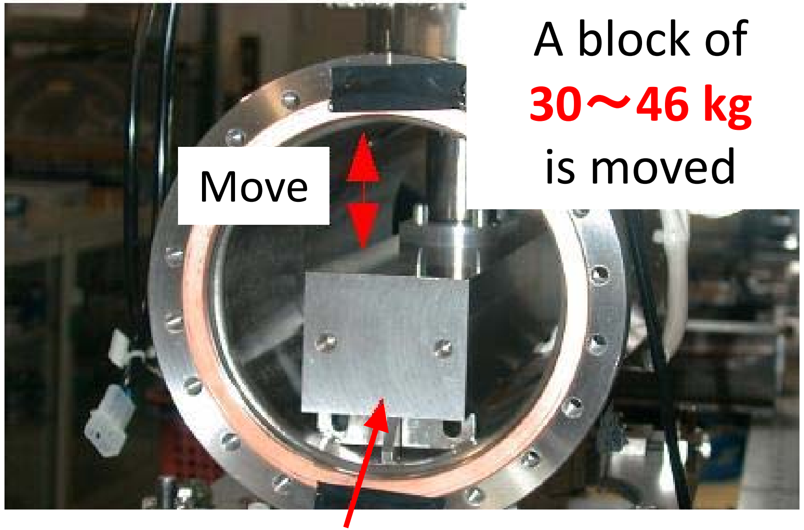

A block of **30～46 kg** is moved

Heavy metal (alloy of tungsten)

the thermal conductivity not so high

After BS is fully opened, Abs is opened.
After Abs is fully closed, BS is closed.
The sequences are essential to keeping safety.

ABS and BS work on ways together to protect us from radiation when we enter the hutch.

*What components remove most “**power**” from ID ?*

For managing heat load

Total power from ID = 14 kW

The power through FE section = 0.6 kW

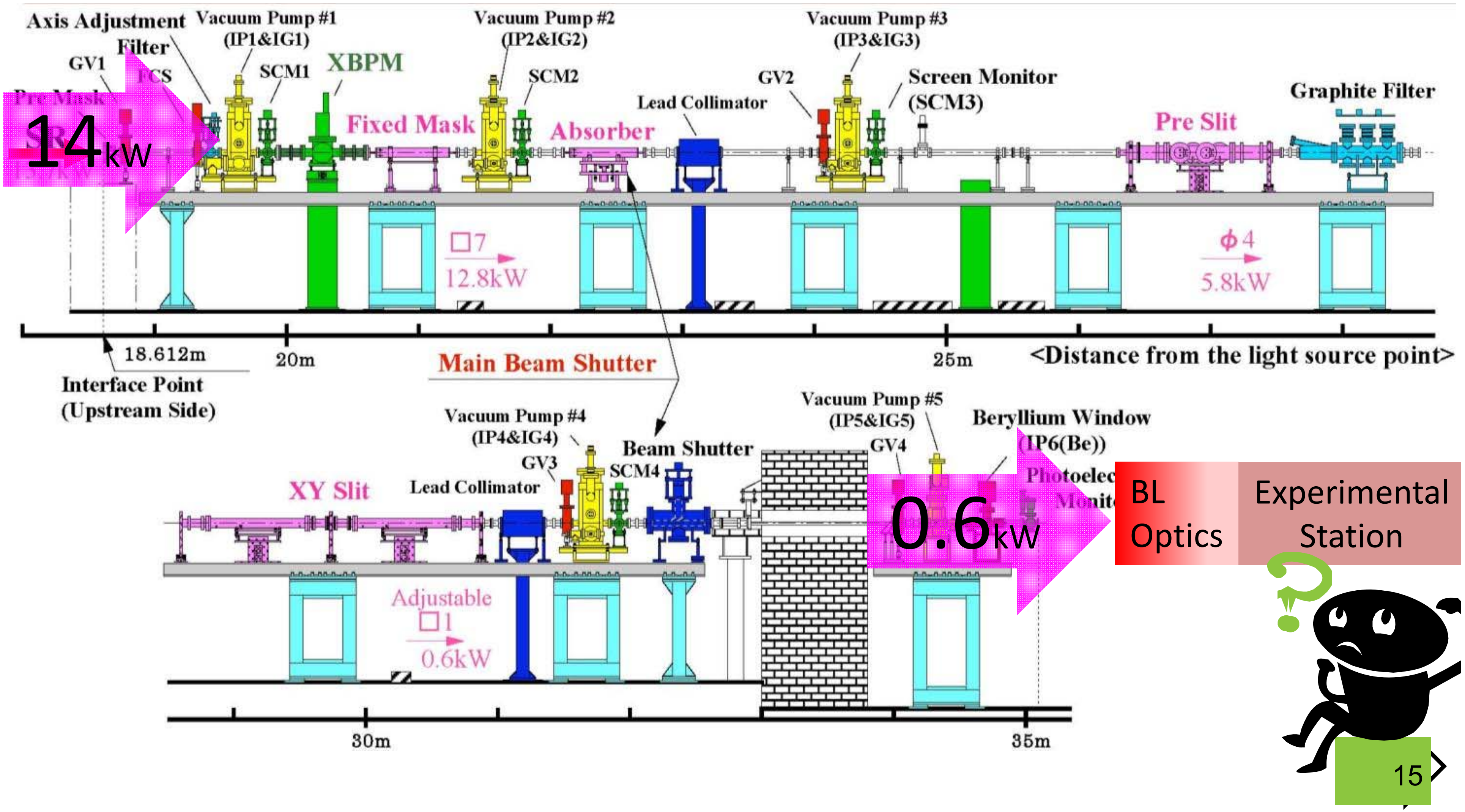

*What components remove most **"power"** from ID ?*

For managing heat load

Absorber, **masks** (to prevent BS from *melting*)

XY slit, filters (to prevent optics from *distorting*)

These components (①, ② and ③) *cut off the power to <u>prevent optics from distorting by heat load.</u>*

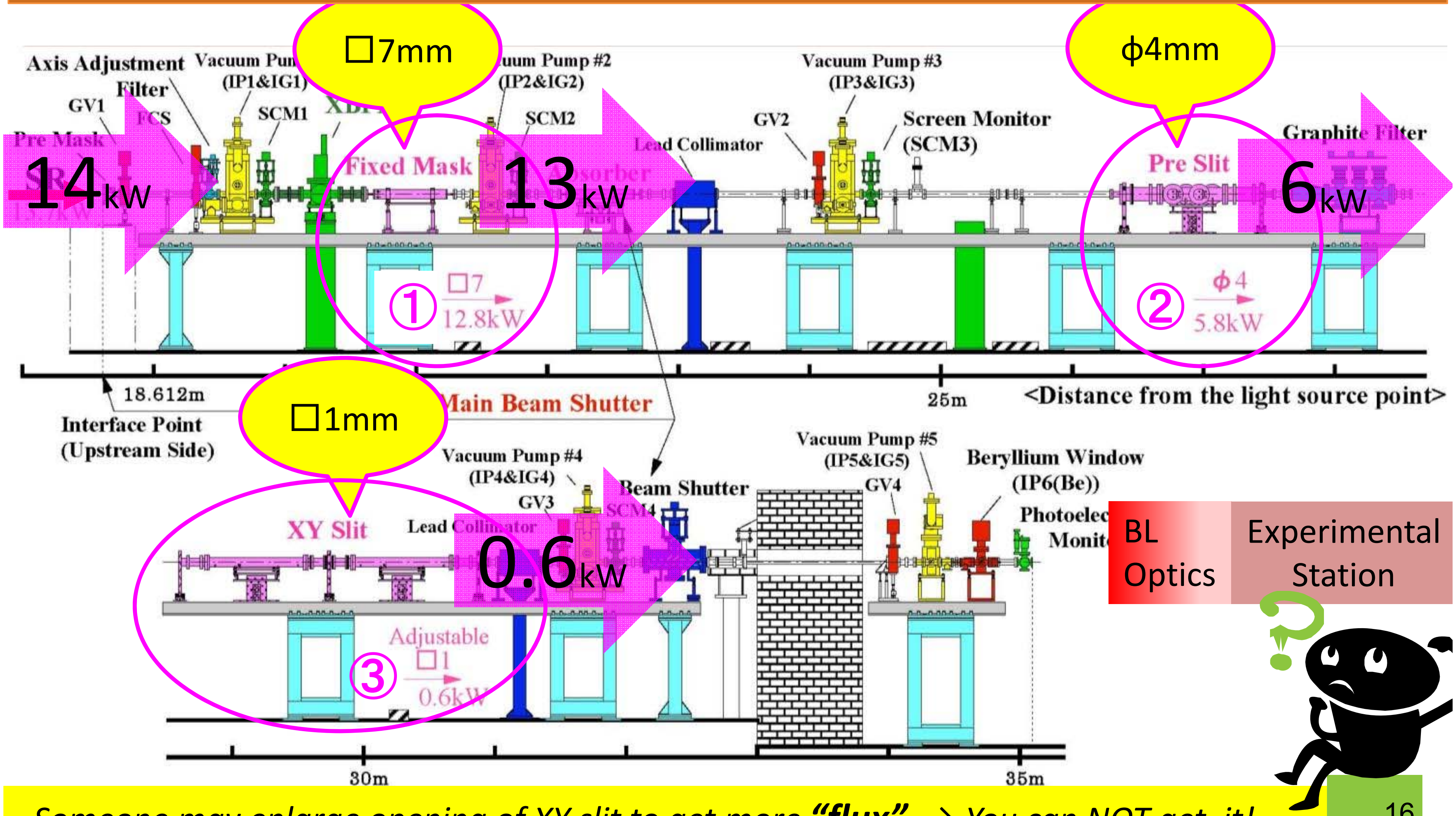

*Someone may enlarge opening of XY slit to get more **"flux"** → You can NOT get it!*

FE: "*For users to take lion's share*"

For managing heat load

Adding a spatial limitation to photon beam,

supplying <u>only a good quality part</u> around the central axis of ID

<u>to transport optical system safely and stably</u>.

The size of XY slit is set to 1.05mm□.
XY slit is installed ～30m away from ID.

①Fixed Mask Aperture
322μrad x 322μrad

②Pre Slit Aperture
ϕ152μrad

③XY Slit Aperture
35μrad x 35μrad

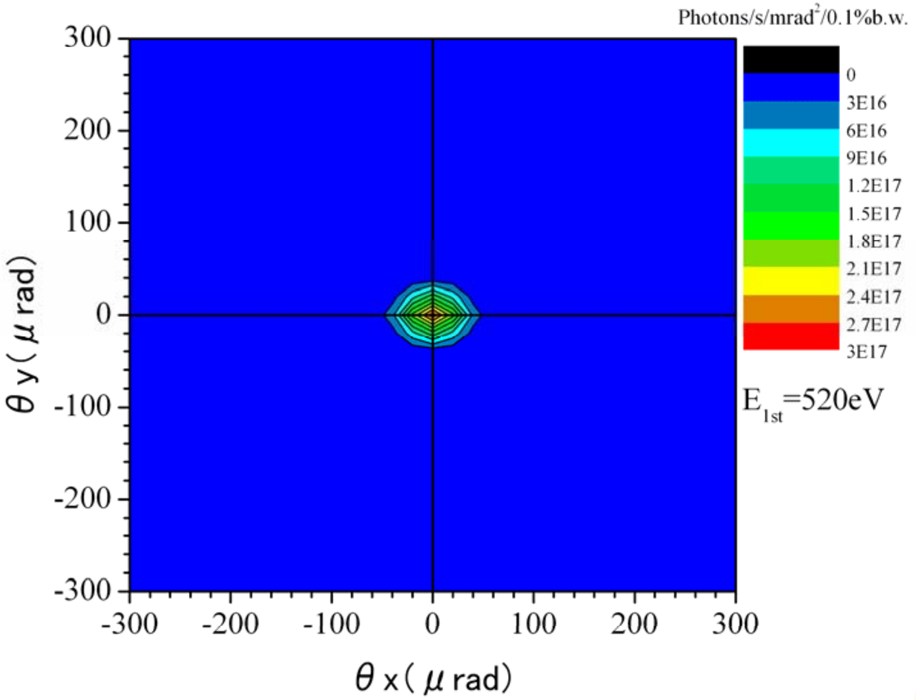

1st harmonic
Flux Density

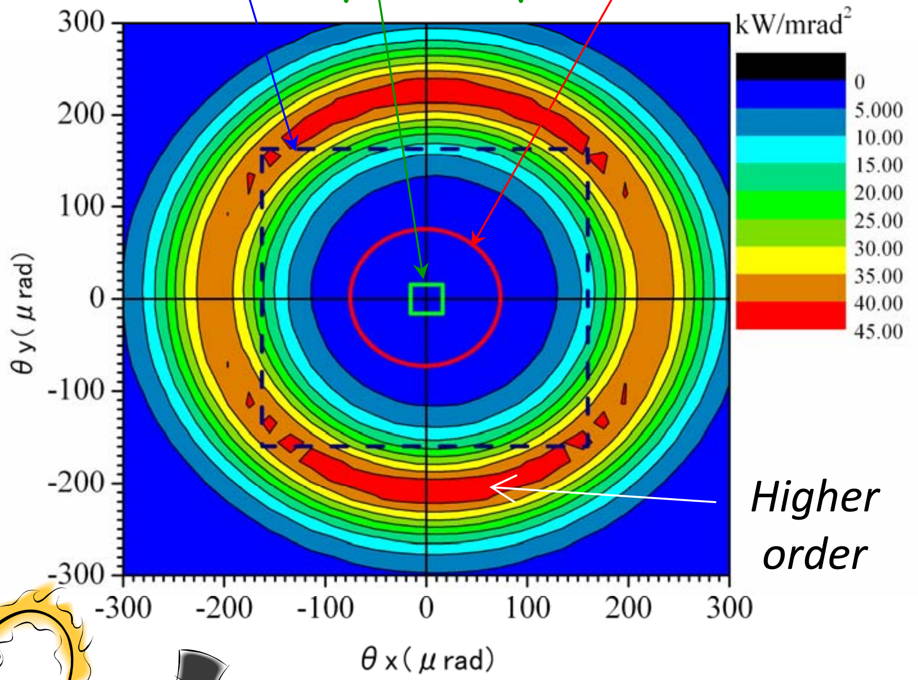

Power Density

Helical Mode Operation
at BL15XU

Comparison of the **Spatial Distribution** between 1^{st} harmonic Flux density and Power density

For managing heat load

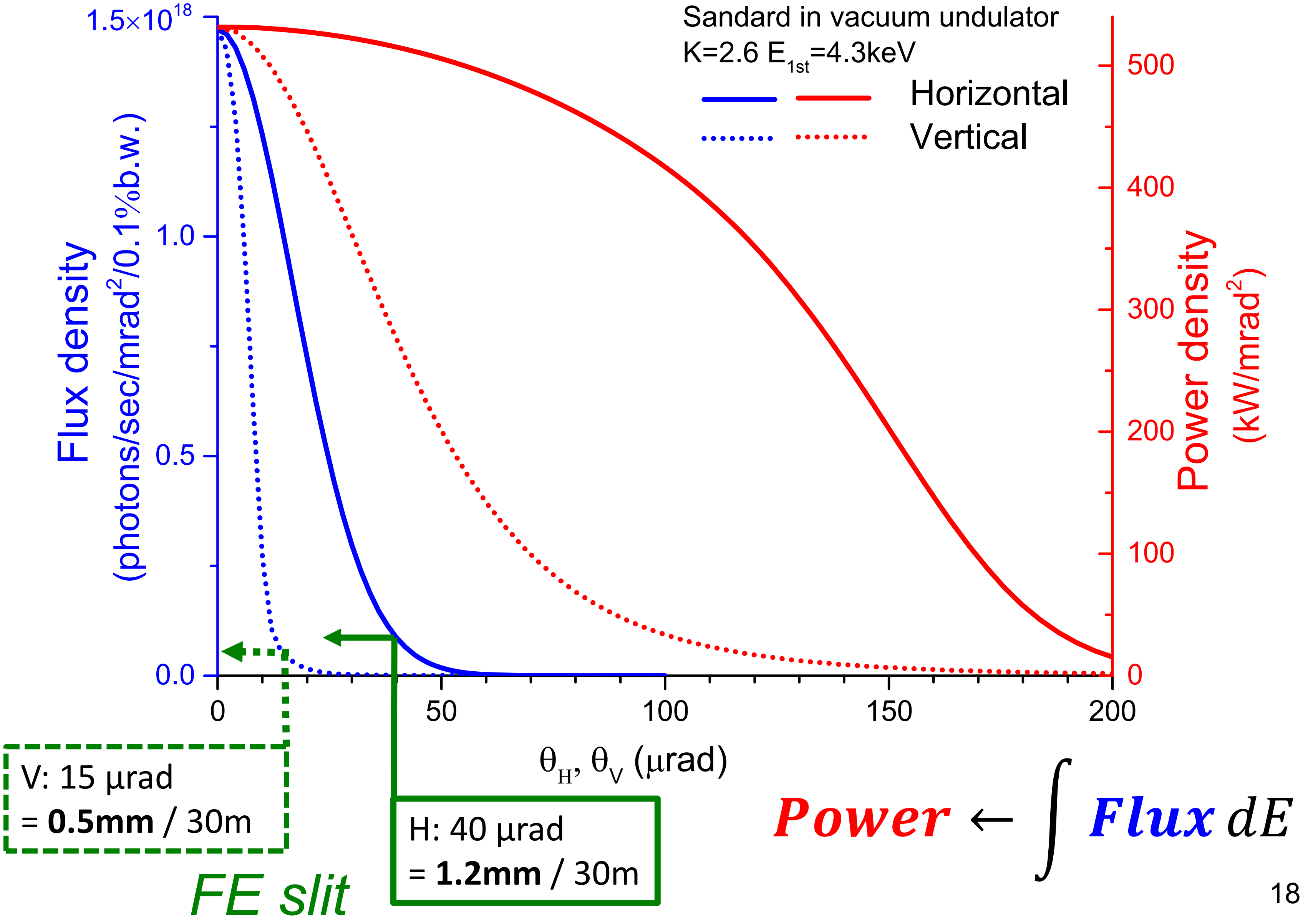

V: 15 μrad
= **0.5mm** / 30m

H: 40 μrad
= **1.2mm** / 30m

FE slit

$$\mathbf{Power} \leftarrow \int \mathbf{Flux}\, dE$$

If an optical component is irradiated by too much power ….

One user opened FE slit excessively.

2kW

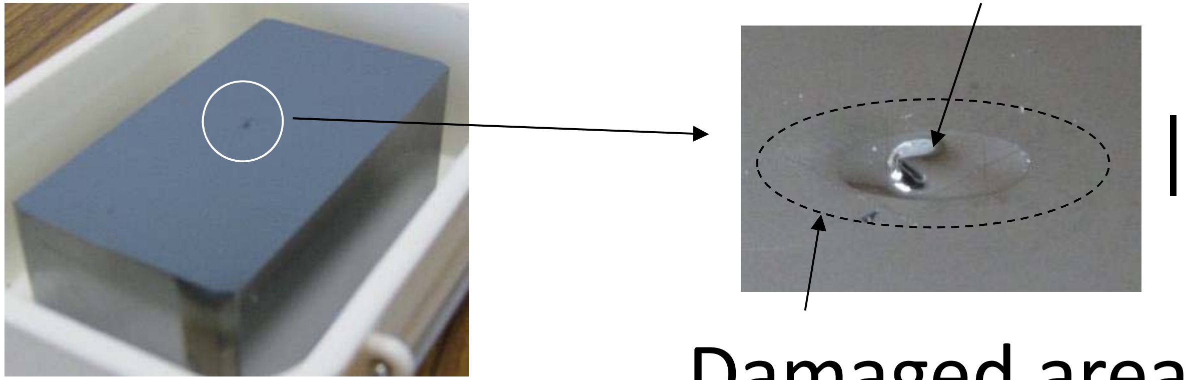

Melted

Damaged area

LN2-cooled
Si crystal

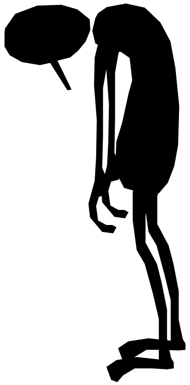

Slit : *“Too much is as bad as too little”*

How to manage high heat load by FE XY slit ?

For managing heat load

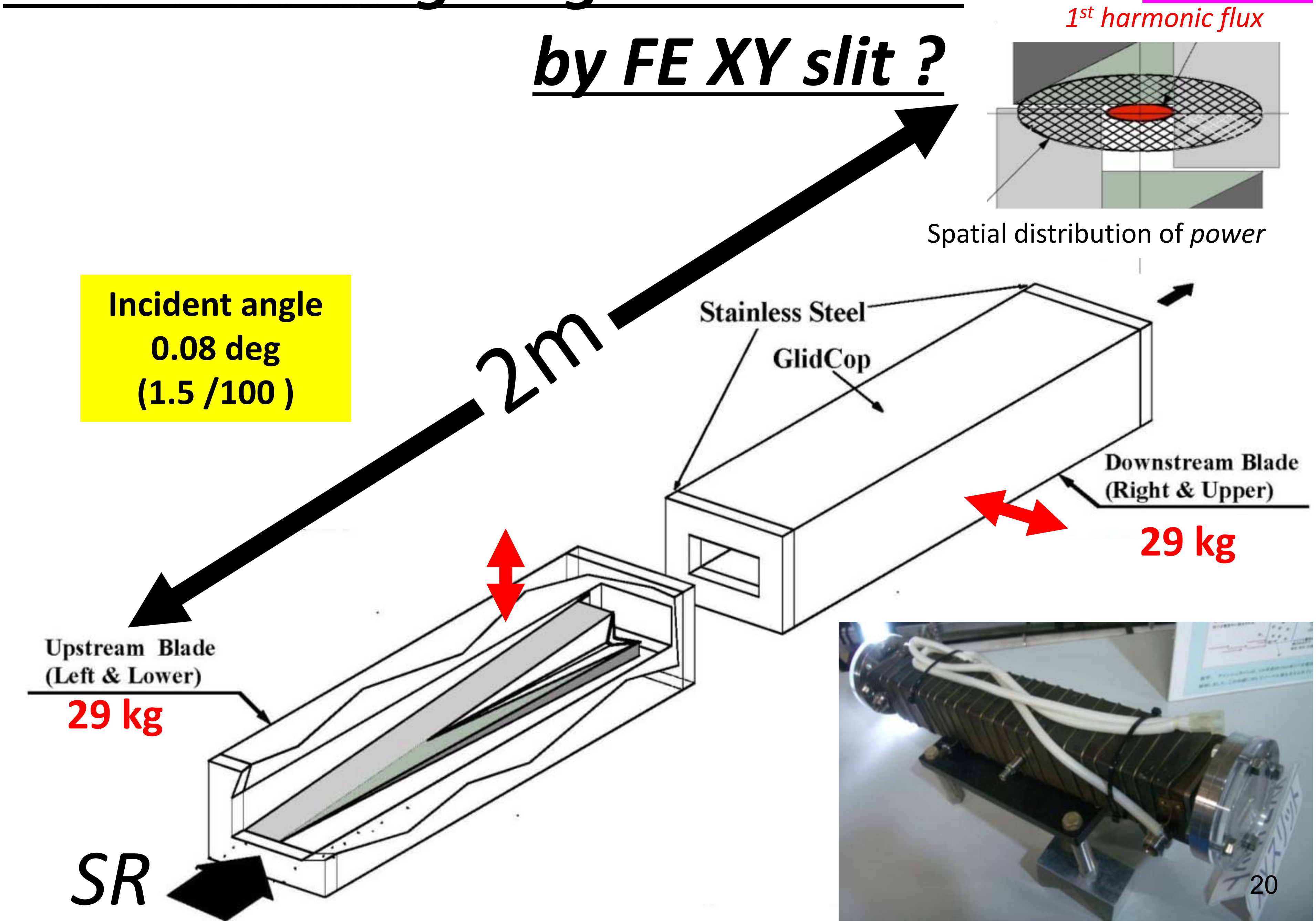

Spatial distribution of *power*

Incident angle
0.08 deg
(1.5 /100)

Key issues of front end

1. Key functions of components in front end :

They have their proper functions, proper missions based on the principles of human radiation safety, vacuum protection, heat-load and radiation damage protection of themselves.

They have to deal with every mode of ring operation and every mode of beamline activities.

2. Any troubles in one beamline should not make any negative effect to the other beamlines.

3. Strongly required to be a reliable and stable system.

We have to adopt key technologies which are reliable, stable and fully established as far as possible.

Higher the initial cost, the lower the running cost from the long-range cost-conscious point of view.

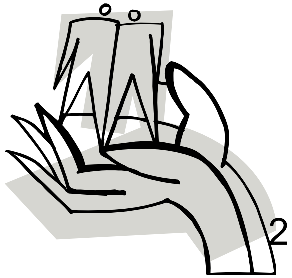

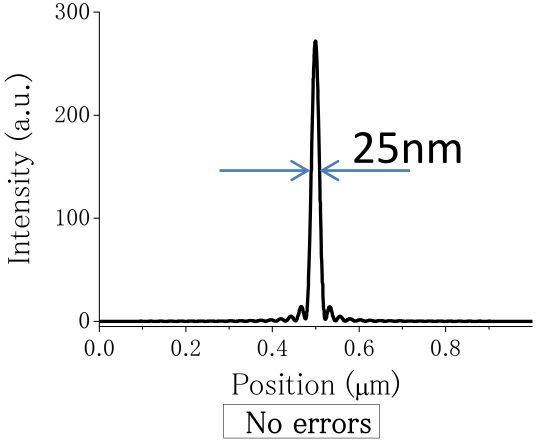

Tailoring x-rays
to application

↓

<u>X-ray mirrors</u>

design, errors, metrology
& alignment

The functions of x-ray mirrors

- ✓Deflecting
- ✓Low pass filter
- ✓Focusing
- ✓Collimating

- Separation from γ-ray
- Branch / switch beamline
- Higher order suppression
- Micro- / nano- probe
- Imaging
- Energy resolution

w. multilayer or crystal mono.

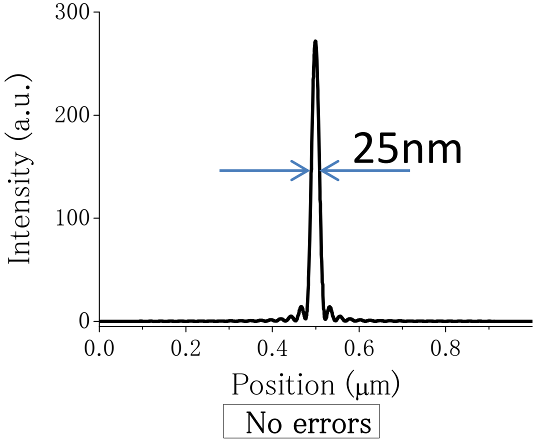

Tailoring x-rays to application

↓

X-ray mirrors

design, errors, metrology & alignment

Design parameters of x-ray mirror

Requirement

the beam properties both *of incident and reflected x-rays*

(*size, angular divergence / convergence, direction, energy region, power…*)

We have to know well what kinds beam irradiate on the mirror.

Design parameters

✓ C h, Pt, N Cr), thickness

ultilay graded ML

✓ Ir razing

How to select

✓ S at, sph tic …

: adaptive (mechanically bent, bimorph)

✓ Substrate sha dal…

✓ Substrate siz dth

✓ w/o cooling ater or LN_2…

✓ Substrate ma op…

In addition,

some errors s ess…

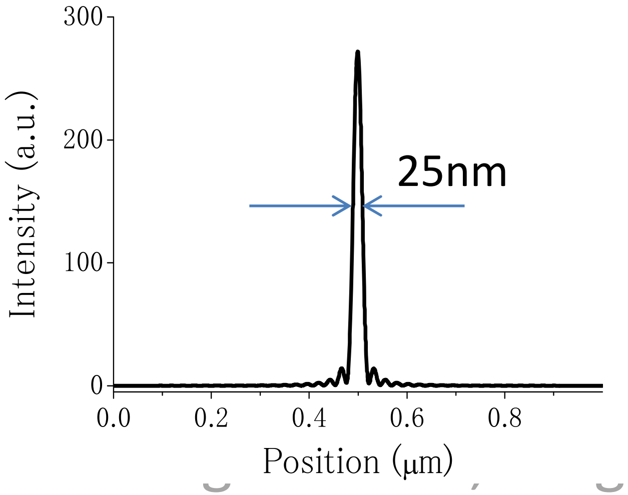

Design parameters of x-ray mirror

Requirement

the beam properties both *of incident and reflected x-rays*

(*size, angular divergence / convergence, direction, energy region, power…*)

We have to know well what kinds beam irradiate on the mirror.

Design parameters

✓ Coating material : Rh, Pt, Ni … (w/o binder , Cr), thickness
: multilayers (ML), laterally graded ML
✓ Incident angle : grazing angle (mrad) ⇨ How to select
✓ Surface shape : flat, sphere, cylinder, elliptic …
: adaptive (mechanically bent, bimorph)
✓ Substrate shape : rectangular, trapezoidal…
✓ Substrate size : length, thickness, width
✓ w/o cooling : indirect or direct, water or LN_2…
✓ Substrate material : Si, SiO2, SiC, Glidcop…

In addition,

some errors such as figure error, roughness…

How to select coating material and incident angle ?

Reflectivity for grazing incident mirrors

$$R(\lambda, \theta, n) = \left| \frac{k_1 - k_2}{k_1 + k_2} \right|^2$$

$$k_1 = \frac{2\pi}{\lambda} \cos\theta, k_2 = \frac{2\pi}{\lambda} \sqrt{n^2 - \cos^2\theta}$$

$$\Downarrow$$

The complex index of refraction

Coating material (1)
“the complex index of refraction”

The complex atomic scattering factor for the *forward scattering*

$$f = f_1 + if_2$$

The complex index of refraction

$$n = 1 - \delta - i\beta \qquad E \propto e^{-i(\varpi t - kr)}$$

$$\begin{cases} \delta = \dfrac{N r_0 \lambda^2}{2\pi} f_1(\lambda) \\ \beta = \dfrac{N r_0 \lambda^2}{2\pi} f_2(\lambda) \end{cases}$$

Small
for x-ray region

	$\delta\ (\times 10^{-5})$	$\beta(\times 10^{-7})$
Si	0.488	0.744
Quartz	0.555	2.33
Pt	3.26	20.7
Au	2.96	19.5

$$r_0 = \frac{e^2}{4\pi m c^2} = 2.82 \times 10^{-15} m$$

N: Number of atoms per volume

$$\beta = \frac{\mu\lambda}{4\pi}$$

*μ: linear **absorption** coefficient*

Coating material (2)

"total reflection"

$$\cos(\theta_1)/\cos(\theta_2) = n_2/n_1$$ ←Snell's law

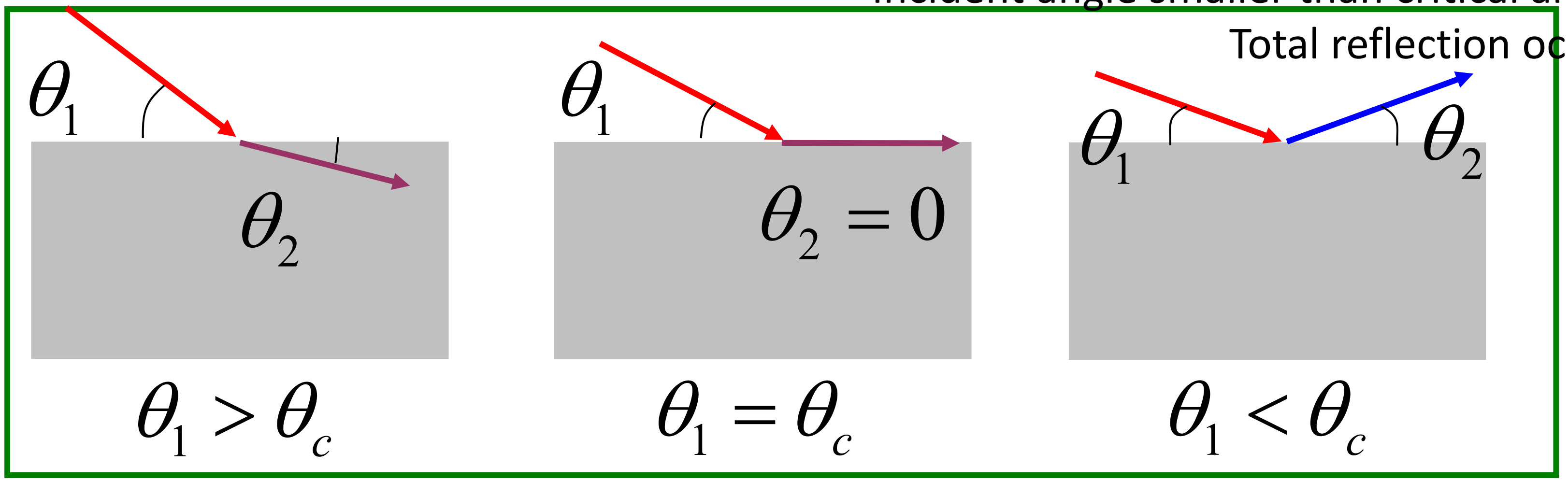

Incident angle smaller than critical angle,
Total reflection occurs

$$\cos(\theta_c) = n = 1-\delta, \cos(\theta_c) \approx 1-\theta_c^{\ 2}/2$$

$$\theta_c \cong \sqrt{2\delta} = 1.6\times10^{-2}\lambda\sqrt{\rho} = 20\sqrt{\rho}/E$$

For example,

θ_c (rad), ρ (g / cm^3) , λ (nm) , E (eV)

Rh (ρ = 12.4 g /cm^3) λ=0.1nm, θ_c =5.68 mrad

Coating material (3) : “*cut off, absorption*”

The cut off energy of total reflection Ec

$$E_c \approx 20\sqrt{\rho}/\theta_i$$

E_c (eV) , ρ (g / cm^3), θ_c (mrad)

Rh (12.4 g / cm^3)

Pt (21.4 g / cm^3)

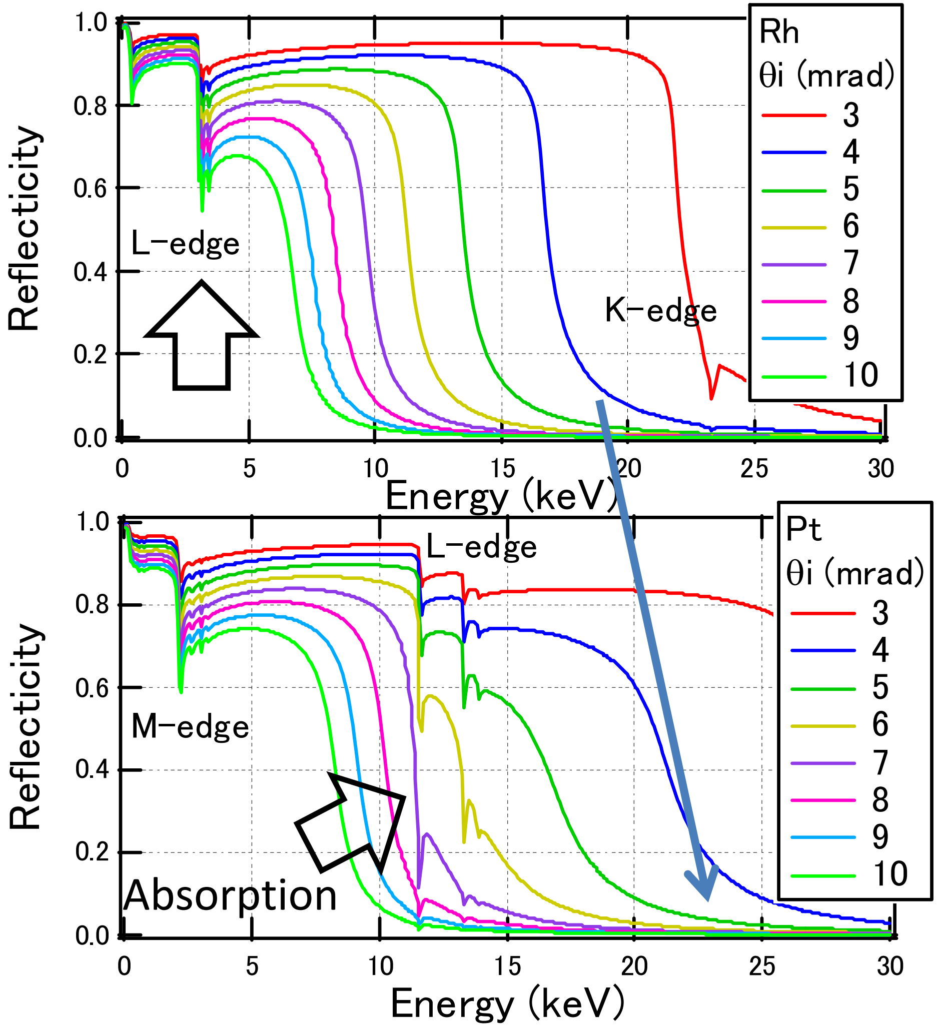

Cut off energy, absorption → incident angle

→ Opening of the mirror, length, width of mirror, power density

Atomic scattering factors, Reflectivity

You can easily find optical property in "X-Ray Data Booklet"
by Center for X-ray Optics and Advanced Light Source,
Lawrence Berkeley National Lab.
In the site the reflectivity of x-ray mirrors can be calculated.

http://xdb.lbl.gov/

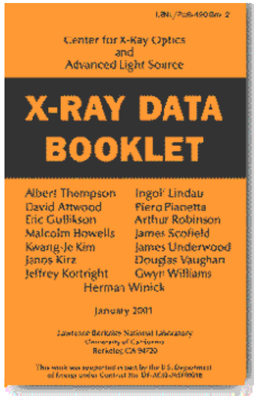

Center for X-Ray Optics
and
Advanced Light Source

X-RAY DATA
BOOKLET

Albert Thompson	Ingolf Lindau
David Attwood	Piero Pianetta
Eric Gullikson	Arthur Robinson
Malcolm Howells	James Scofield
Kwang-Je Kim	James Underwood
Janos Kirz	Douglas Vaughan
Jeffrey Kortright	Gwyn Williams

Herman Winick

January 2001

Lawrence Berkeley National Laboratory
University of California
Berkeley, CA 94720

<u>Many thanks to the authors !</u>

Surface shape (1)

Purpose of the mirror

- deflecting
- low pass filter
- focusing
- collimate

- meridional
- sagittal

for example,	Easy to make or cost
flat	◎
spherical	◎
cylindrical	○
toroidal	○
elliptical	△
parabolic…	△
adaptive	△

Take care of aberration

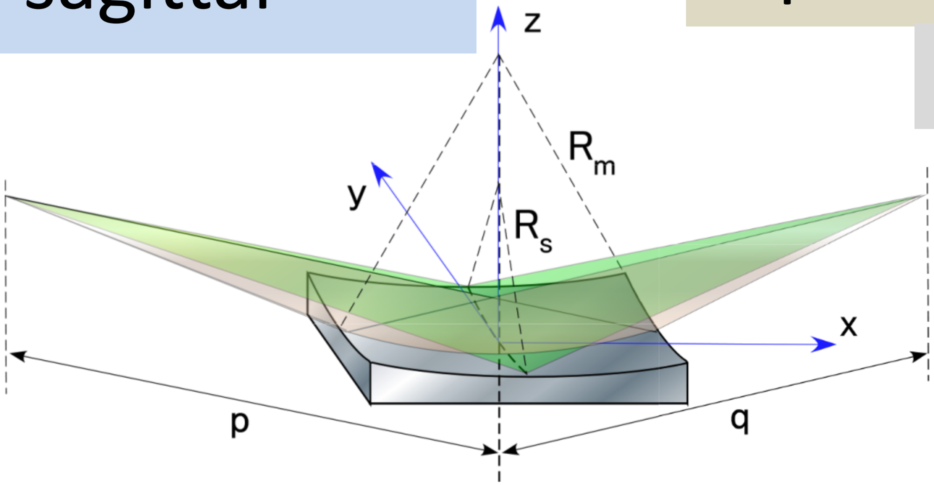

Surface shape (2) radius and depth

add photos

$$R_m = \frac{2}{\left(1/p + 1/q\right)\sin\left(\theta_i\right)}$$

$$R_s = \frac{2\sin\left(\theta_i\right)}{\left(1/p + 1/q\right)} = R_m \sin^2\left(\theta_i\right)$$

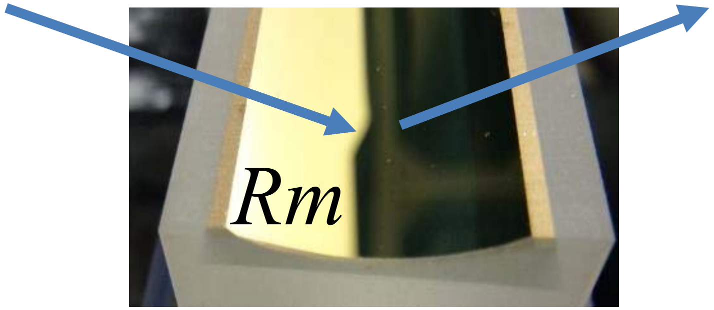

Meridional focusing

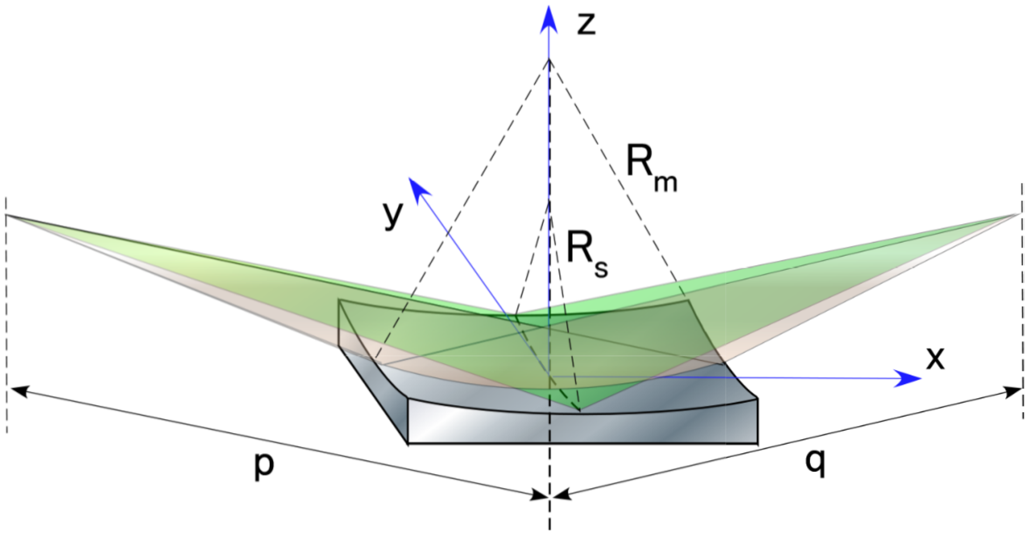

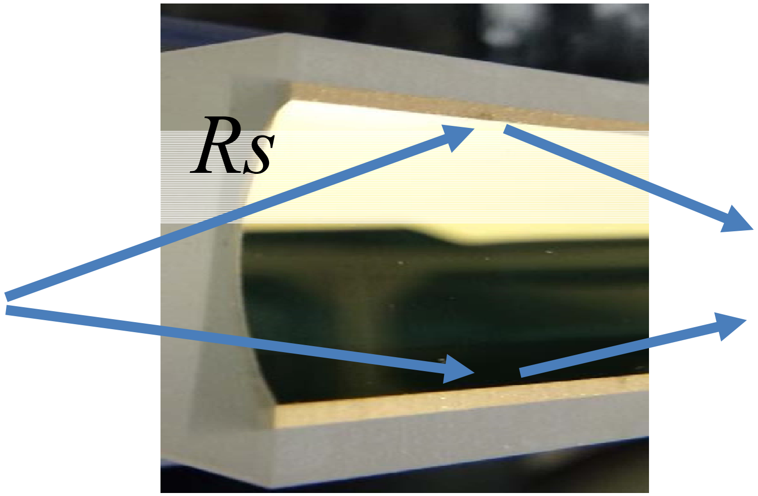

Sagittal focusing

Surface shape (2) radius and depth

$$R_m = \frac{2}{\left(1/p + 1/q\right)\sin\left(\theta_i\right)}$$

$$R_s = \frac{2\sin\left(\theta_i\right)}{\left(1/p + 1/q\right)} = R_m \sin^2\left(\theta_i\right)$$

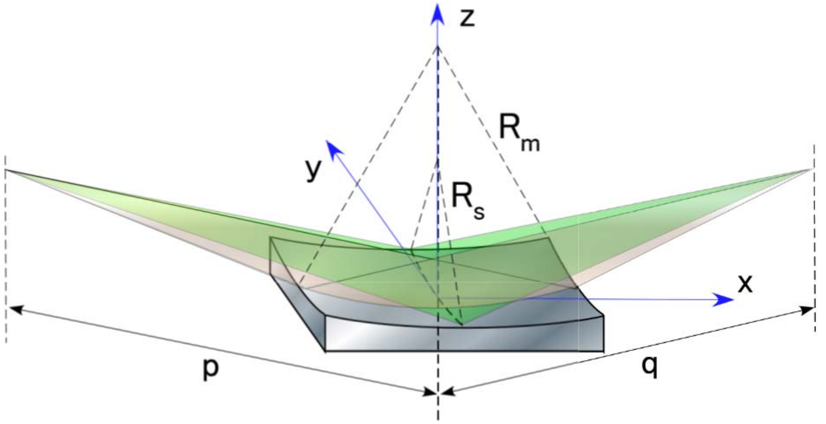

For parallel beam $q \to \infty, 1/q = 0$

Depth at the center

$$D = R - \sqrt{R^2 - \left(\frac{L}{2}\right)^2} \approx \frac{L^2}{8R}$$

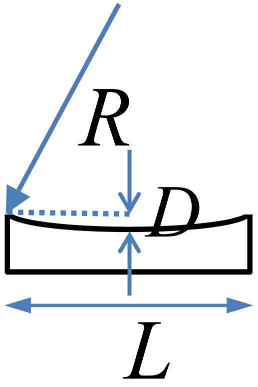

For example,

p=15～50m, q=5～20m, θ_i=1～10mrad

R_m=0.1～10 km, R_s= 30～100 mm

R_m= 1 km, L=1m → D = 125 µm

R_s=30 mm, L=20mm → D = 1.7 mm

Sagittal focusing mirror

R_s～30mm

Surface shape (3) elliptical

$$\frac{x^2}{a^2}+\frac{y^2}{b^2}=1$$

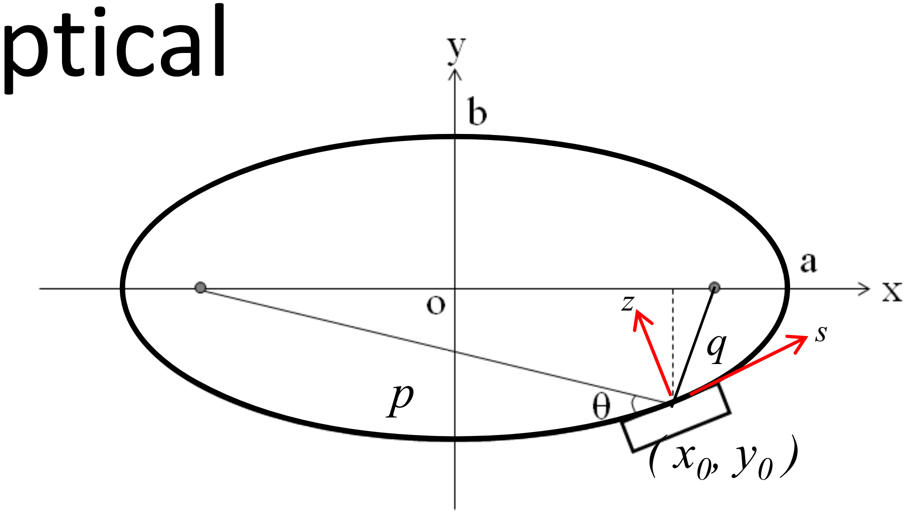

For example,

$$p = 975\,m\,, q = 50\,mm\,, \theta = 3\,mrad$$

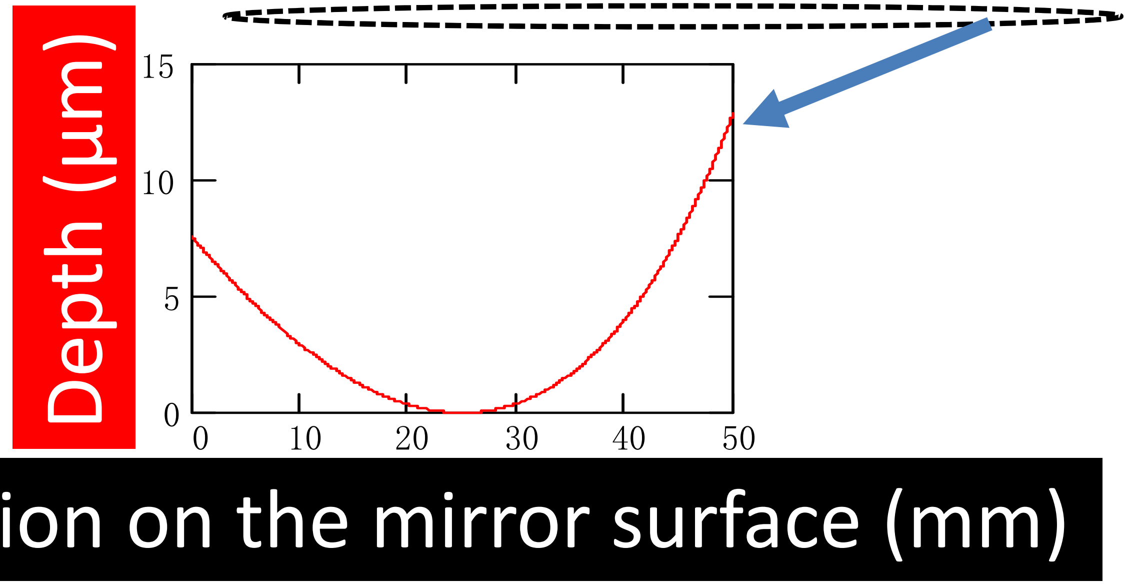

Precise fabrication is not easy.

Design parameters of x-ray mirror

Requirement

the beam properties both *of incident and reflected x-rays*

(*size, angular divergence / convergence, direction, energy region, power…*)

Design parameters

- ✓ Coating material : Rh, Pt, Ni … (w/o binder , Cr), thickness
  : multilayers (ML), laterally graded ML
- ✓ Incident angle : grazing angle (mrad)
- ✓ Surface shape : flat, sphere, cylinder, elliptic …
  : adaptive (mechanically bent, bimorph)
- ✓ Substrate shape : rectangular, trapezoidal…
- ✓ Substrate size : length, thickness, width
- ✓ **w/o cooling : indirect or direct, water or LN$_2$…**
- ✓ **Substrate material : Si, SiO2, SiC, Glidcop…**

In addition,

some errors such as figure error, roughness…

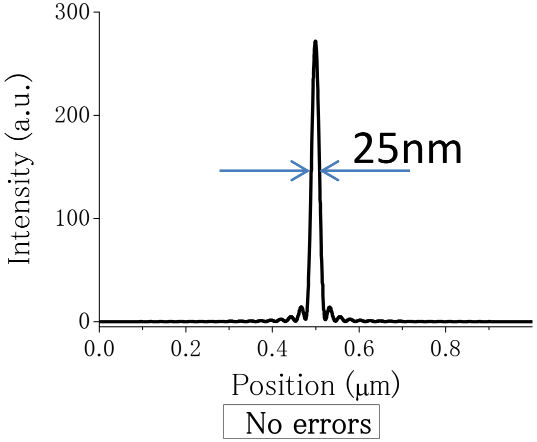

Tailoring x-rays
to application

↓

<u>X-ray mirrors</u>

design, errors, metrology
& alignment

“An actual mirror has some errors.”

The tolerance should be specified to order the mirror

☐ *Roughness*
☐ *Density of coating material*
☐ *Radius error*
☐ *Figure error*

- Reflectivity
- Beam size
- Distortion
- Deformation …

The cost (price and lead time) depends entirely on tolerance.
We must consider or discuss how to measure it.

✓ Deformation by self-weight, coating and support …
✓ Figure error of adaptive mechanism
✓ Misalignment of mirror
✓ Stability of mirror’s position (angle)
✓ Deposition of contamination by use
✓ Decomposition of substrate by use

- Environment
- Manipulator
- Cooling system …

Contamination and removal

before

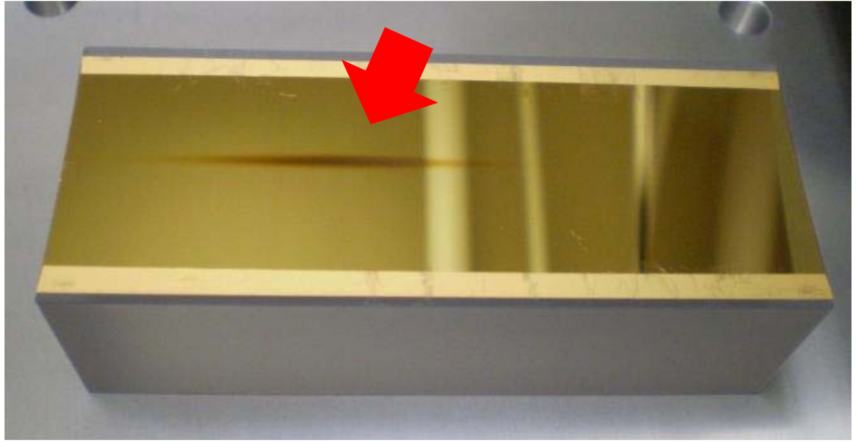

After cleaning

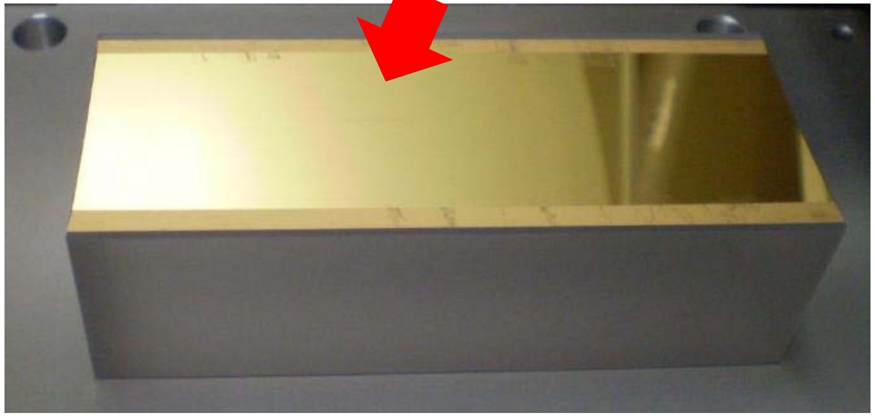

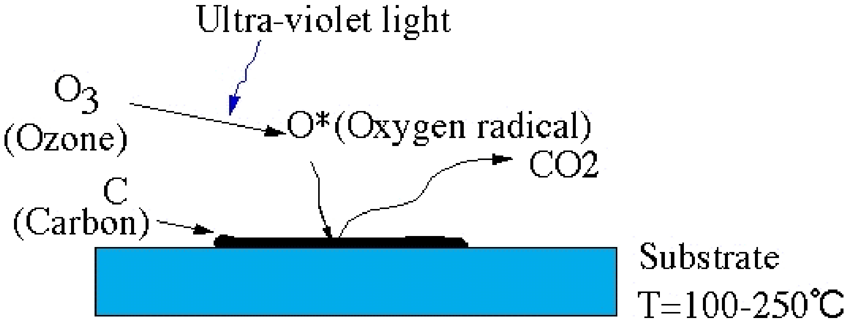

Advantage of UV/ozone cleaning

1. Low Damage
2. Contamination-free
3. Non-contact

UV / ozone cleaning

It takes from 10 min to a few hours.

Errors (1)

*“Density **ρ** and surface roughness **σ** ”*

$$E_c \approx 20\sqrt{\rho}/\theta_i$$

$$R = R_0 e^{-\left(\frac{4\pi\sigma\sin(\theta_i)}{\lambda}\right)^2}$$

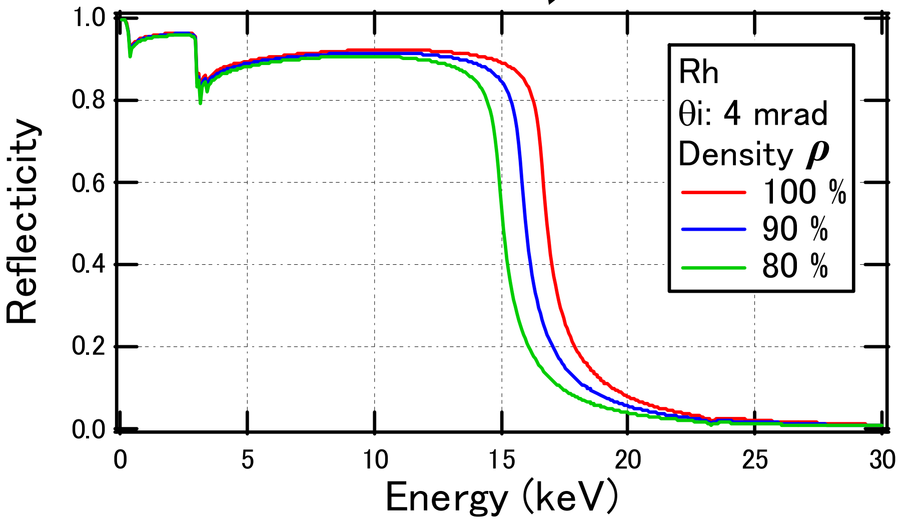

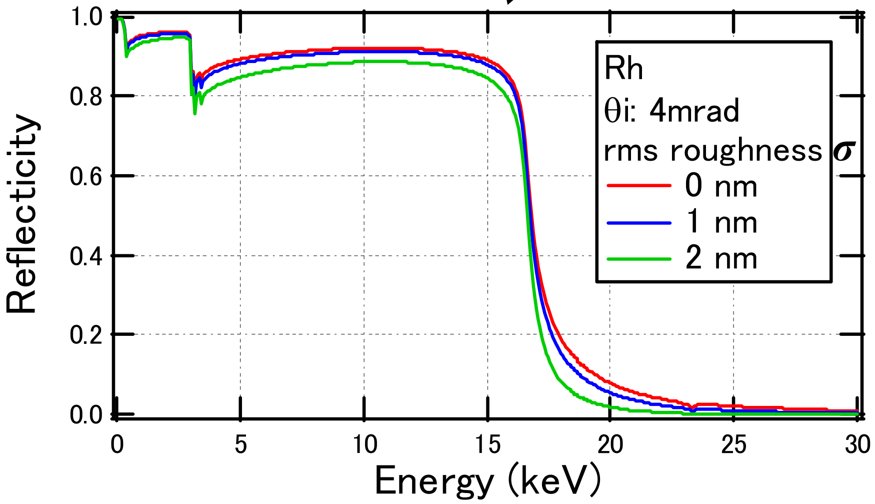

Coating on sample wafer at the same time is helpful to evaluate the density and roughness.

Errors (2)

“the self-weight deformation”

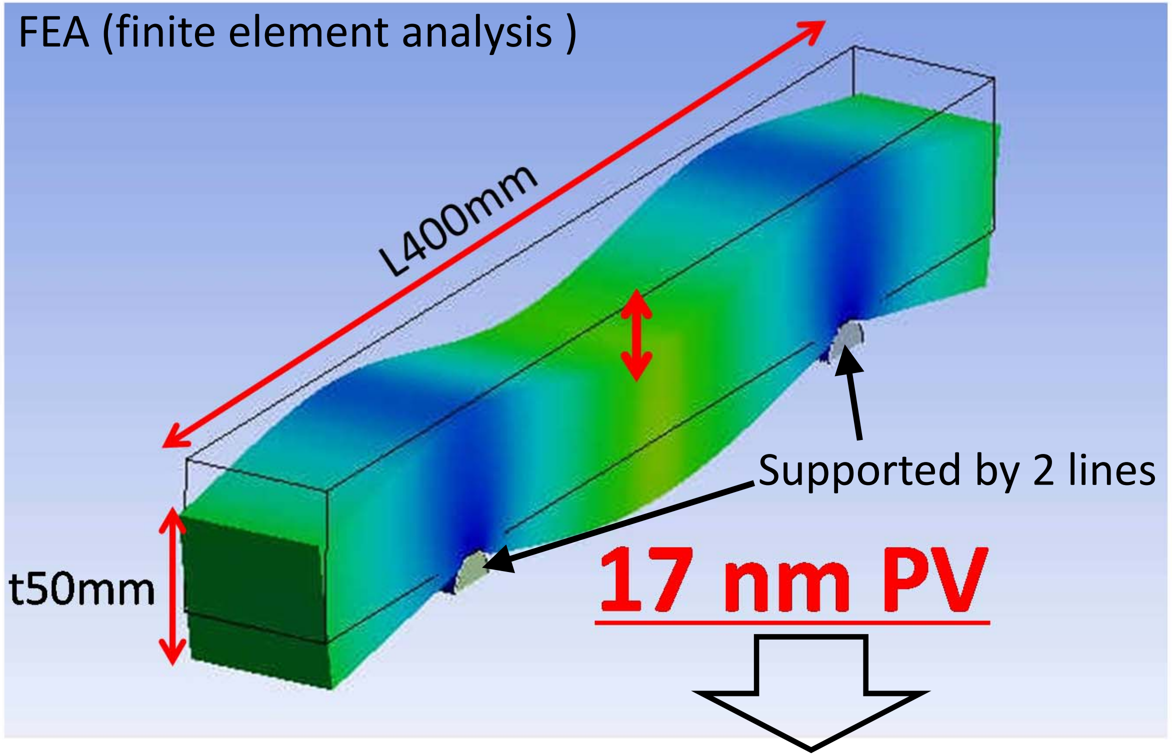

17 nm PV

Material	SiO_2
Density	2.2 g / cm^3
Poisson's ratio	0.22
Young’s modulus	E = 70 Gpa

$$D \propto \frac{L^4}{E \times t^3}$$

This value for nano-focusing is larger than figure error by Rayleigh’s rule.

(→See next page)

Improvement for nano-focusing

a) Substrate → Si (E 〜 190 GPa)

b) Optimization of supporting points and method

c) Figuring the surface in consideration of the deformation

Errors (3a)

“figure error estimated by Rayleigh’s rule ”

$$\phi = 2hk\sin(\theta) \rightarrow {}^{\pi}\!/_{2} \qquad h_{\lambda/4} = {}^{\lambda}\!/_{8\theta}$$

0.06nm (20keV)	3mrad	2nm
0.08nm (15keV)	3mrad	3nm
1 nm (1keV)	10mrad	12nm

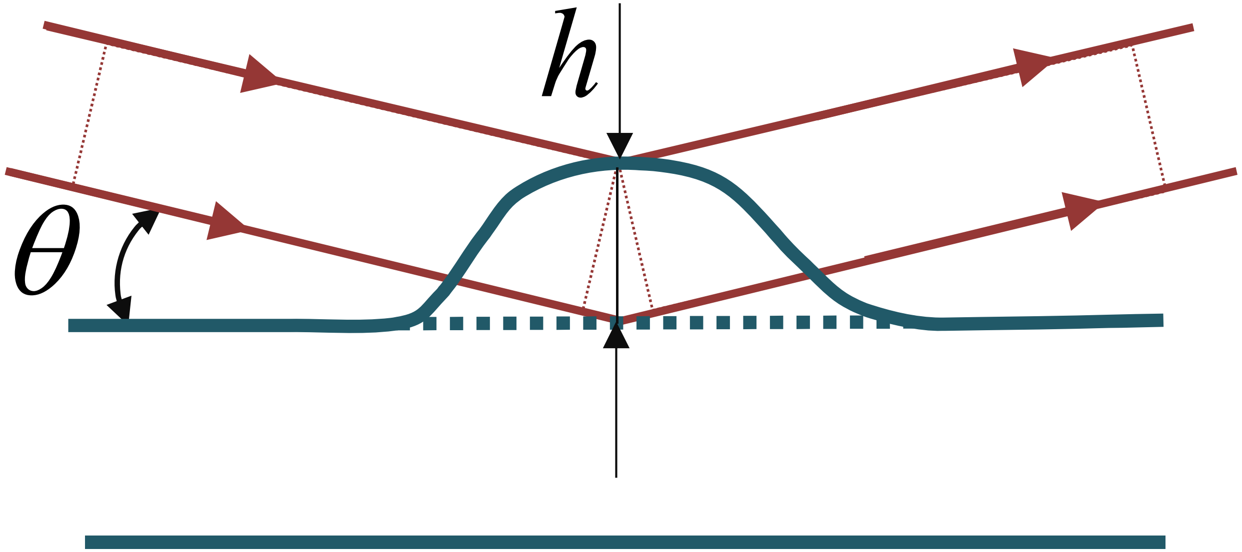

Errors (3b)

“ estimation by wavefront simulation ”

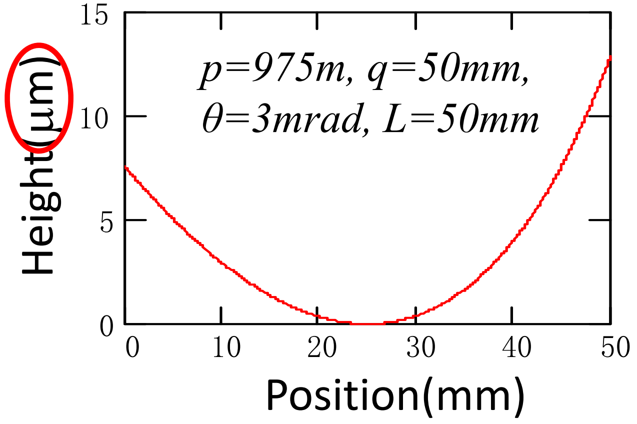

Designed surface

+

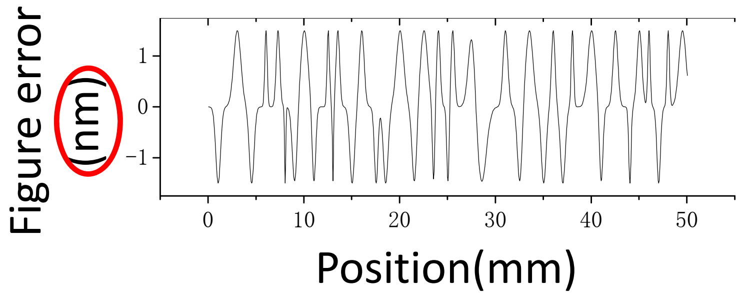

Errors of ***short*** range order

Intensity profiles of focusing beam by wavefront simulation

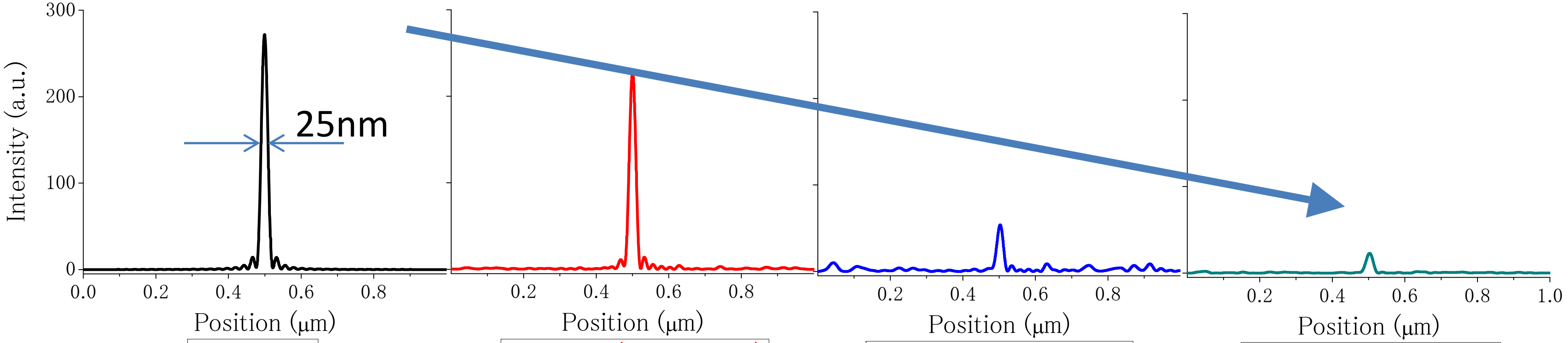

No errors

3nmPV (0.85nmRMS)

9nmPV (2.5nmRMS)

30nmPV (8.5nmRMS)

Errors of ***short*** range order ***decreases intensity***. → Roughness

Errors (3c)

“ estimation by wavefront simulation ”

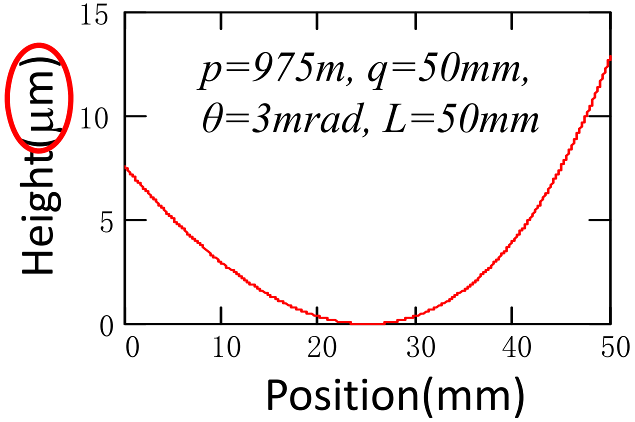

Designed surface

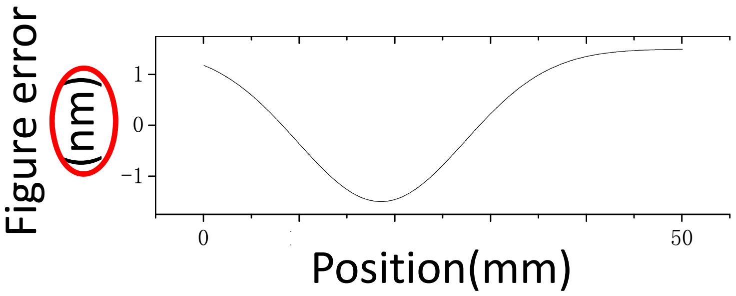

Errors of ***long*** range order

Intensity profiles of focusing beam by wavefront simulation

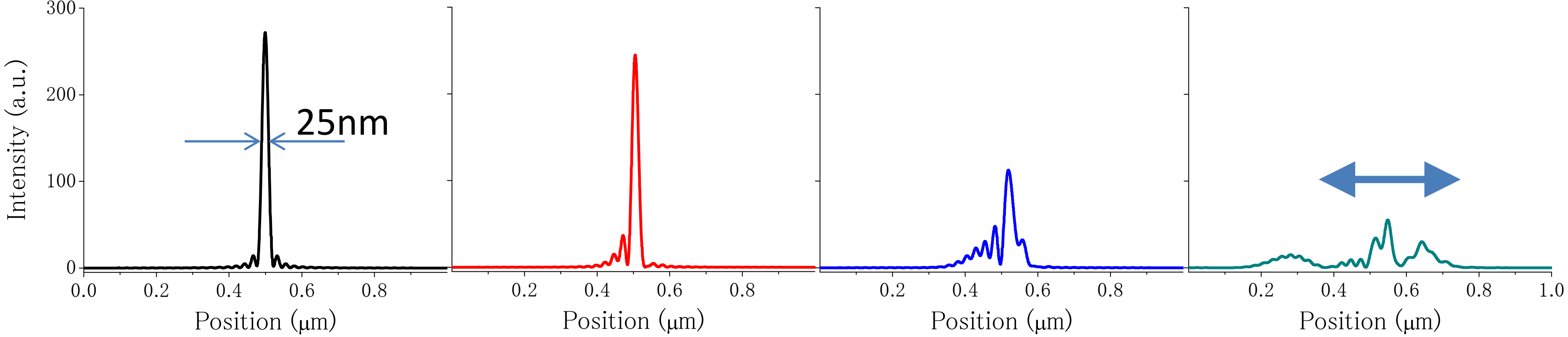

No errors

3nmPV (1.1nmRMS)

9nmPV (3.2nmRMS)

30nmPV (11nmRMS)

Errors of ***long*** range order ***loses shape***. → Figure

“ estimation by wavefront simulation ”

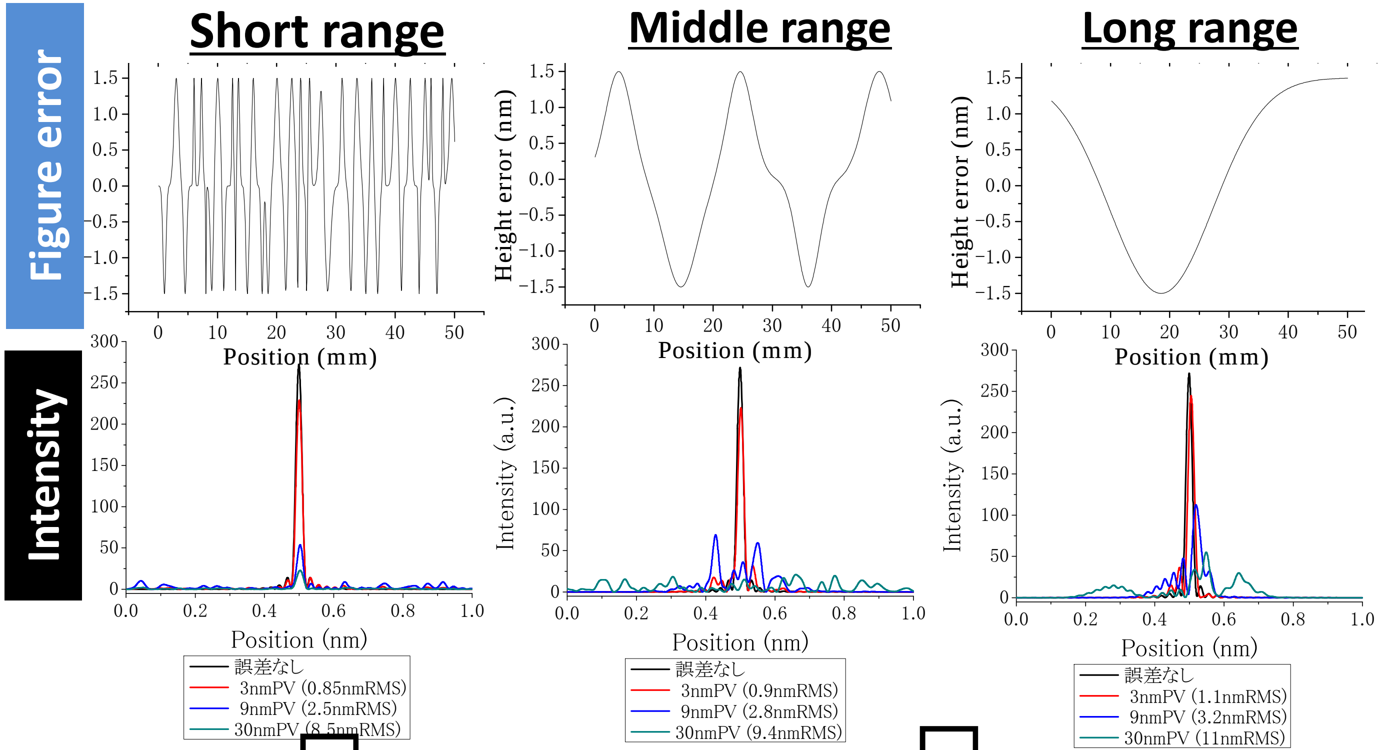

Short range **Middle range** **Long range**

Figure error

Intensity

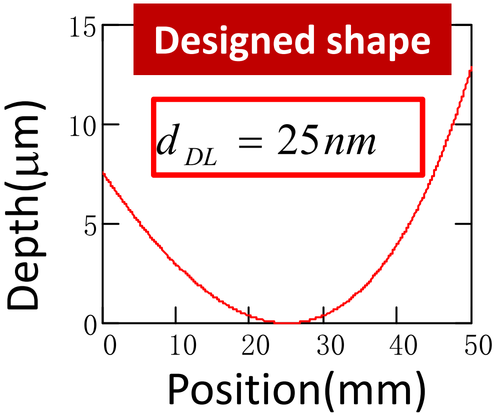

Designed shape

$d_{DL} = 25nm$

Intensity reduced **Shape loses**

If the figure error < 3nmPV ***for all spatial range***,

the estimated focusing size performs 25 nm.

The value corresponds to the result of Rayleigh’s rule.

Performed 25nm

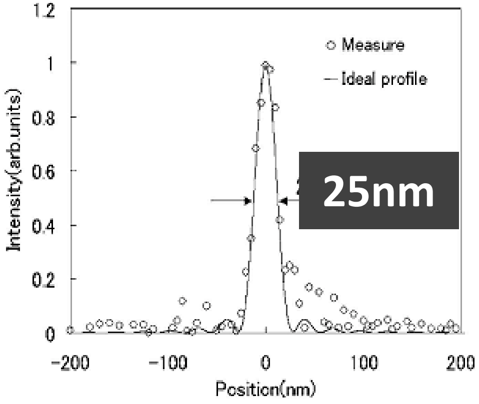

The focusing beam of 25 nm was realized

using high precision mirror with figure error of 3 nm PV

*H. Mimura, H. Yumoto, K. Yamauchi et.al, Appl. Phys. Lett. **90**, 051903 (2007).

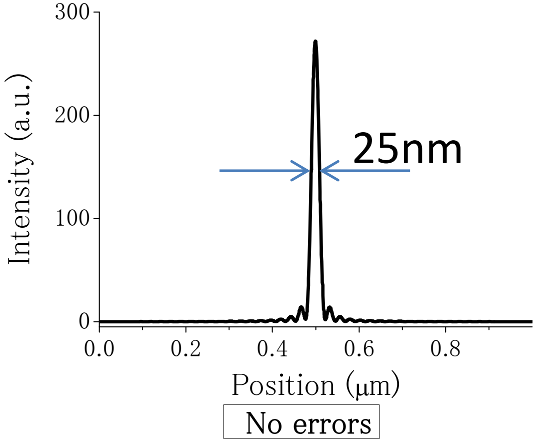

Tailoring x-rays
to application

↓

<u>X-ray mirrors</u>

design, errors, metrology
& alignment

How to evaluate the errors ?

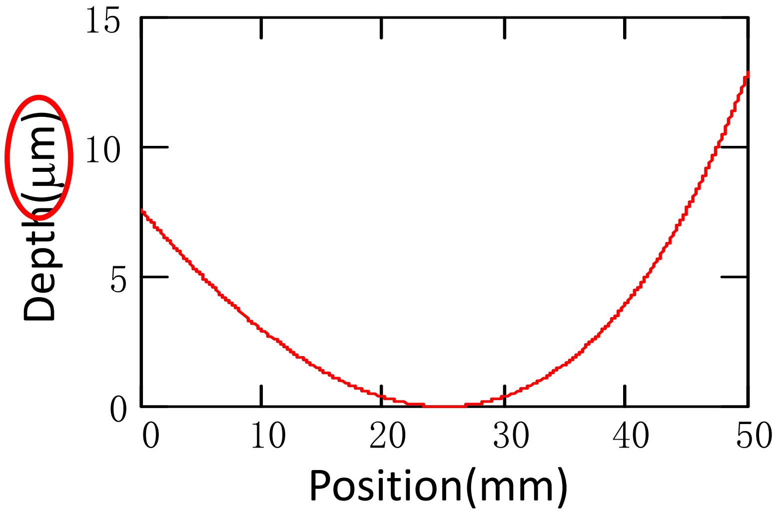

Designed surface

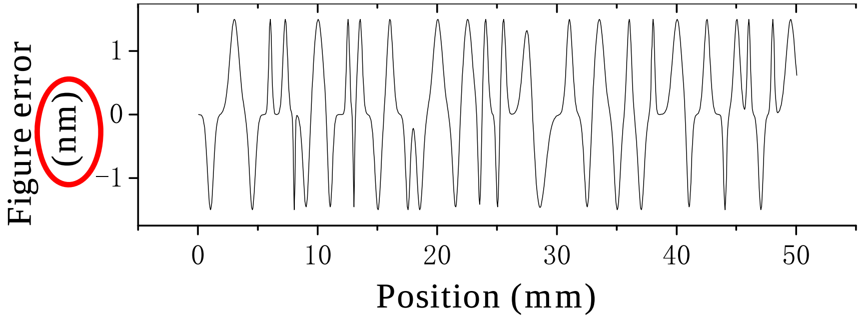

Errors (short range)

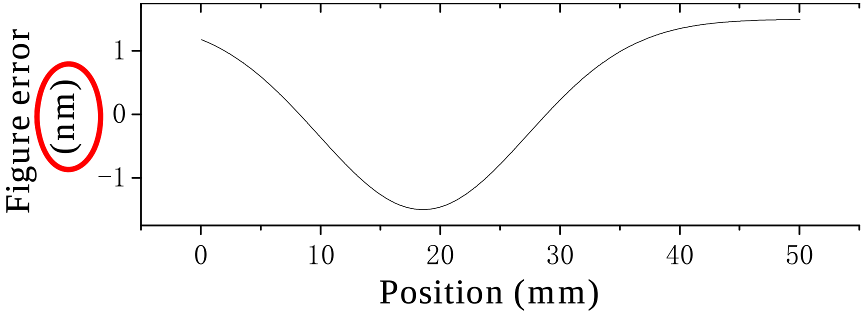

Errors (long range)

Metrology instruments for x-ray optics

Field of view, lateral resolution

Short

～10 µm,

0.1 nm

Roughness

Scanning probe microscope

z (0.1nm)

Short / middle

～10 mm,

1 µm

Roughness, figure

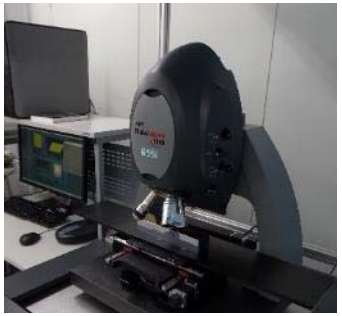

Scanning white light interferometer

z (0.1nm)

Long / middle

～ 0.1 m,

0.1 mm

Figure

Fizeau interferometer

z (0.1nm)

Long / middle

～1m,

1 mm

Slope

Long Trace Profiler (LTP)

slope (0.1µrad)

Vertical resolution (rms)

Scanning white light interferometer

Short range

Interference fringe → **Height**

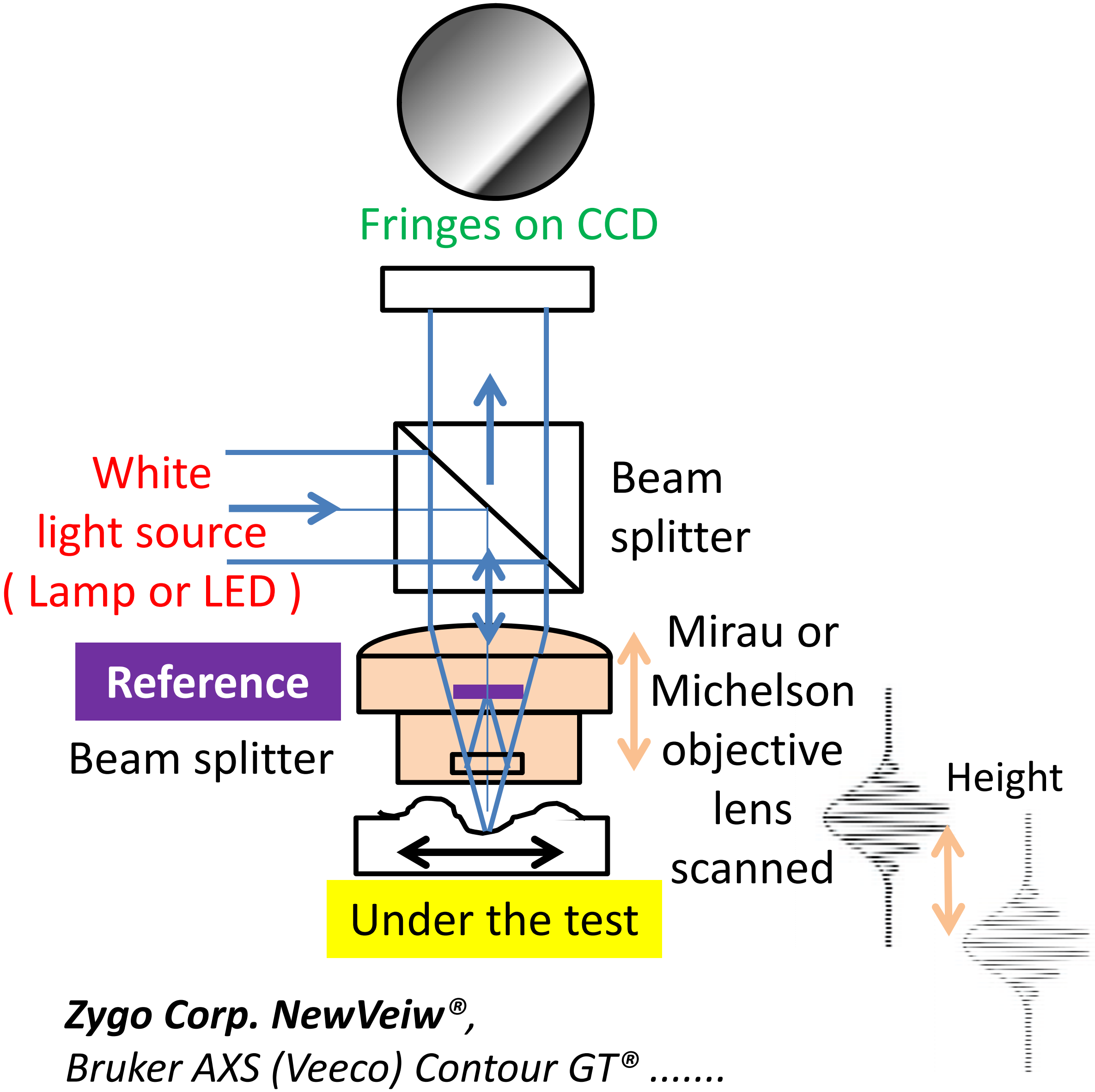

Fringes on CCD

White light source (Lamp or LED)

Beam splitter

Reference

Beam splitter

Mirau or Michelson objective lens scanned

Height

Under the test

Commercially available

FOV (=lens) 50um～10 mm
Lateral resolution 1 µm～
Vertical resolution 0.1 nm

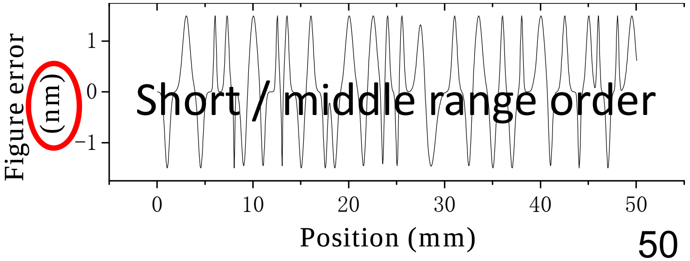

Short / middle range order

Zygo Corp. NewVeiw®,
Bruker AXS (Veeco) Contour GT® …….

Fizeau interferometer

Long / mid range

Interference pattern → **Height**

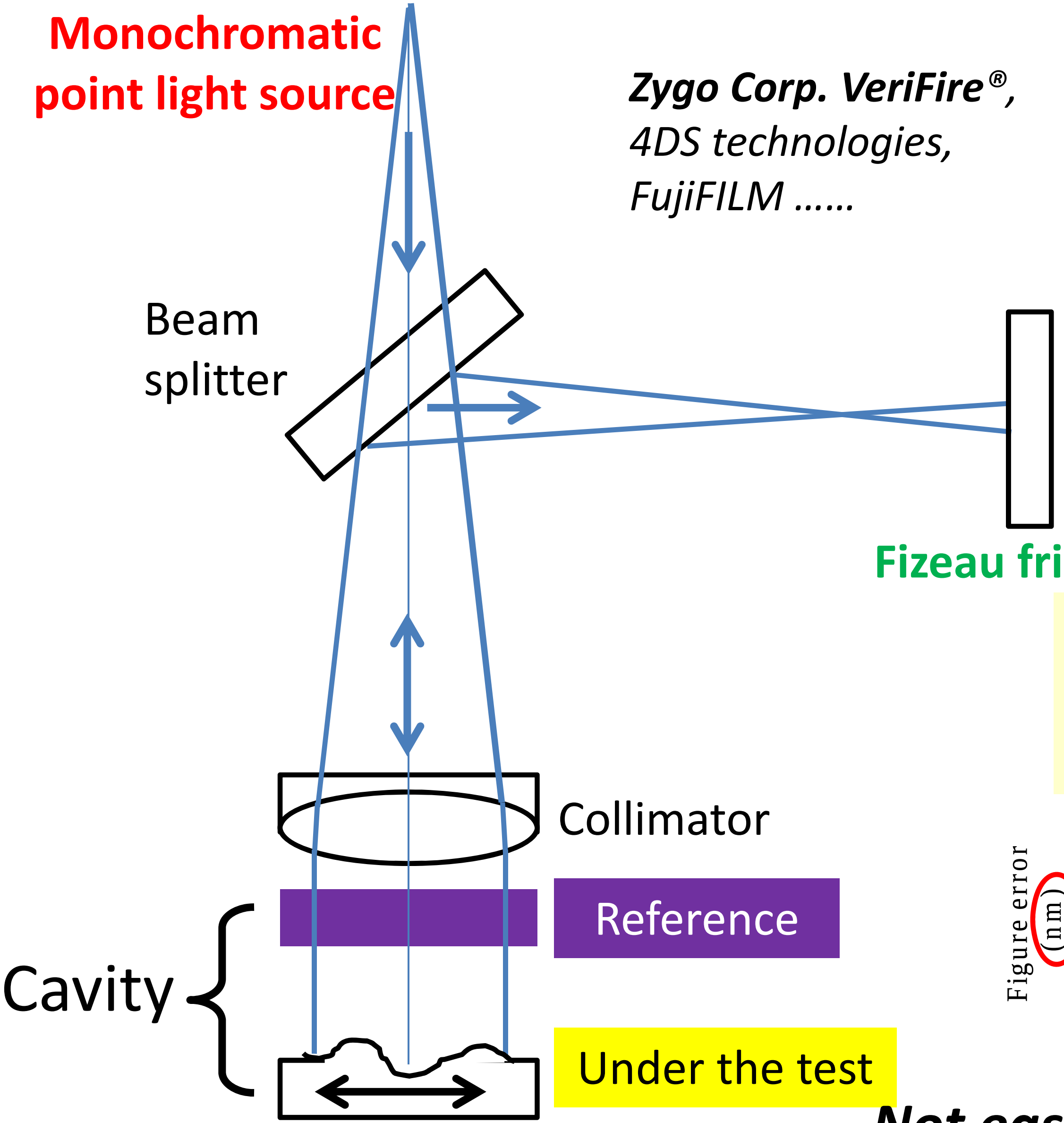

Commercially available

Zygo Corp. VeriFire®,
4DS technologies,
FujiFILM ……

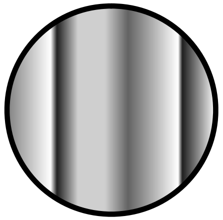

Fizeau fringes on CCD

FOV (=reference) ∼0.1 m
Lateral resolution ∼0.1 mm
Vertical resolution 0.1 nm

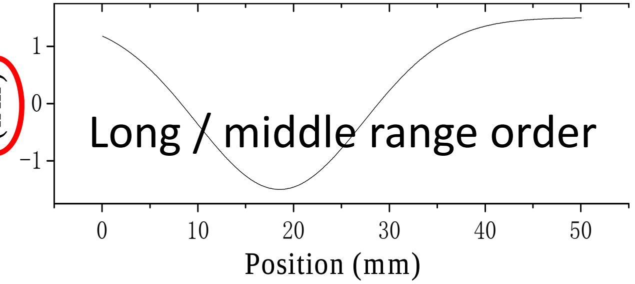

Not easy to measure large mirror

Long trace profiler (LTP)

Long / mid range

Homemade

Direction of laser reflected on the surface → **Slope**

FOV (=stage) ～2 m
Lateral resolution mm～
Vertical resolution 0.1 μrad

Slope

$$Z' = \frac{d}{2F}$$

d μm
F 1m
$Z' <$ sub-μrad

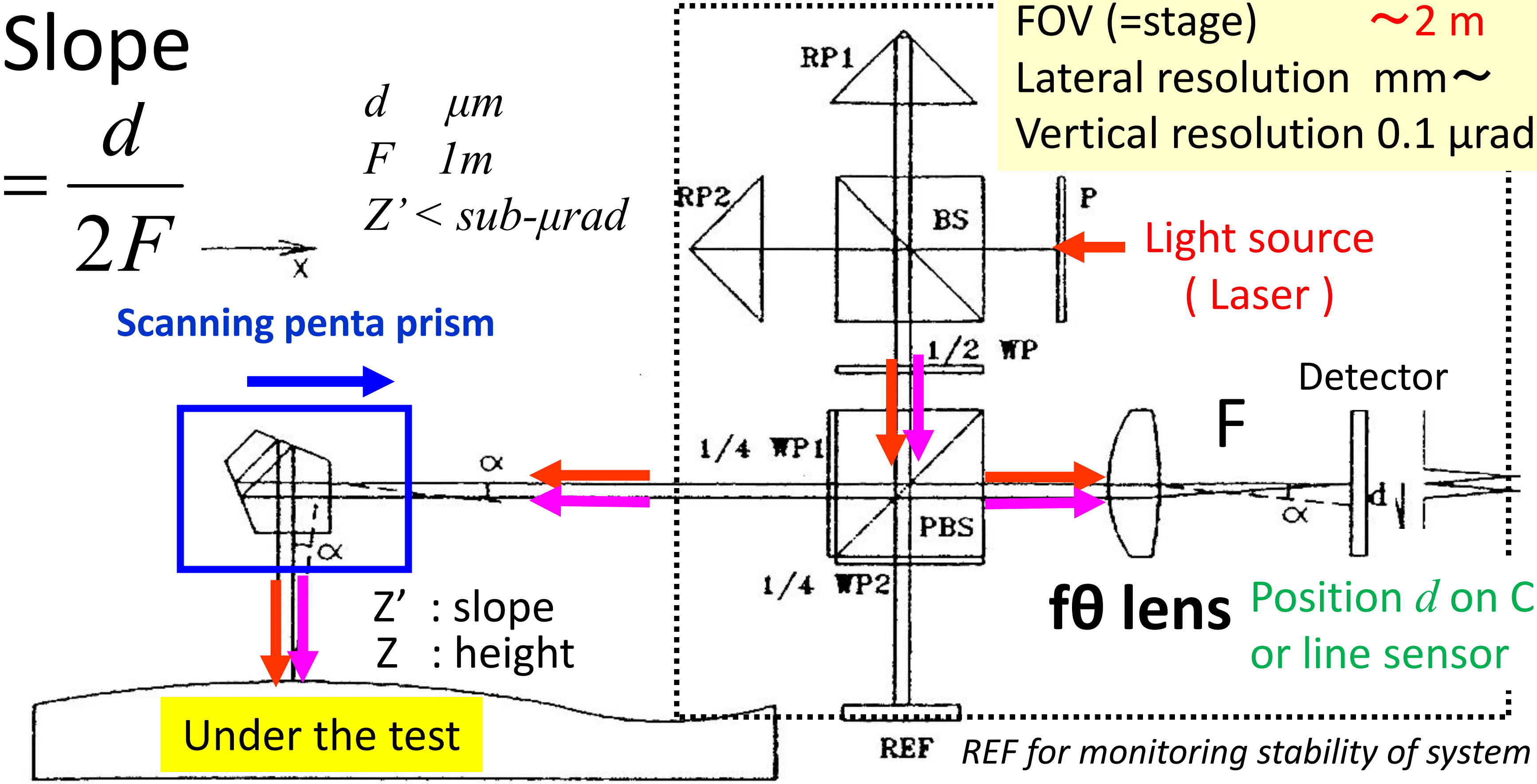

Scanning penta prism

Light source
(Laser)

Detector

F

fθ lens

Position d on CCD
or line sensor

Z' : slope
Z : height

Under the test

REF for monitoring stability of system

Easy to measure slope of sub-μrad on large mirror by NO reference

Many kinds of LTPs are developing among SR facilities.

For example, S. Qian, G. Sostero and P. Z. Takacs, Opt. Eng. **39**, 304-310 (2000).

Long / mid/ short range

Stitching interferometer for large mirror

Homemade

MSI

(micro-stitching interferometer)

RADSI

(relative angle determinable stitching interferometer)

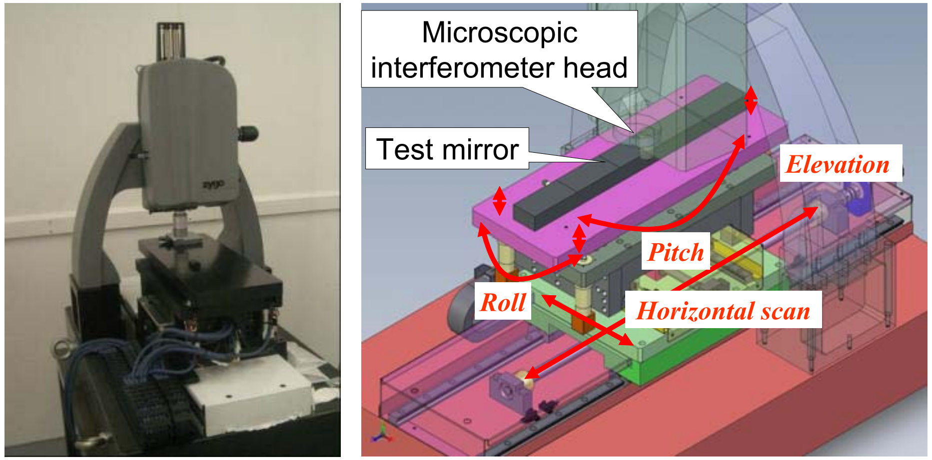

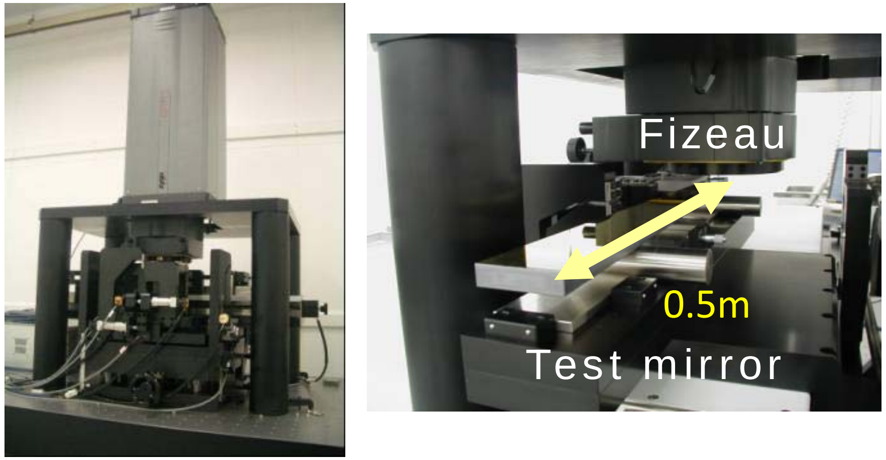

Collaboration with Osaka Univ., JTEC and SPring-8

H. Ohashi et al., Proc. Of SPIE **6704**, 670405-1 (2007).

Height error of wide range order for a long and aspherical mirror with 1μm of lateral and 0.1 nm of vertical resolution.

Necessity is the mother of invention.

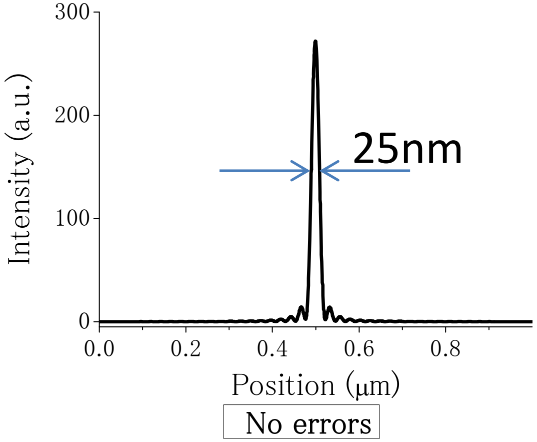

Tailoring x-rays to application

↓

<u>X-ray mirrors</u>

design, errors, metrology & alignment

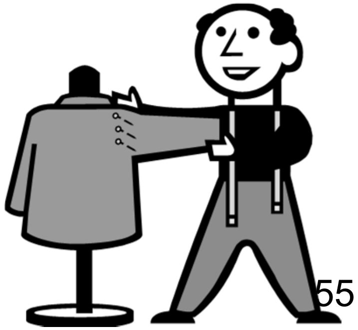

Introduction of KB mirrors

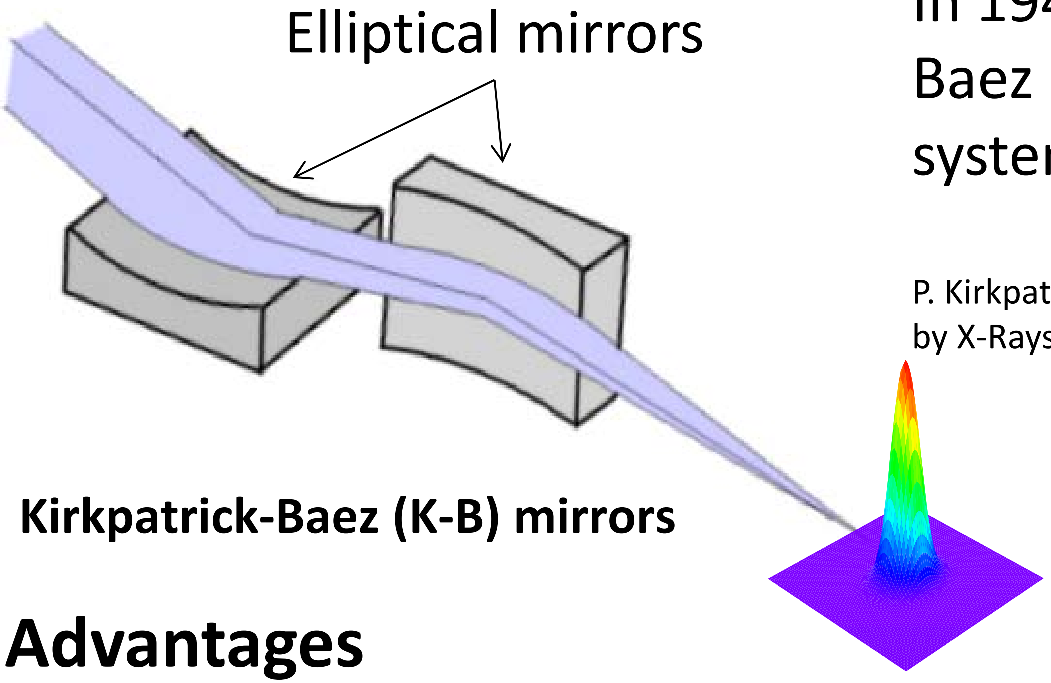

Kirkpatrick-Baez (K-B) mirrors

In 1948, P. Kirkpatrick and A. V. Baez proposed the focusing optical system.

P. Kirkpatrick and A. V. Baez, "Formation of Optical Images by X-Rays", J. Opt. Soc. Am. **38**, 766 (1948).

Advantages

- ●Large acceptable aperture and High efficiency
- ●No chromatic aberration
- ●Long working distance

Suitable for x-ray nano-probe

Disadvantages

- ●<u>Difficulty in mirror alignments</u>
- ●<u>Difficulty in mirror fabrications</u>
- ●Large system

Overview of x-ray focusing devices

Diffraction	focus size, focal length [energy]	energy range	aberration -coma -chromatic -figure error
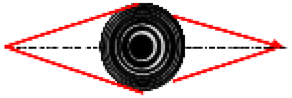 Fresnel Zone Plate	12 nm, f = 0.16 mm [0.7 keV], 30 nm, f = 8 cm [8 keV]	soft x-ray hard x-ray	-coma small -chromatic exist -figure error small
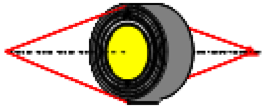 Sputter sliced FZP	0.3 μm, f = 22 cm [12.4 keV], 0.5 μm, f = 90 cm [100 keV]	8-100 keV	-coma small -chromatic exist -figure error large→small
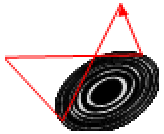 Bragg FZP	2.4 μm, f = 70 cm [13.3 keV]	mainly hard x-ray	-coma small -chromatic exist -figure error small
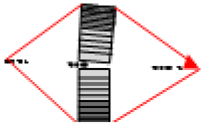 Multilayer Laue Lens	16 nm(1D), f = 2.6 mm [19.5 keV], 25nm × 40nm, f=2.6mm,4.7mm [19.5 keV]	mainly hard x-ray	-coma large -chromatic exist -figure error small

Refraction	focus size, focal length [energy]	energy range	aberration -coma -chromatic -figure error
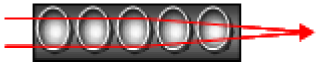 Pressed Lens	1.5 μm, f = 80 cm [18.4 keV], 1.6 μm, f = 1.3 m [15 keV]	mainly hard x-ray	-coma small -chromatic exist -figure error large
 Etching Lens	47nm × 55nm, f = 1cm, 2cm [21 keV]	mainly hard x-ray	-coma small -chromatic exist -figure error small

Reflection

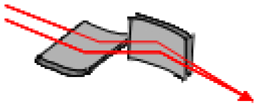 Kirkpatrick-Baez Mirror	7 nm × 8nm, f=7.5cm [20 keV]	soft x-ray hard x-ray	-coma large -chromatic not exist -figure error small
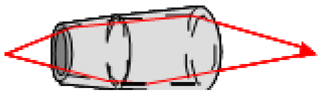 Wolter Mirror	0.7 μm, f = 35 cm [9 keV]	<10 keV	-coma small -chromatic not exist -figure error large
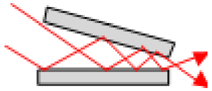 X-ray Waveguide	95 nm, [10 keV]	soft x-ray hard x-ray	-coma large -chromatic not exist -figure error large

How small is x-ray focused ?

For example, by elliptical mirror

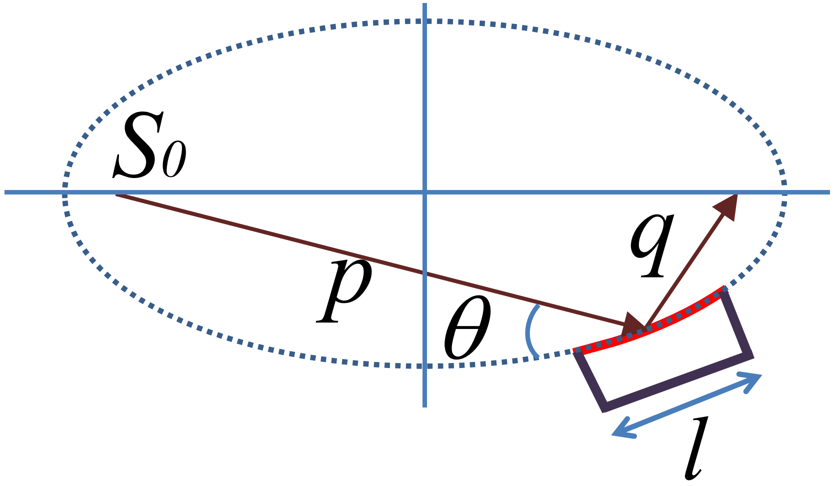

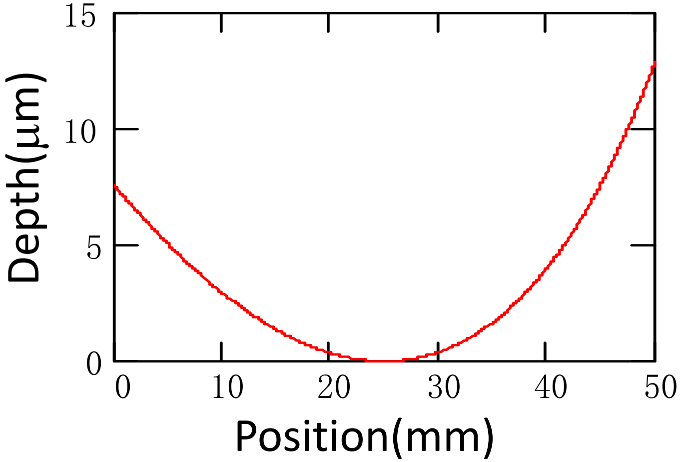

Geometrical size

$$d_G = \frac{q}{p} \times S_0$$

Diffraction limited size(FWHM)

$$d_{DL} = \lambda \times \frac{0.88q}{l\sin(\theta)}$$

$$p = 975\,m, q = 50\,mm, \theta = 3mrad, l = 50\,mm, \lambda = 0.083\,nm, S_0 = 100\,\mu m$$

(15keV)

Mag. = 1 / 19500 !

$$d_G = 5nm < \boxed{d_{DL} = 25nm}$$

The opening of the mirror restricts the focused size even if magnification is large.

Nano-focusing by KB mirror History since the century

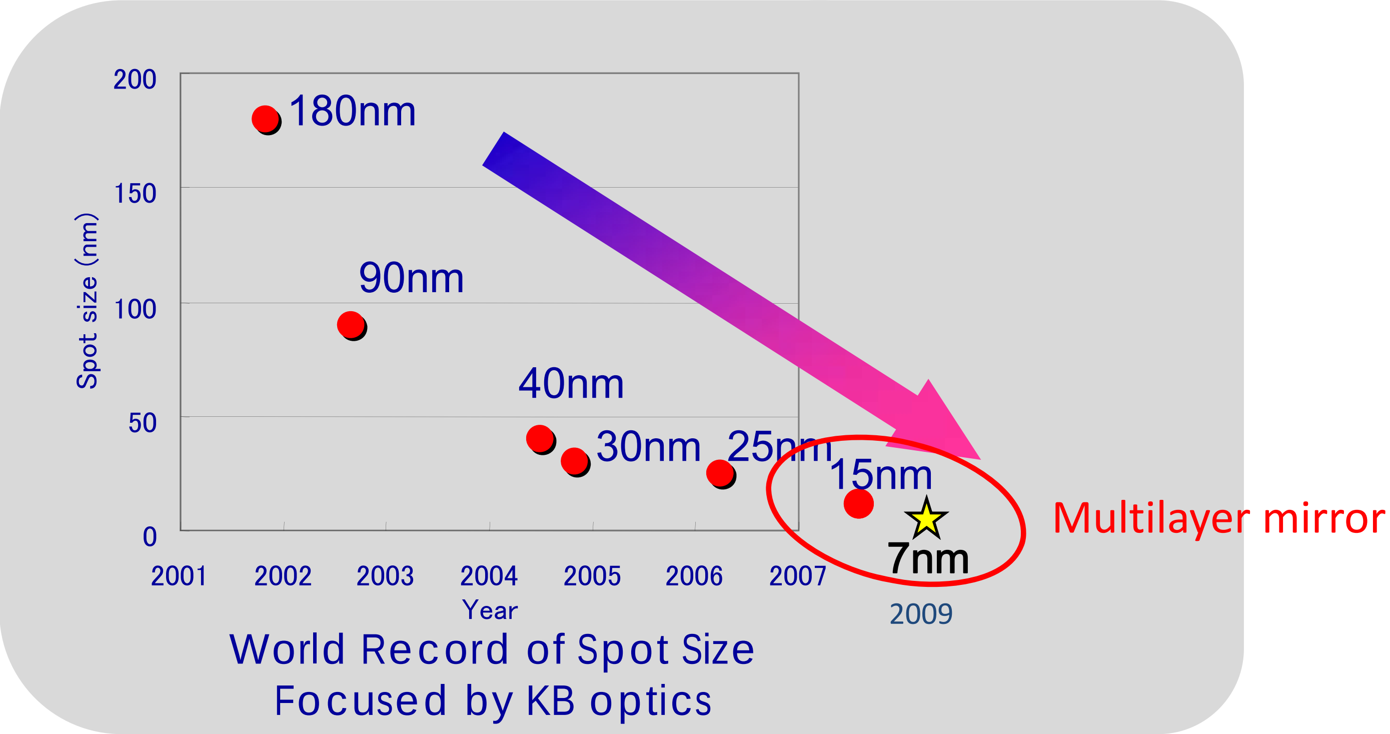

World Record of Spot Size Focused by KB optics

World Record of spot size is **7** nm (by Osaka Univ., in 2009 *).

*Routinely obtained spot size is up to **30** nm.*

Ref * : H. Mimura et al., “Breaking the 10 nm barrier in hard-X-ray focusing”, Nature Physics **6**, 122 (2010).

Difficulty in mirror alignments

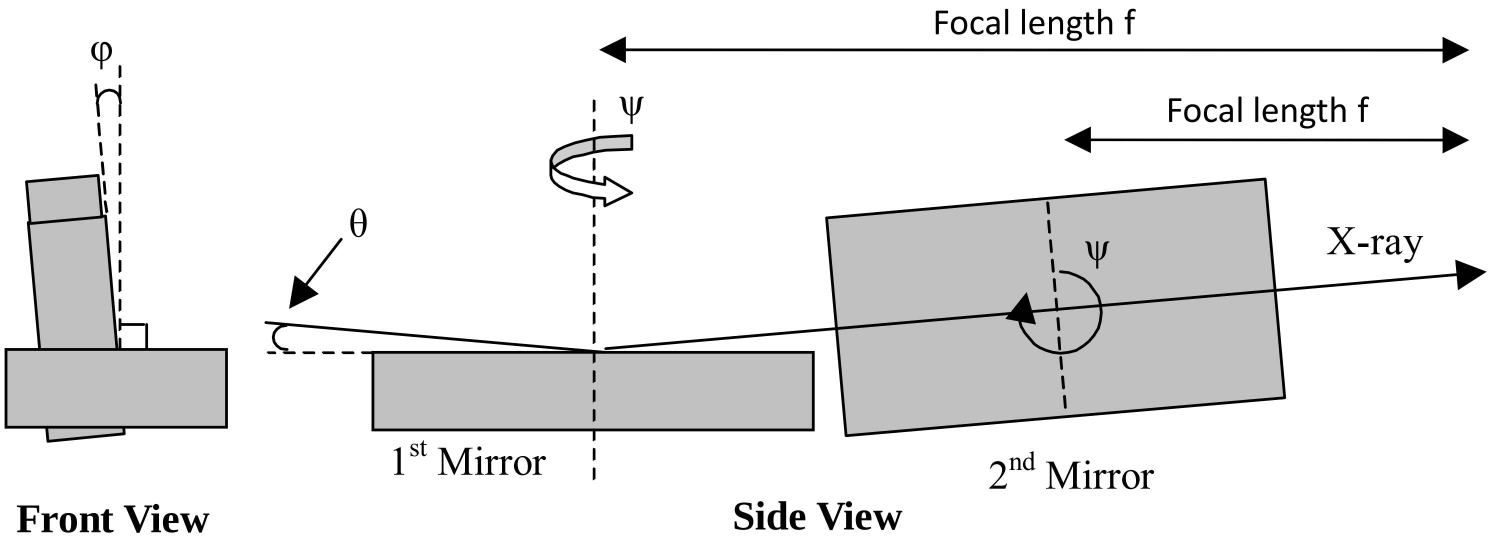

Positioning two mirrors is difficult
because there are at least 7 degree of freedom.

It is difficult to use KB mirrors.

Pitching	θ1, θ2
Yawing	Ψ1, Ψ2
Orthogonality	Φ
Focal length	f1, f2

KB optics installed in BL29XU-L

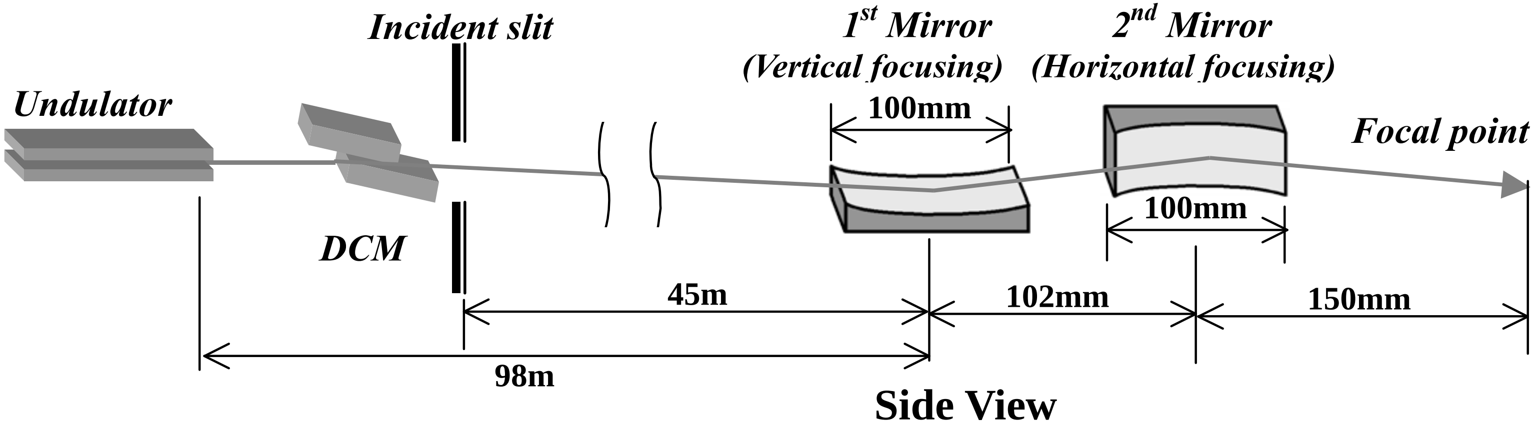

	1st Mirror	2nd Mirror
Glancing angle (mrad)	3.80	3.60
Mirror length (mm)	100	100
Mirror aperture (µm)	382	365
Focal length (mm)	252	150
Demagnification	189	318
Numerical aperture	0.75×10^{-3}	1.20×10^{-3}
Coefficient *a* of elliptic function (mm)	23.876×10^{3}	23.825×10^{3}
Coefficient *b* of elliptic function (mm)	13.147	9.609
Diffraction limited focal size (nm, FWHM)	48	29

Ref :H. Mimura, H. Yumoto, K. Yamauchi et.al, Appl. Phys. Lett. **90**, 051903 (2007).

Tolerance limits of mirror alignments

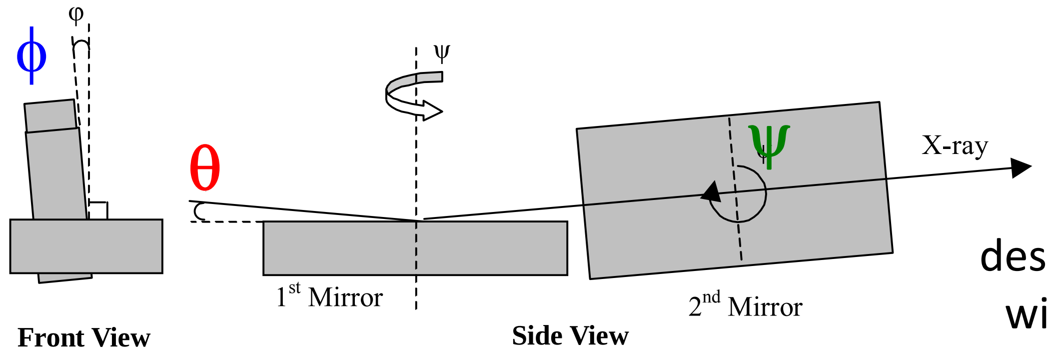

Severe positioning of two mirrors is required.

The manipulator should be designed for these freedom of axis with the resolution & the range.

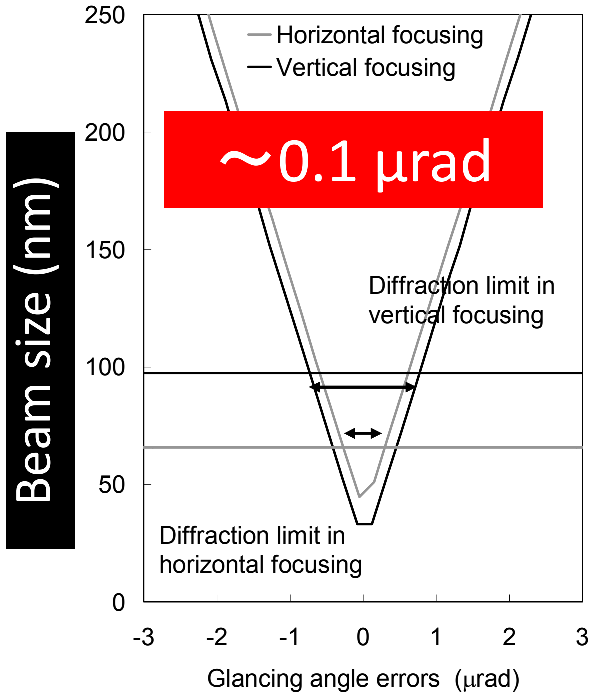

Errors of θ

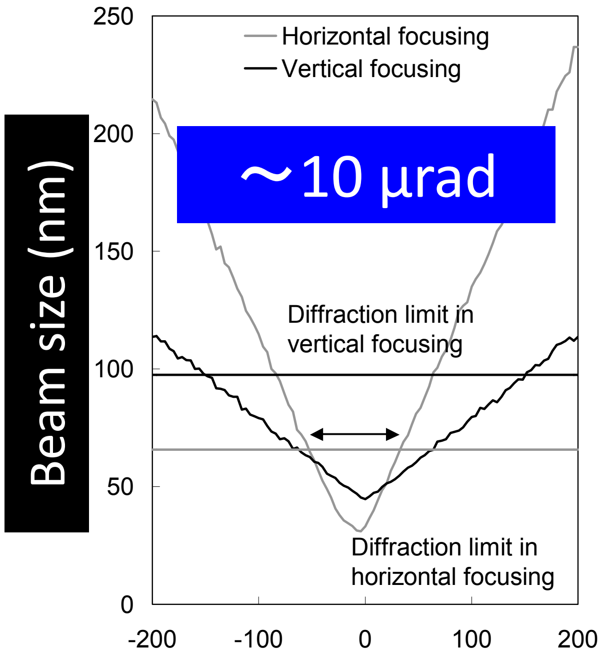

Perpendicularity errors Δϕ (µrad)

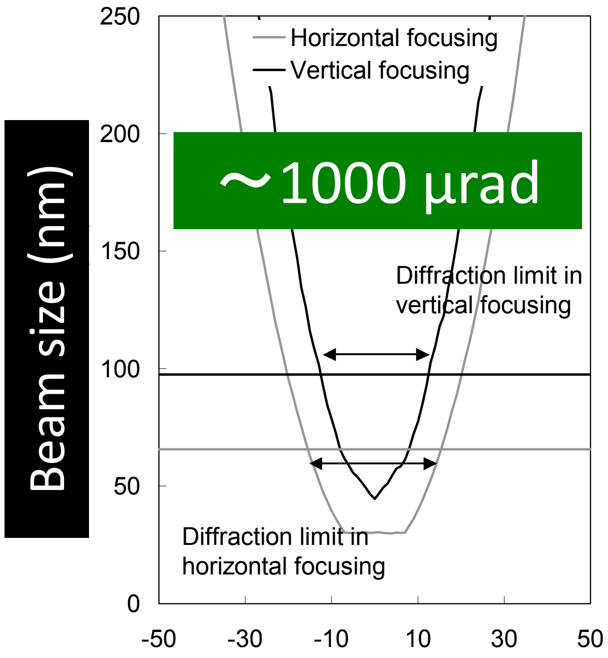

In-plane rotation errors Δψ (mrad)

Freedom of axis, Resolution, range

Ref: S. Matsuyama, H. Mimura, H. Yumoto et al., “Development of mirror manipulator for hard-x-ray nanofocusing at sub-50-nm level”, Rev. Sci. Instrum. **77**, 093107 (2006).

A typical manipulator of KB optics

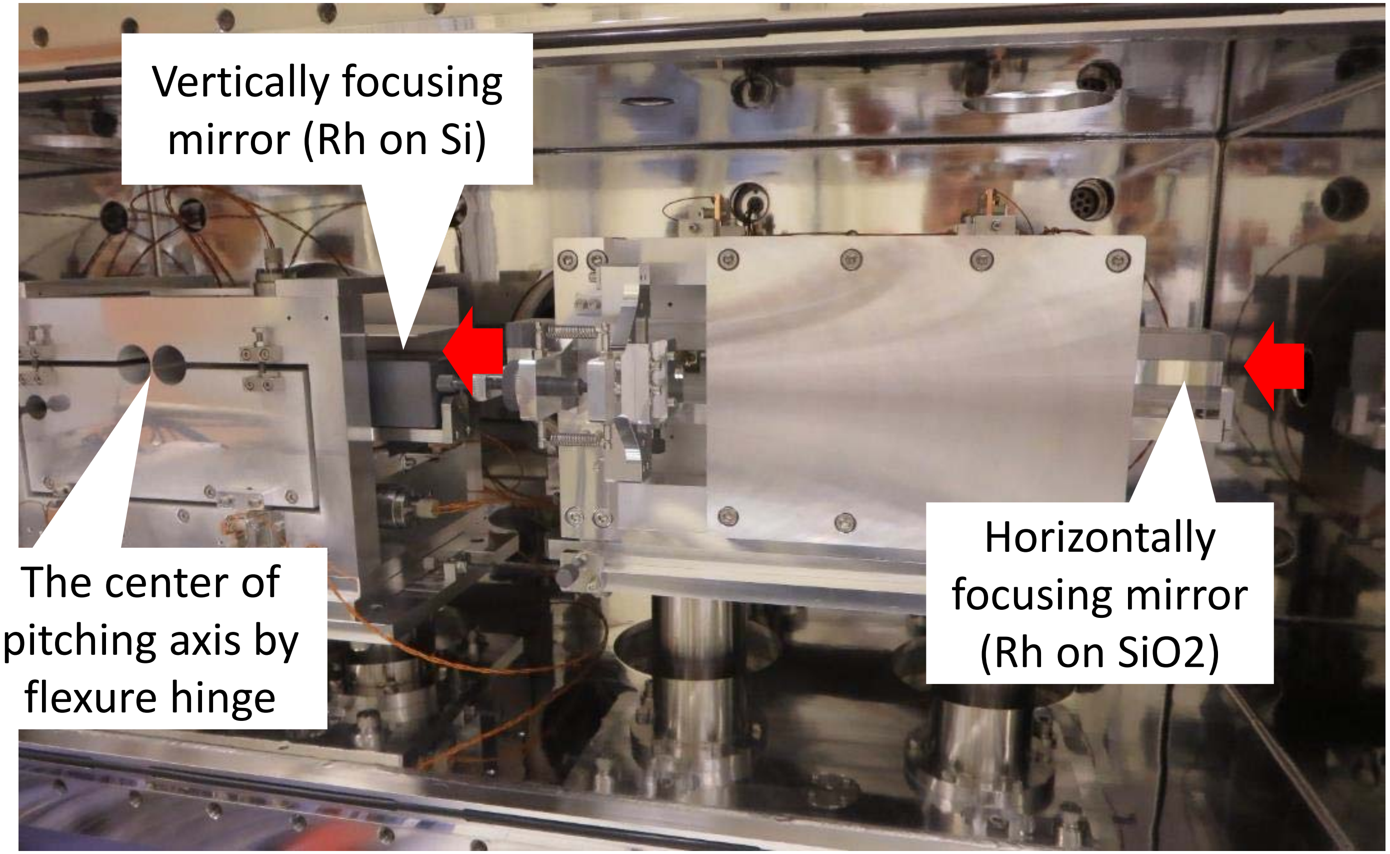

- ✓ Precise manipulation of mirrors
- ✓ Highly stable system
- ✓ Ultra-high vacuum
  (or He environment)

For example,

☐ *Resolution of pitching axis = 0.1 μrad*

→ *Res. of the actuator at 100 mm = 10 nm*

☐ *The focal length = 1 m and beam size = 1 μm*

→ *Angular stability of the mirror* ～ *0.1 μrad*

Alignment

Image on X-ray CCD camera

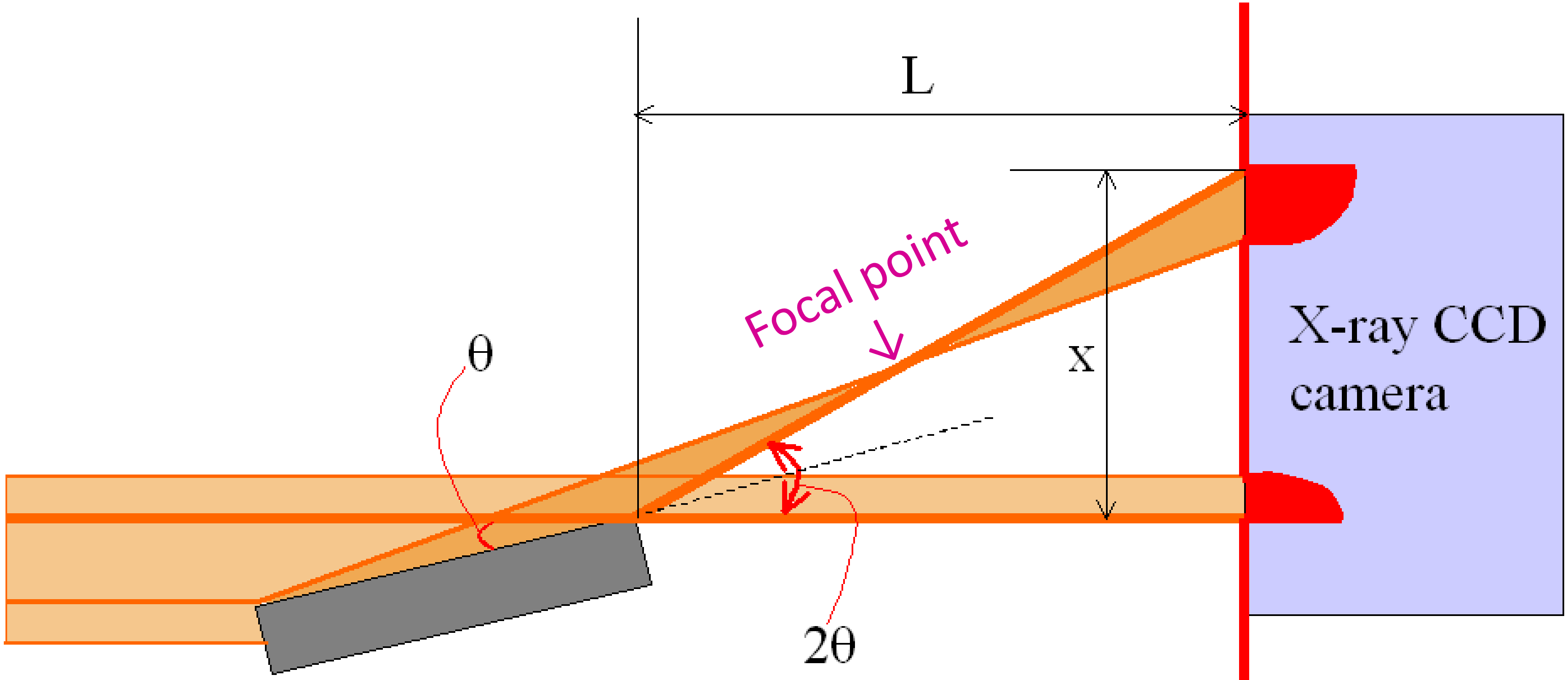

$$L \times 2\theta = x$$

$$\theta = \frac{x}{2L}$$

Alignment

Image of reflected x-ray

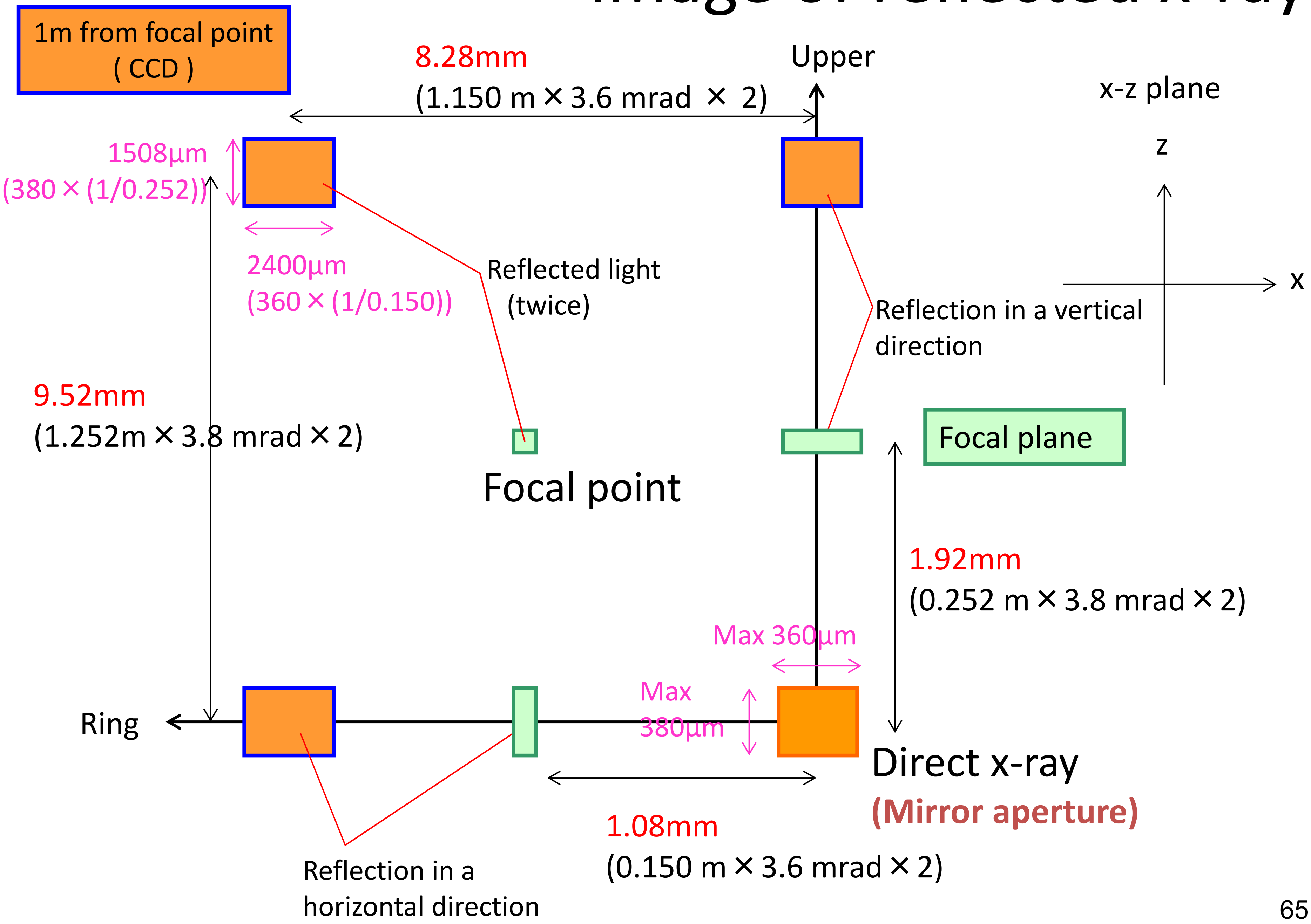
1m from focal point (CCD)

8.28mm

(1.150 m × 3.6 mrad × 2)

Upper

x-z plane

1508μm

(380 × (1/0.252))

2400μm

(360 × (1/0.150))

Reflected light (twice)

Reflection in a vertical direction

9.52mm

(1.252m × 3.8 mrad × 2)

Focal plane

Focal point

1.92mm

(0.252 m × 3.8 mrad × 2)

Max 360μm

Max 380μm

Ring

Direct x-ray

(Mirror aperture)

1.08mm

(0.150 m × 3.6 mrad × 2)

Reflection in a horizontal direction

Alignment

Alignment of in-plane rotation (Horizontal focusing mirror)

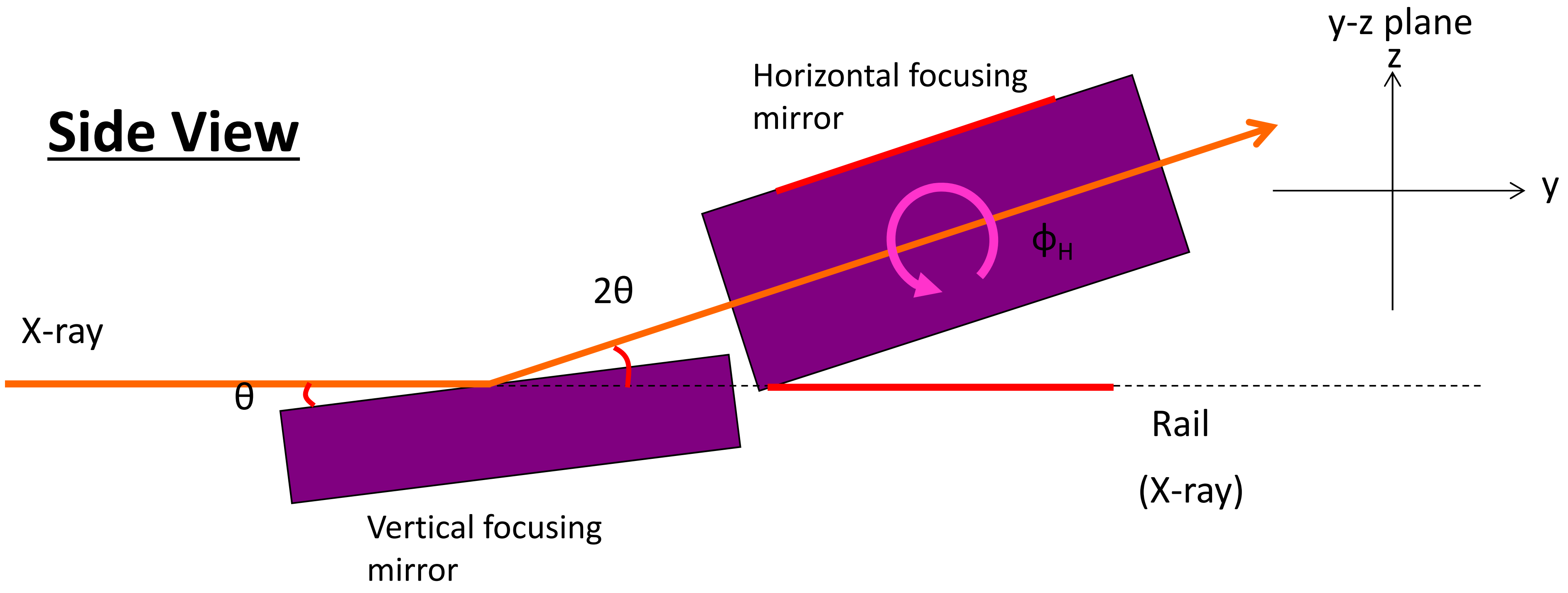

θ: 3.8mrad→ 2θ: 7.6mrad

Reflected angle of vertical-focusing mirror needs to be considered, in the alignment of in-plane rotation of horizontal-focusing mirror.

Alignment of incident angle

- **Foucault test**

  Rough assessment of focusing beam profile.
  This method is used for *seeking focal point*.

- **Wire (Knife-edge) scan method**

  Final assessment of *focusing beam profile*.

Precise adjustment of the glancing angle and focal distance is performed until the best focusing is achieved, while monitoring the intensity profile.

Alignment of incident angle

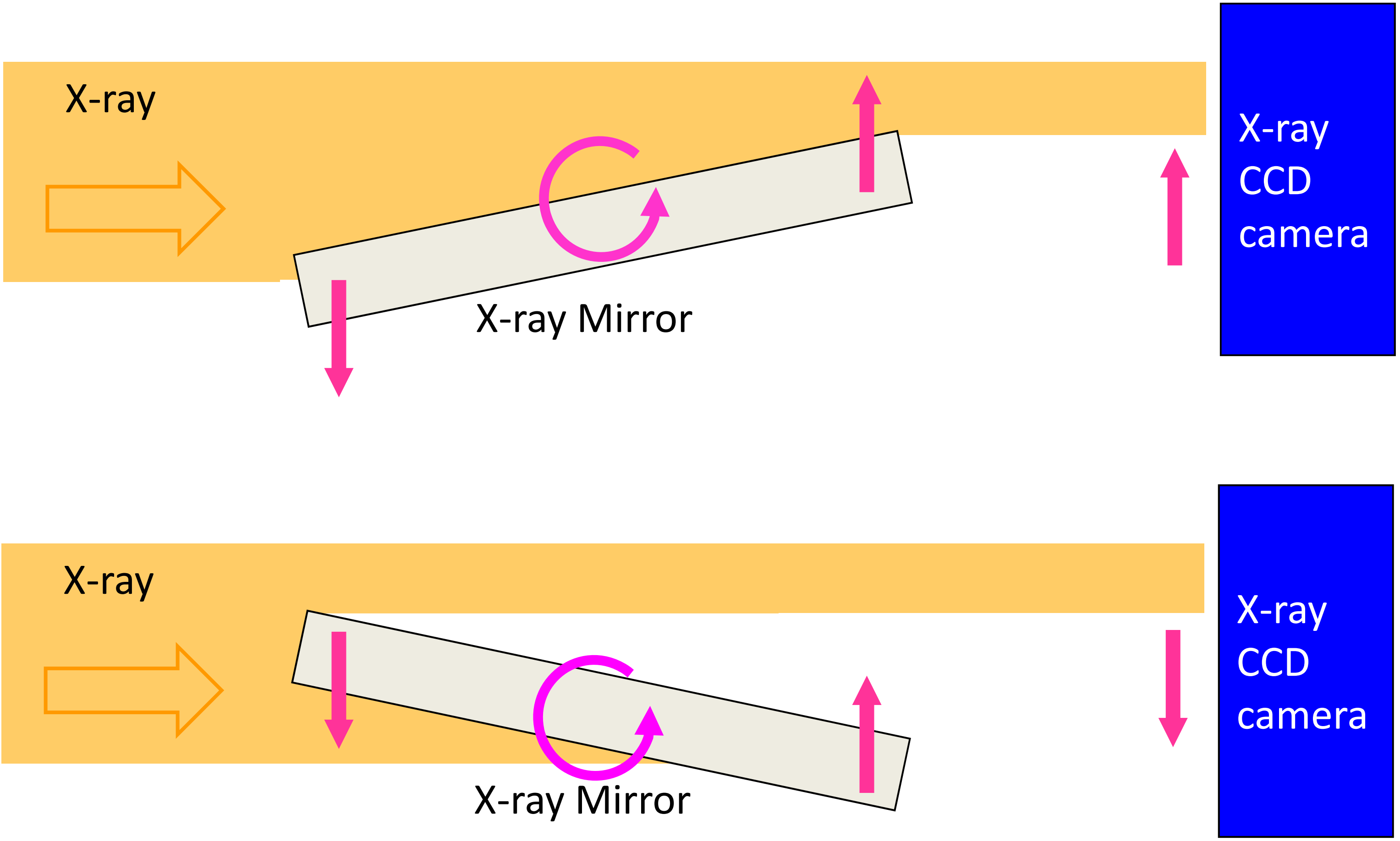

Foucault test

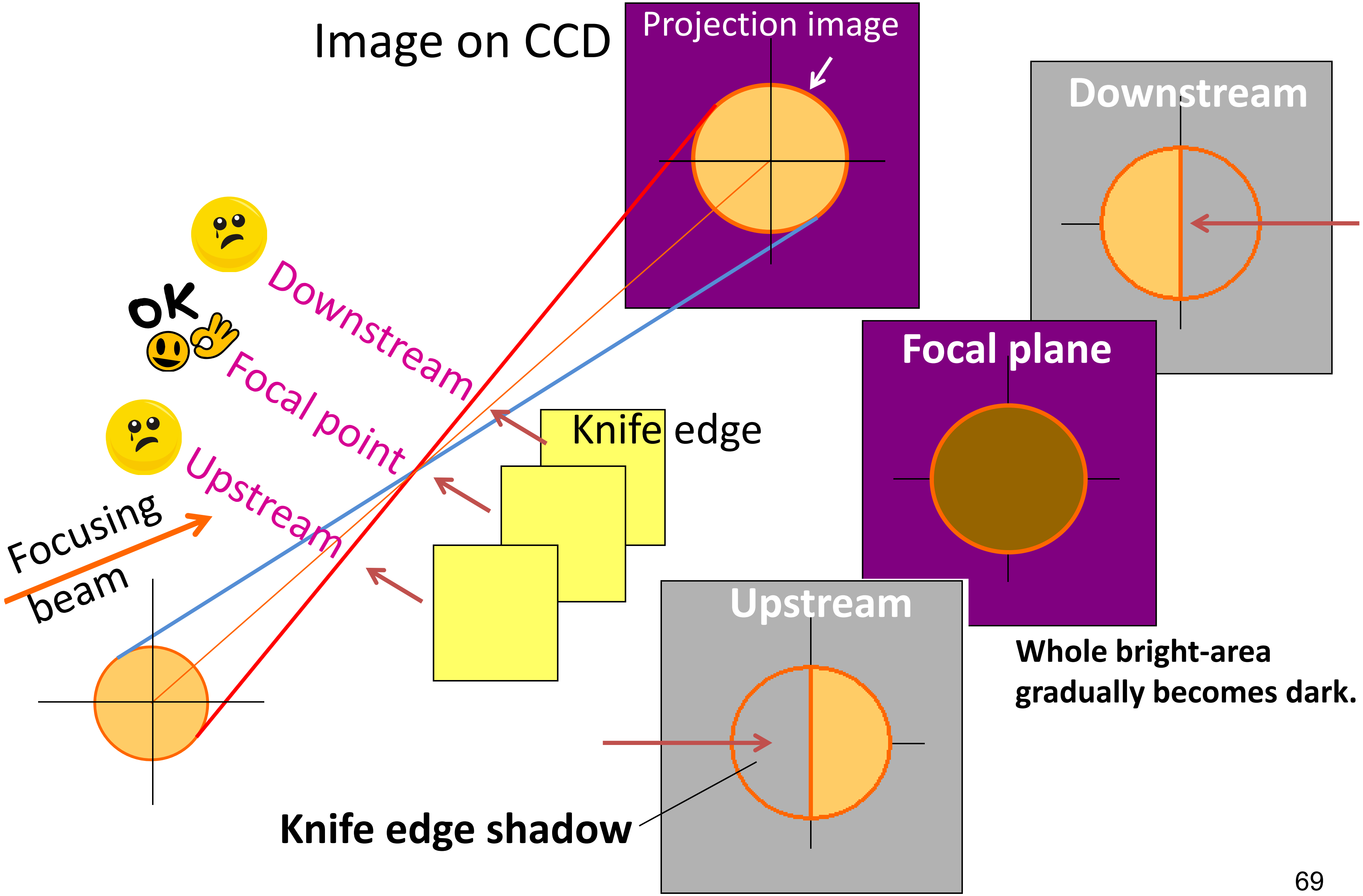

Whole bright-area gradually becomes dark.

Foucault test 1

Alignment

Wire is at downstream of focal point.
Image on CCD become dark from lower side.

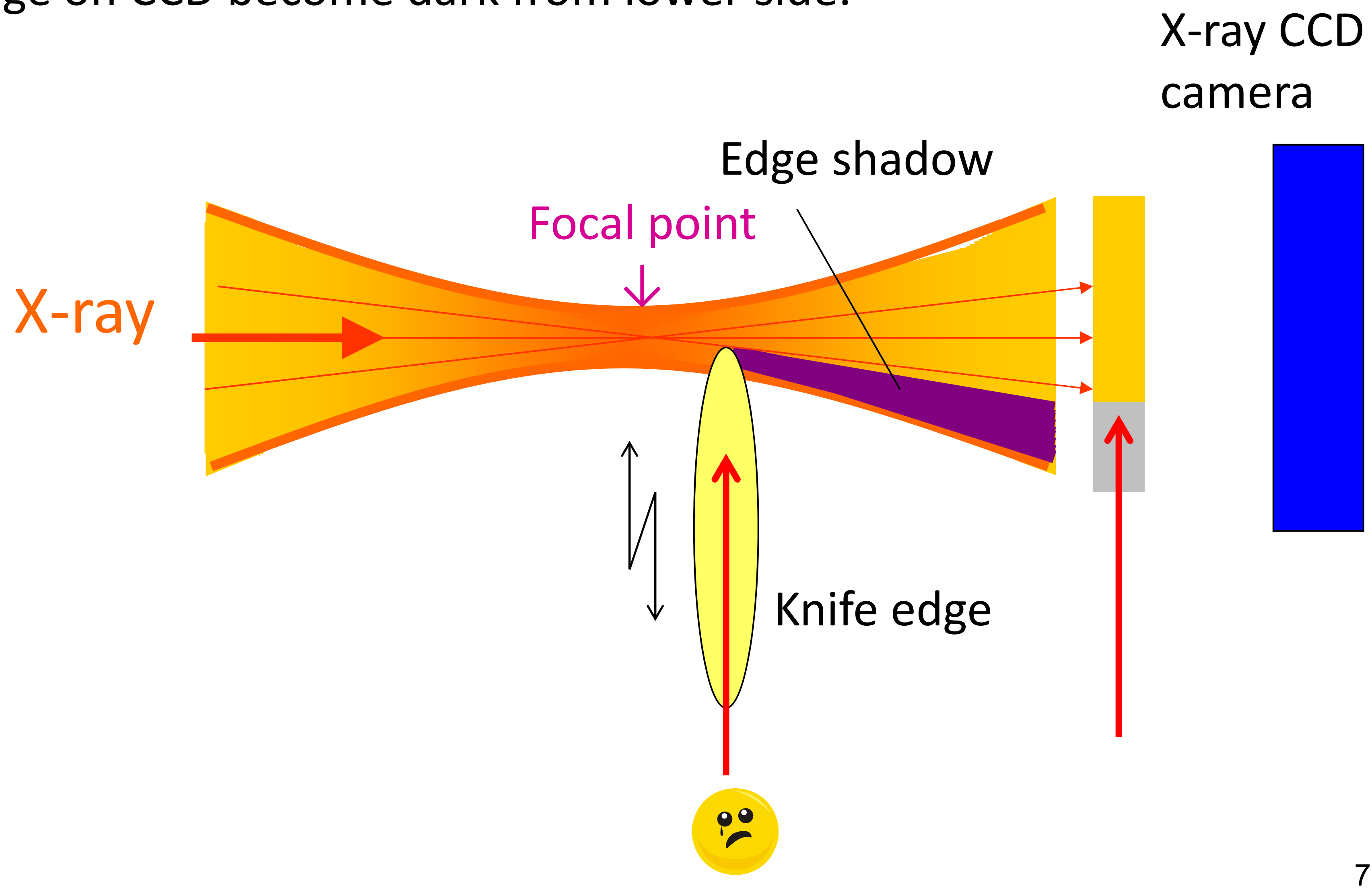

Foucault test 2

Wire is at upstream of focal point.
Image on CCD become dark from upper side.

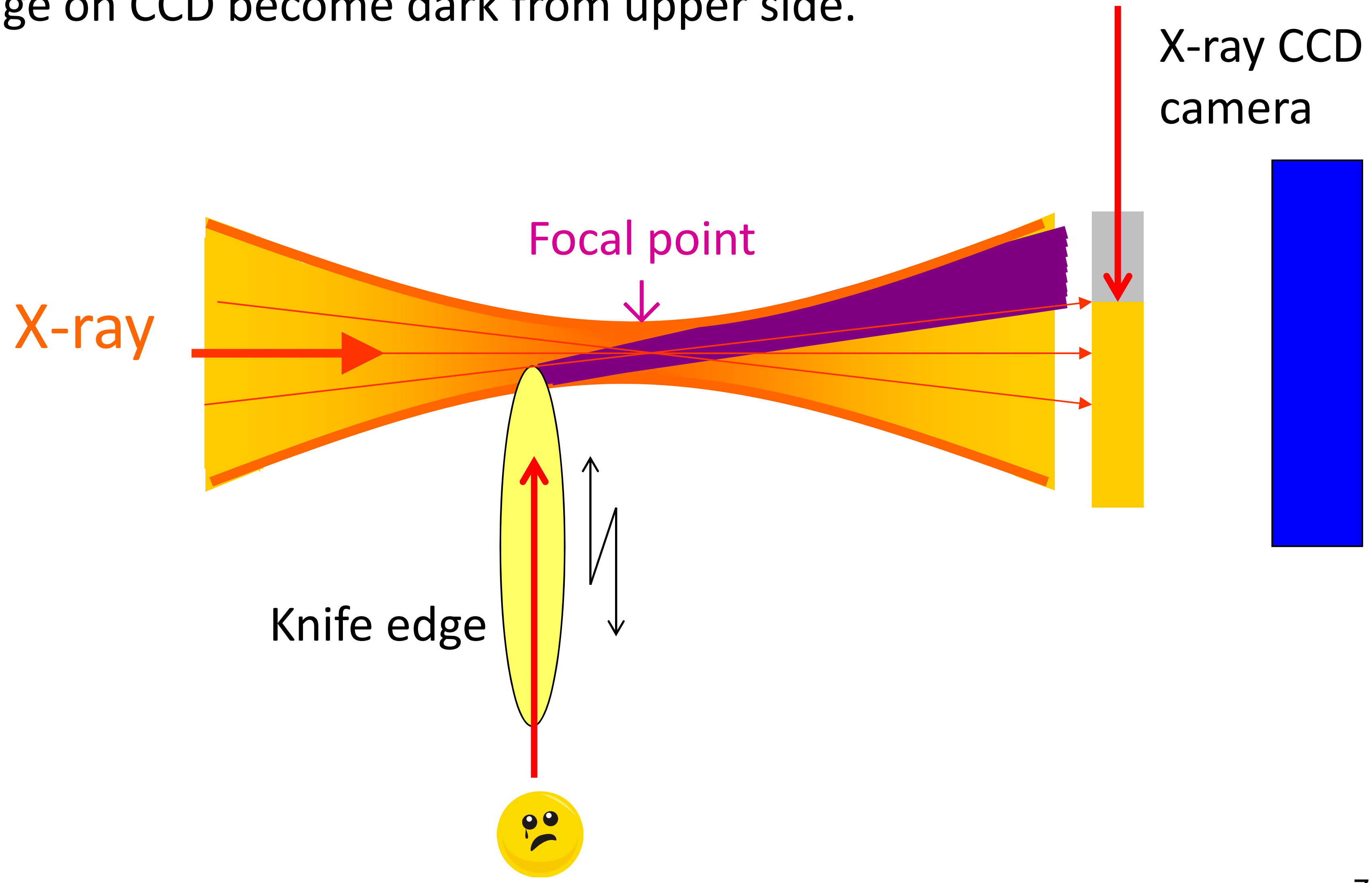

Foucault test 3

Alignment

Wire is at the focal point.
Whole bright-area gradually becomes dark.

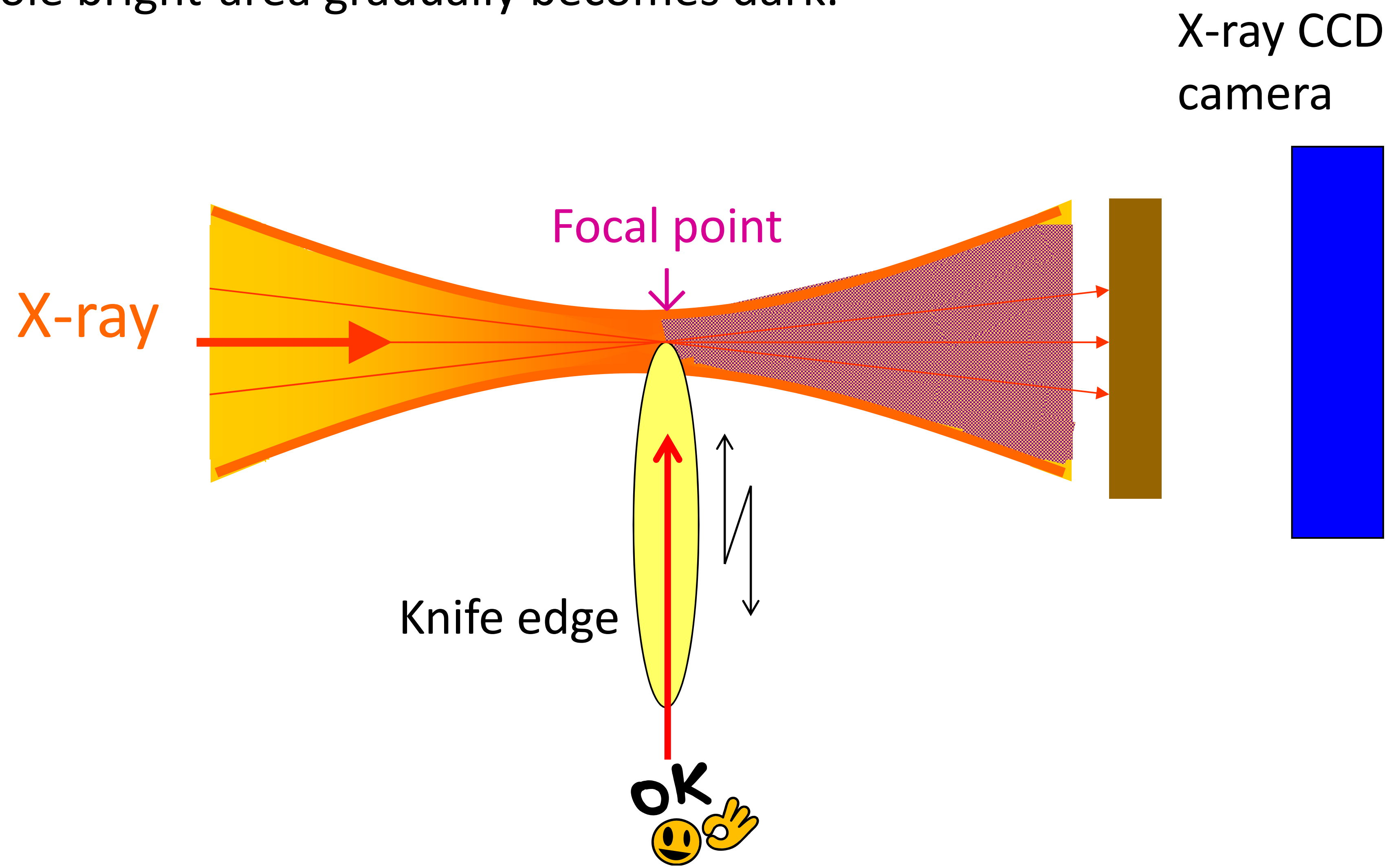

Alignment

Relationship between incident angle and focal position

Tolerance of the incident angle
→ only a few micro-rad

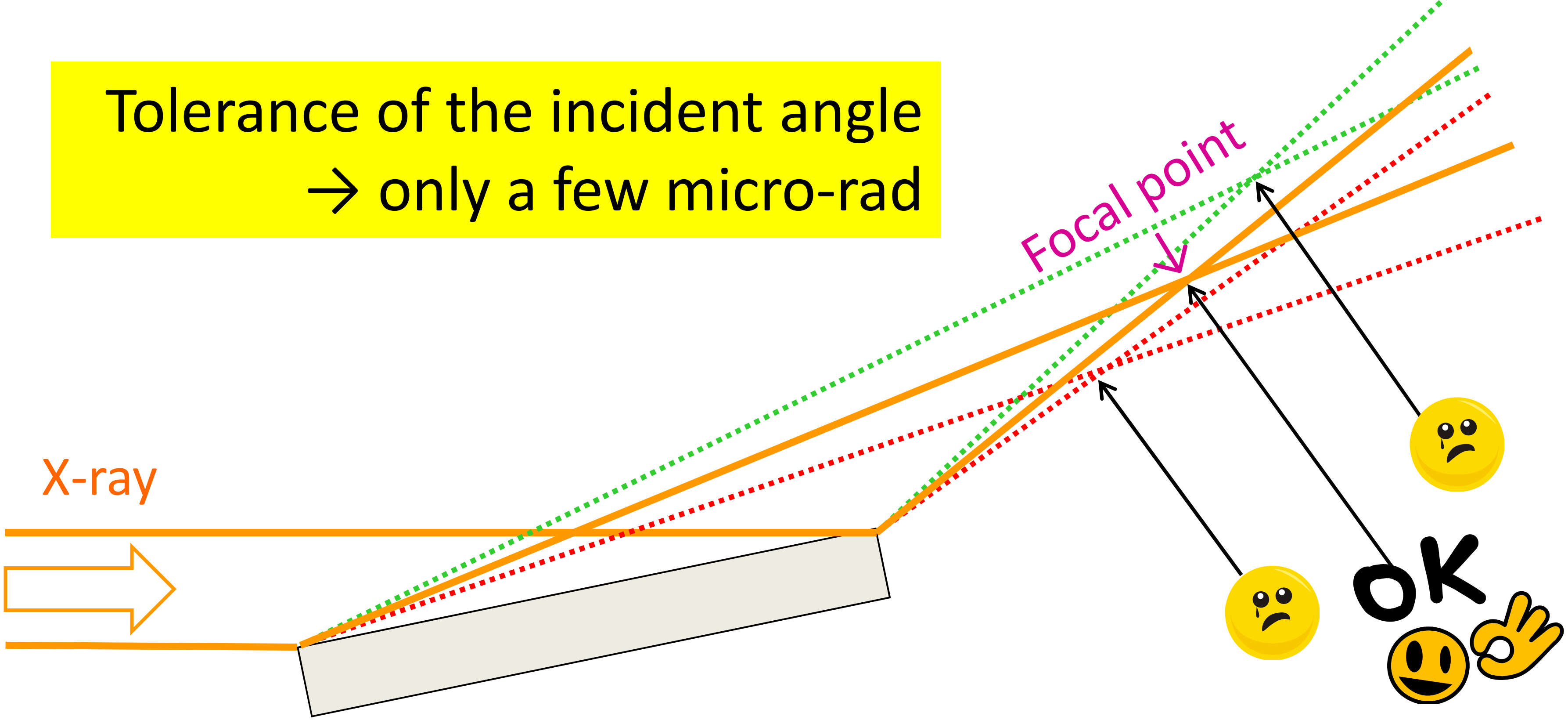

Incident angle→Large ⇒ Focal point → downstream

Incident angle→Small ⇒ Focal point → upstream

Wire (Knife-edge) scan method for measuring beam profiles

The sharp knife edge is scanned across the beam axis, and the total intensity of the transmitting beam is recorded along the edge position.

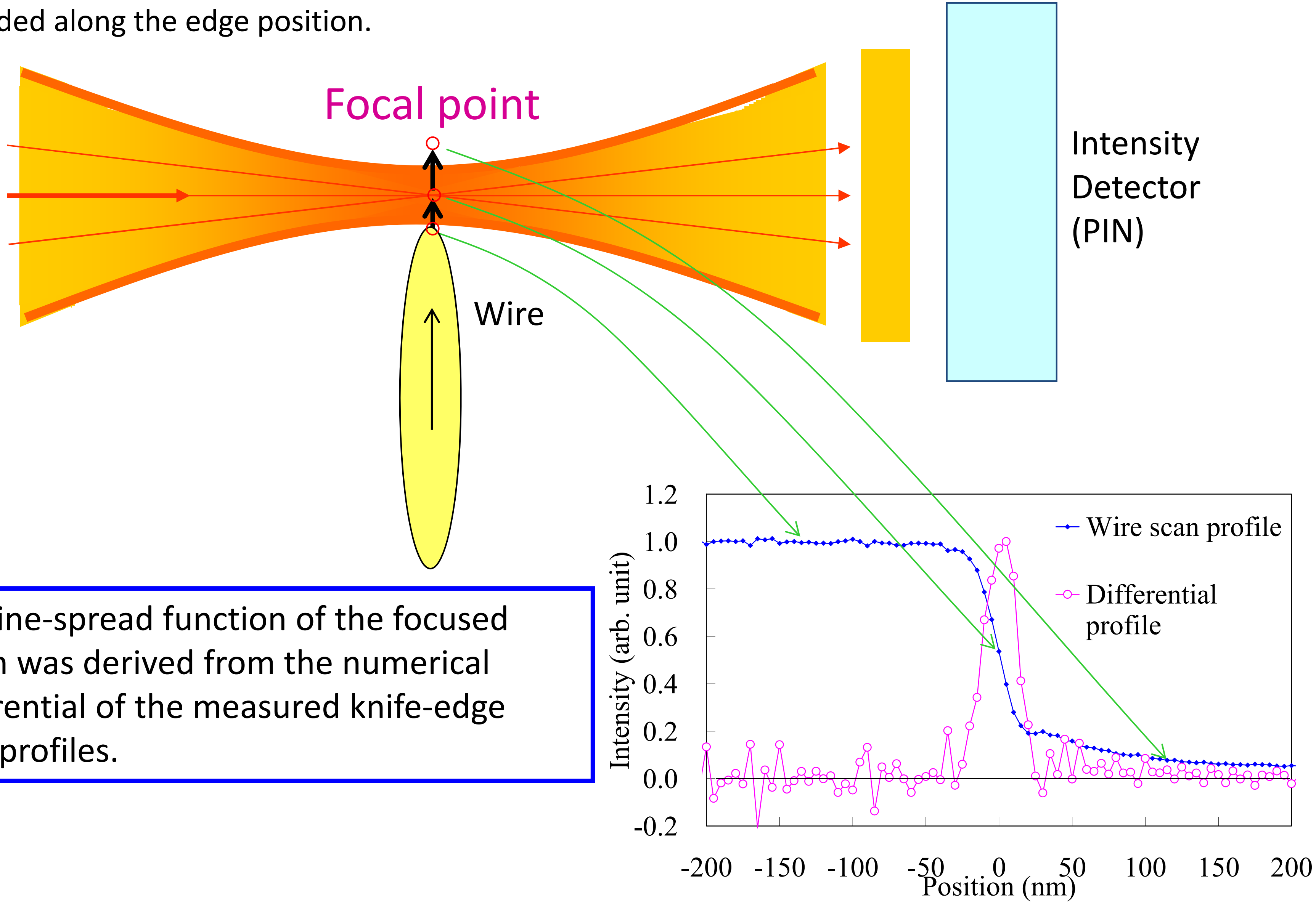

The line-spread function of the focused beam was derived from the numerical differential of the measured knife-edge scan profiles.

Relationship between Beam size and Source size

Beam size changes depending on source size (or virtual source size).

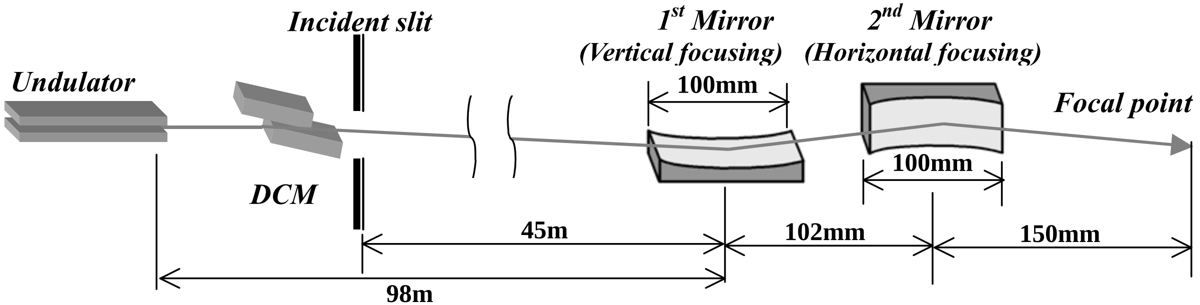

Side View

Beam size = Source size / M (M: demagnification)
AND
Beam size ≥ Diffraction limit

Beam size is selectable for each application.

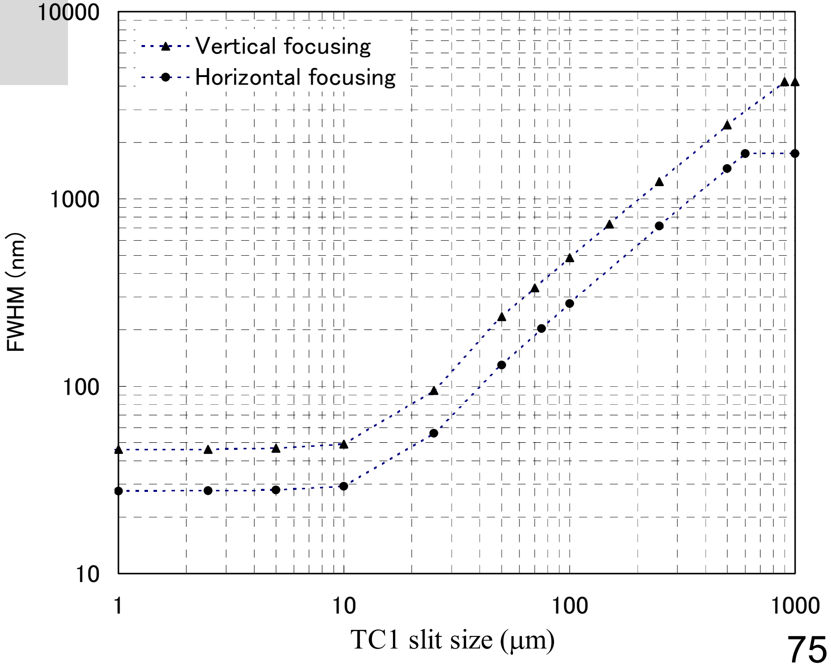

Scanning X-ray Fluorescence Microscope: SXFM

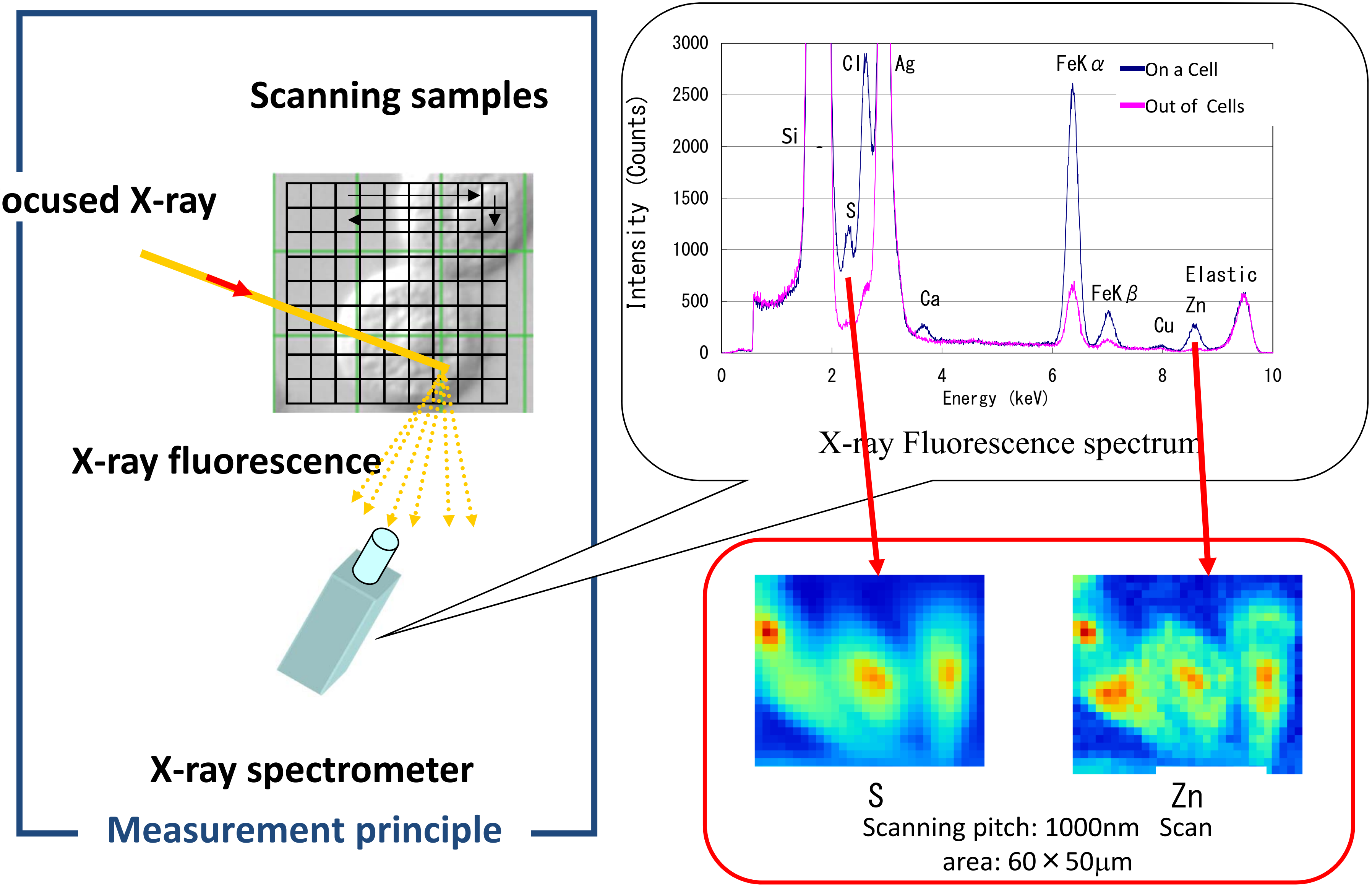

Scanning samples

Focused X-ray

X-ray fluorescence

X-ray spectrometer

Measurement principle

X-ray Fluorescence spectrum

S

Zn

Scanning pitch: 1000nm Scan area: 60×50μm

Ref: M. Shimura et al., “Element array by scanning X-ray fluorescence microscopy after cis-diamminedichloro-platinum(II) treatment”, Cancer research **65**, 4998 (2005).

Key issues of x-ray mirror

1. *To select the functions of x-ray mirror*

   Deflecting, low pass filtering, focusing and collimating → Shape of the mirror

2. *To specify the incident and reflected beam properties*

   Energy range , flux
      → absorption, cut off energy → coating material → incident angle
   The beam size and the power of incident beam
      → opening of the mirror, incident angle
      → absorbed power density on the mirror → w/o cooling, substrate
   Angular divergence / convergence, the reflected beam size
      → incident angle, position of the mirror (source, image to mirror)
   Direction of the beam
      → effect of polarization, self-weight deformation

4. *To specify the tolerance of designed parameters*

   Roughness, density of coating material, radius error, figure error

   The cost (price and lead time) depends entirely on the tolerance.

5. *To consider the alignment*

   The freedom, resolution and range of the manipulator

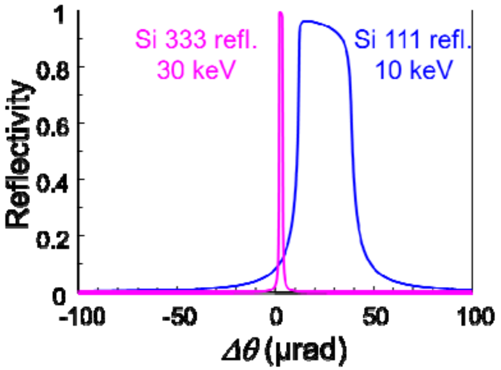

Tailoring x-rays to application

↓

X-ray monochromator

■Principle

- ✓ Introduction of diffraction theory
- ✓ Dynamical theory
- ✓ DuMond diagram

■ Engineering

X-ray Monochromator

X-ray monochromator is key component for SR experiments:

- ✓ length gauge for structure analysis,
- ✓ energy gauge for spectroscopy,...

Principle of x-ray monochromator

- ✓ Photon energy tuning ← Bragg's law
- ✓ Energy resolution ← source divergence, *Darwin width*,..
- ✓ Flux (throughput) ← related to *Darwin width*

➔ Understanding ***the dynamical theory*** for large & perfect crystal

Practical of the monochromator

- ✓ Double-crystal monochromator for fixed-exit
- ✓ Crystal cooling to manage high heat load

➔ ***Mechanical engineering*** issues

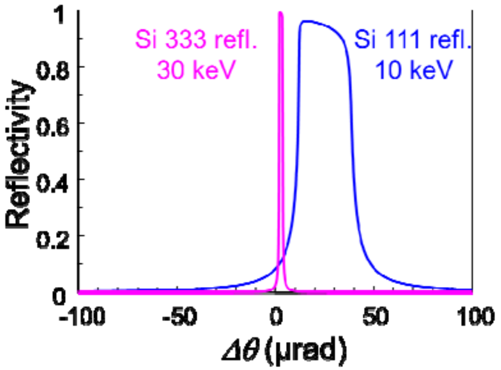

Tailoring x-rays
to application

↓

X-ray monochromator

■ Principle

- ✓ Introduction of diffraction theory
- ✓ Dynamical theory
- ✓ DuMond diagram

■ Engineering

Review

Bragg reflection (*kinematical*)

Bragg's law
in real space

Laue condition
in reciprocal space

$$\boxed{2d\sin\theta = m\lambda}$$

$$\boxed{\mathbf{Q} = \mathbf{h}}$$

Scattering vector $\mathbf{Q}$ = Reciprocal lattice vector $\mathbf{h}$

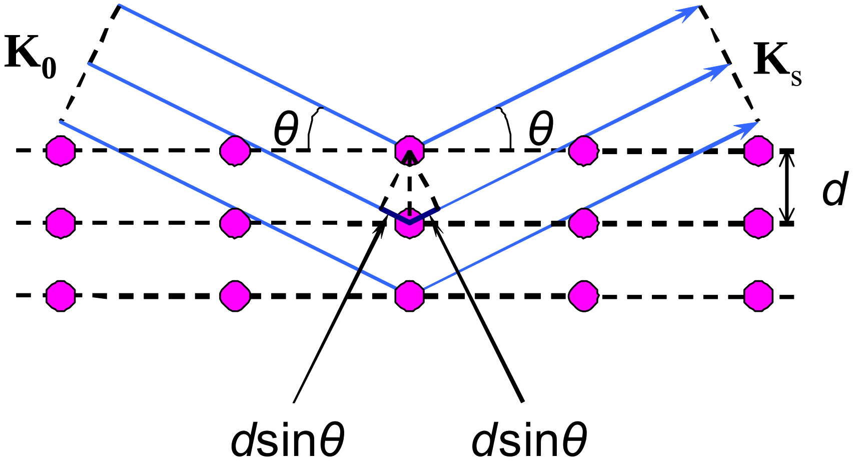

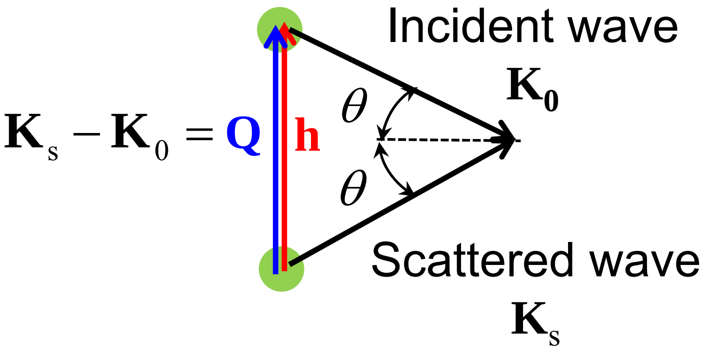

1) Phase matching on the single net plane by mirror-reflection condition.
2) Phase matching between net planes.

Reciprocal lattice vector $\mathbf{h}$
- Normal to net plane
- Length = $1/d$

$$|\mathbf{K}_s| = |\mathbf{K}_0| = k = 1/\lambda$$

$$\boxed{|\mathbf{Q}| = 2k\sin\theta} = \boxed{|\mathbf{h}| = 1/d}$$

Laue condition equivalent to Bragg's law

Ewald sphere

Ewald sphere:

$$Radius = 1/\lambda = K_0$$

$$\mathbf{K}_s - \mathbf{K}_0 = \mathbf{h}$$

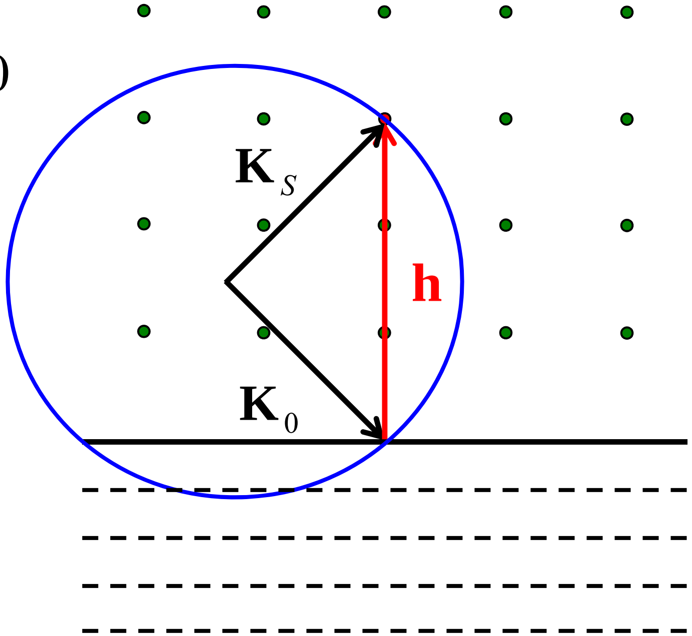

Reciprocal lattice points

When a reciprocal lattice point is ***on the Ewald sphere****,*
Bragg reflection occurs.

Review

Miller indices and *d*-spacing for silicon

$$d = \frac{a}{\sqrt{h^2 + k^2 + l^2}}$$

Top view

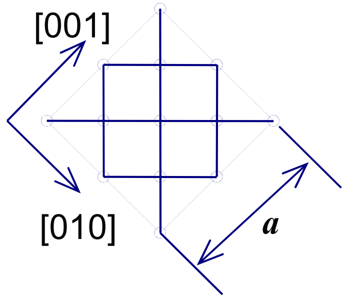

Silicon: $a = 5.431\,\text{Å}$

d-spacing

(400) : 1.3578 Å
(111) : 3.1356 Å
(311) : 1.6375 Å
(511) : 1.0452 Å

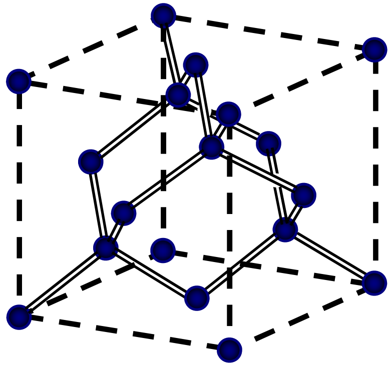

Side view

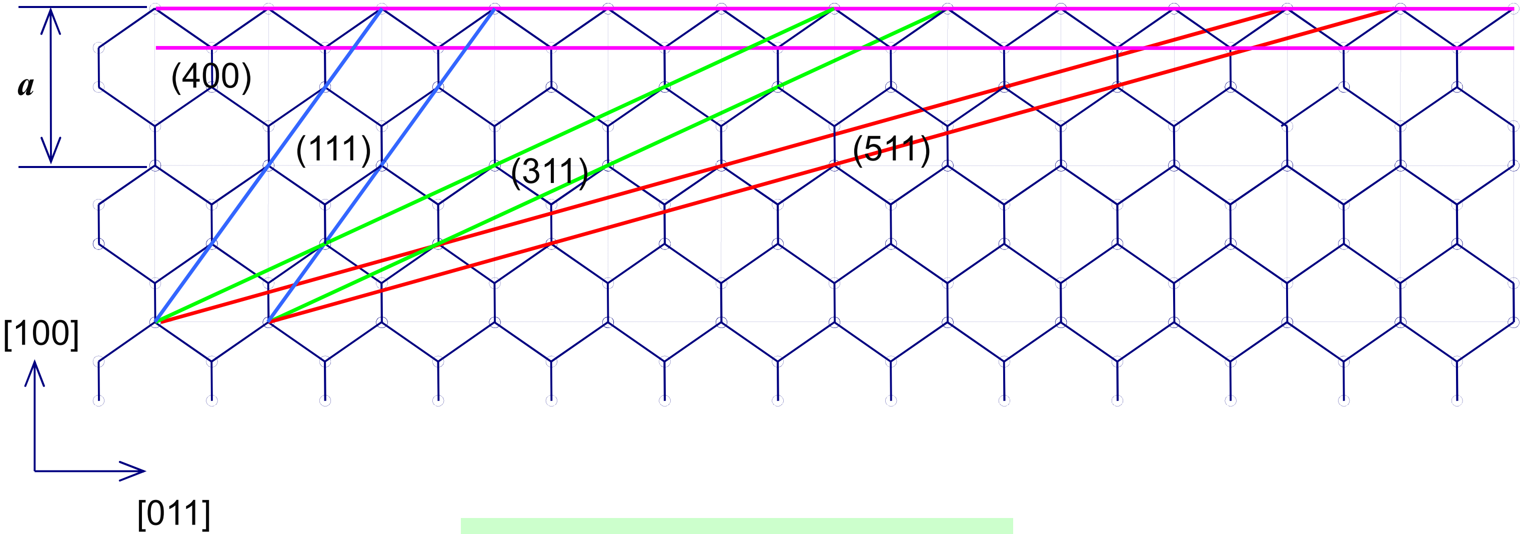

Diamond : $a = 3.567\,\text{Å}$

Review

Crystal structure factor for diamond structure

Structure factor ➔ Sum of atomic scattering with phase shift in the unit cell

$$F(\mathbf{h}) = \sum_j \underline{\underline{f_j(\mathbf{h}, E)}} \exp(2\pi i \mathbf{h} \cdot \mathbf{r}_j)$$

Atomic scattering factor

$$\boxed{F(\mathbf{h}) = \sum_j f_j(\mathbf{h}, E) \exp\{2\pi i (hx_j + ky_j + lz_j)\}}$$

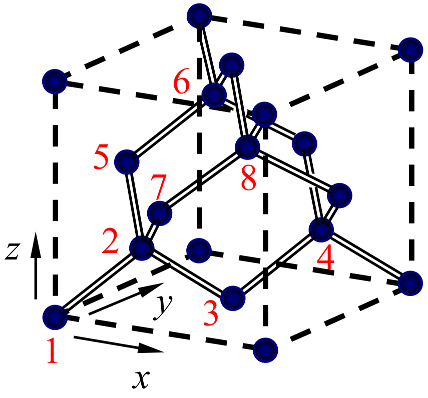

Position of atoms in the unit cell for diamond structure

$(x_j, y_j, z_j) =$

$(0, 0, 0)_1$, $(1/4, 1/4, 1/4)_2$,

$(1/2, 1/2, 0)_3$, $(3/4, 3/4, 1/4)_4$,

$(0, 1/2, 1/2)_5$, $(1/4, 3/4, 3/4)_6$,

$(1/2, 0, 1/2)_7$, $(3/4, 1/4, 3/4)_8$

For diamond structure

h, k, l Mixture of odd and even numbers

$$F = 0$$

h, k, l All odd, or, all even numbers, and m: integer,

$$\begin{cases} h + k + l = 4m & F = 8f \\ h + k + l = 4m \pm 1 & F = 4(1 \pm i)f \\ h + k + l = 4m \pm 2 & F = 0 \end{cases}$$

← 8 atoms in phase

← Half contribute with phase shift $\pm\pi/2$

← Half cancel with π

Review

Crystal structure factor for diamond structure

(400), (220),...

All in phase

➔ $F = 8f$

(111), (311),...

Half contribute with phase shift $\pm\pi/2$

➔ $F = 4(1 \pm i)f$

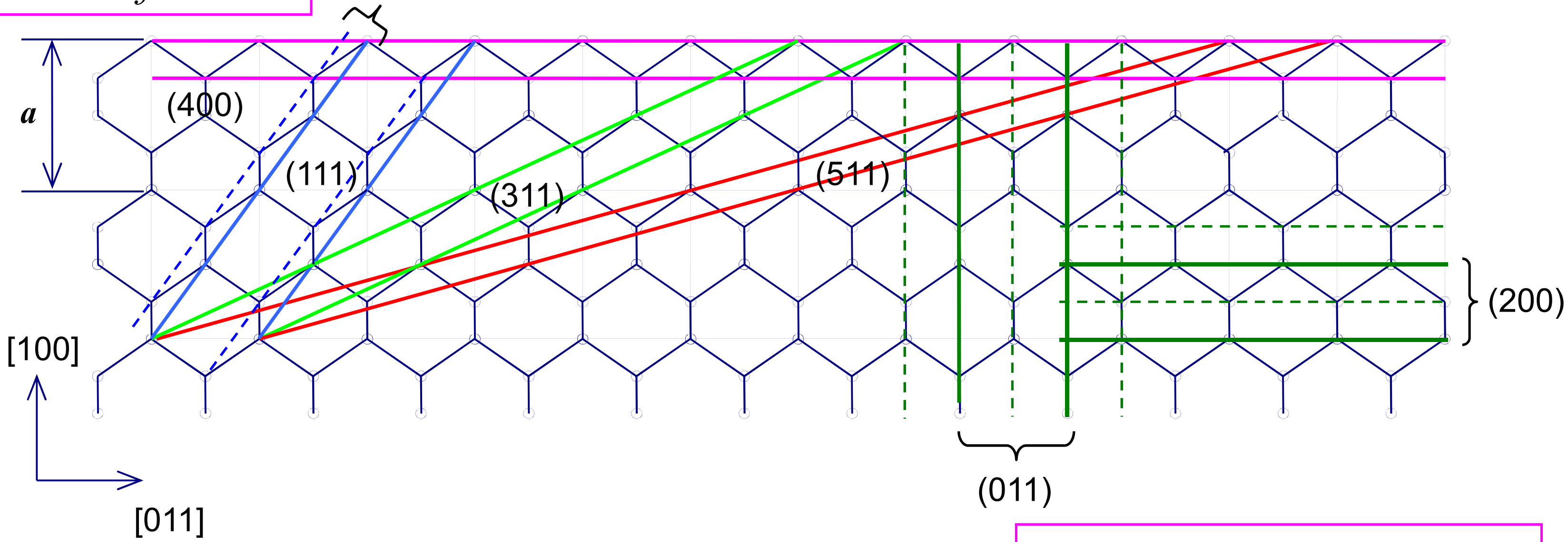

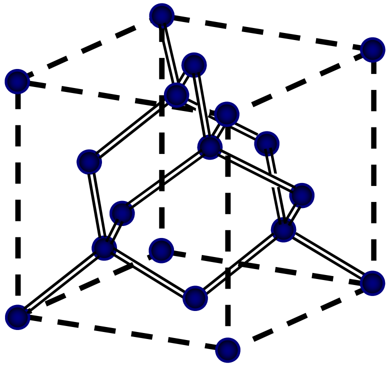

(011), (200),...

Half cancel with π

➔ Forbidden reflection

$F = 0$

Review

Total intensity in *kinematical* approximation

3-dimensional periodic structure of unit cell with number N_x, N_y, N_z
Total scattering intensity becomes:

$$I = I_e \left|F(\mathbf{Q})\right|^2 \cdot \left|G(\mathbf{Q})\right|^2$$

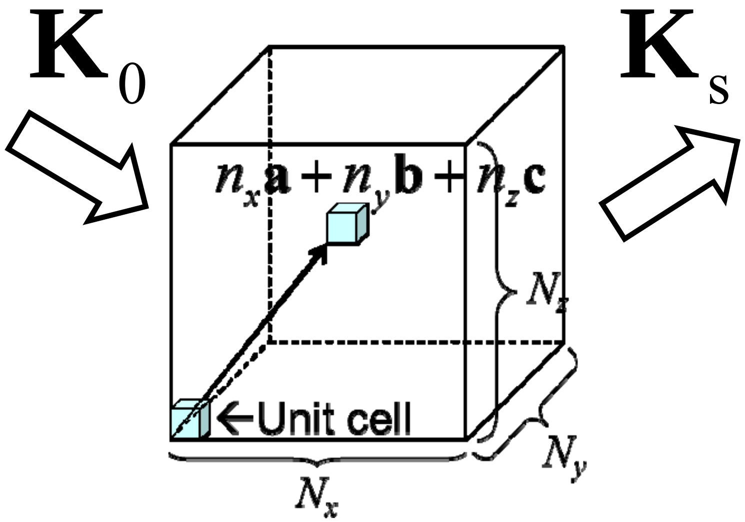

Laue function:

$$\left|G(\mathbf{Q})\right|^2 = \frac{\sin^2(\pi N_x h)}{\sin^2(\pi h)} \cdot \frac{\sin^2(\pi N_y k)}{\sin^2(\pi k)} \cdot \frac{\sin^2(\pi N_z l)}{\sin^2(\pi l)}$$

h, k, l: integer→ Intense peaks

➔ (*hkl*) reflection

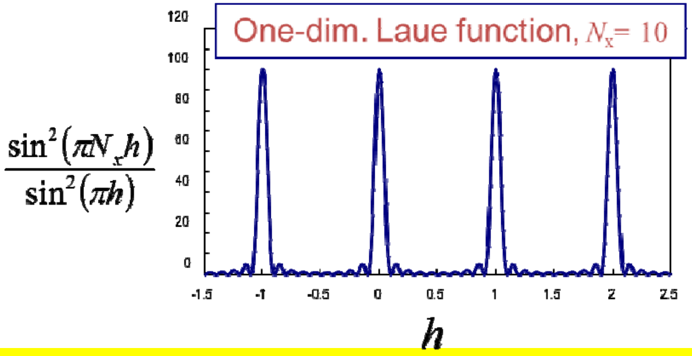

Peak intensity $N_x^{\ 2}$

FWHM $\Delta h \approx 0.8858/N_x \sim 1/N_x$

Crystal size (N) becomes larger
➔ *narrower & higher, approaching delta function*

X-ray monochromator using *perfect crystal*

→ **Perfect single crystal: silicon, diamond,..**

Photon energy tuning:

- ✓ Crystal & lattice plane
- ✓ Bragg angle range

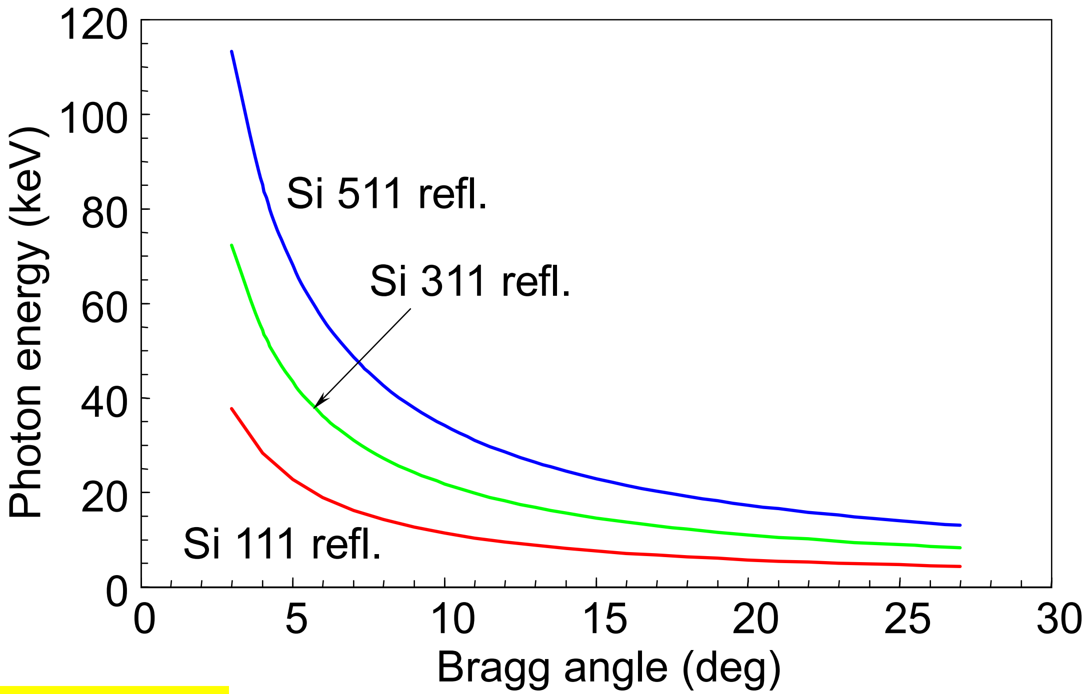

$$E\,[\mathrm{keV}] = \frac{12.3984}{2d_{hkl}\,[\mathrm{\AA}]\sin\theta_{\mathrm{B}}}$$

ex) for SPring-8 standard DCM

Bragg angle: 3~27°

Total intensity in *kinematical* approximation

3-dimensional periodic structure of unit cell with number N_x, N_y, N_z

Total scattering intensity becomes:

$$I = I_e \left|F(\mathbf{Q})\right|^2 \cdot \left|G(\mathbf{Q})\right|^2$$

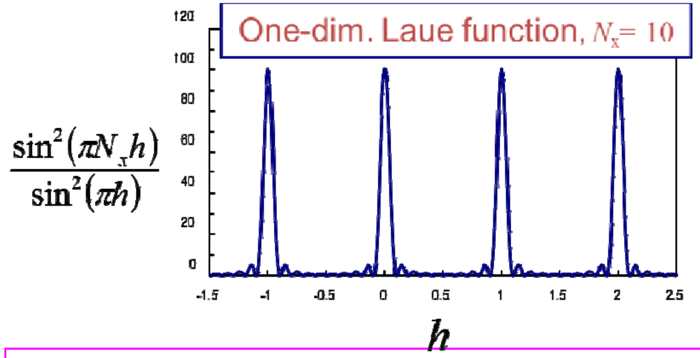

Laue function:

$$\left|G(\mathbf{Q})\right|^2 = \frac{\sin^2(\pi N_x h)}{\sin^2(\pi h)} \cdot \frac{\sin^2(\pi N_y k)}{\sin^2(\pi k)} \cdot \frac{\sin^2(\pi N_z l)}{\sin^2(\pi l)}$$

Peak intensity $N_x^{\ 2}$

FWHM $\Delta h \approx 0.8858/N_x \sim 1/N_x$

Crystal size (N) becomes larger

➔ *narrower & higher, approaching delta function*

$$N \uparrow$$

$$FWHM \to 0, I \to \infty$$

Diffraction theory *for large and perfect crystal*
kinematical to dynamical theory

“Large & perfect” single crystal:

1) Multiple scattering in crystal
2) Extinction (Diffraction by “**finite**” number of net planes)

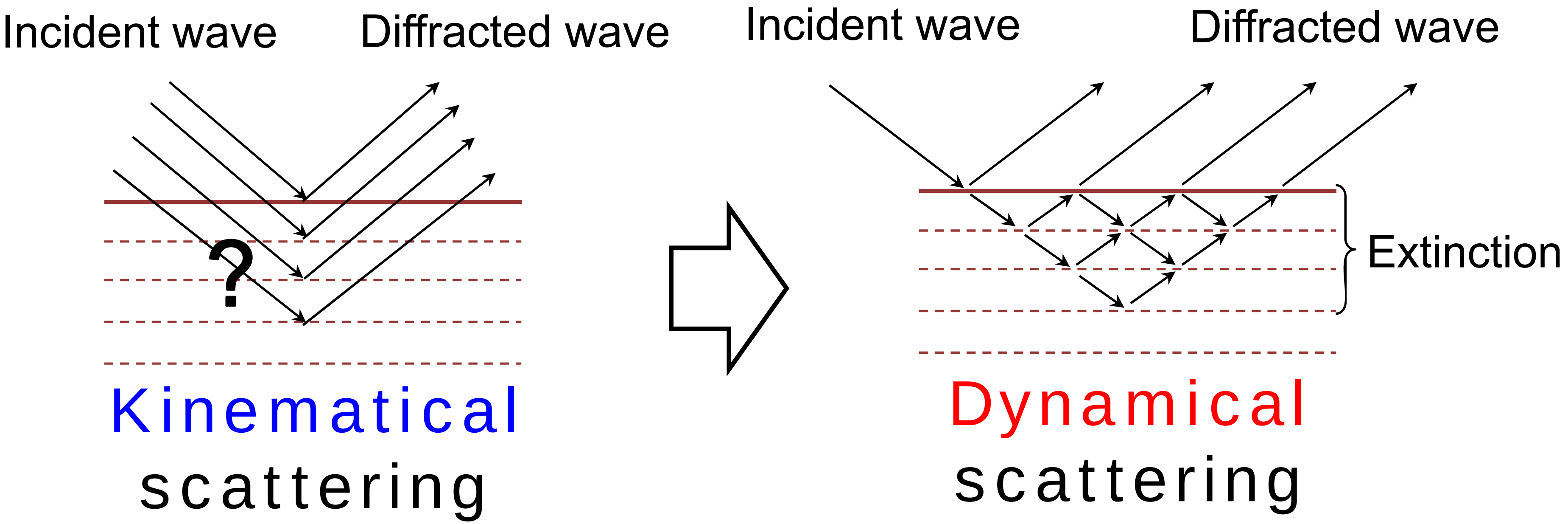

Incident wave

Diffracted wave

?

Kinematical scattering

Incident wave

Diffracted wave

Extinction

Dynamical scattering

Kinematical diffraction is invalid ***for large and perfect crystal****.*
Dynamical theory *must be applied.*

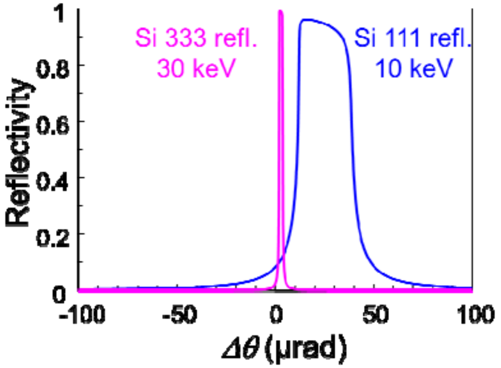

Tailoring x-rays
to application

↓

X-ray monochromator

■ Principle

- ✓ Introduction of diffraction theory
- ✓ Dynamical theory
- ✓ DuMond diagram

■ Engineering

Dynamical theory

C. G. Darwin (1914)

the crystal as an finite stack of atomic planes

→*difference equation*

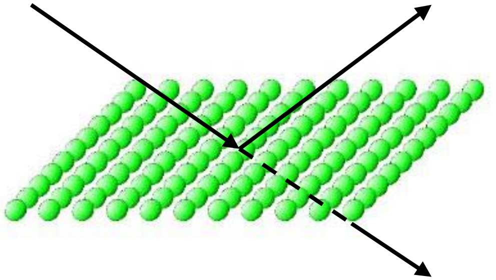

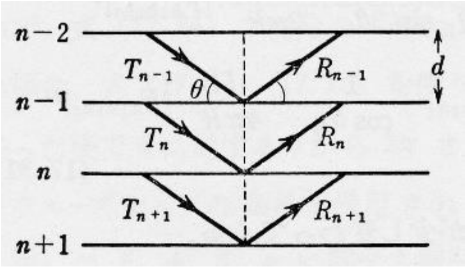

$$T_n = t\,T_{n-1}e^{i\phi} + r\,R_n e^{2i\phi}$$

$$R_n = r\,T_n + t\,R_n e^{i\phi}$$

$$T_0 = 1,\ R_{-1} = 0$$

$$\phi = Kd\sin\theta$$

P. P. Ewald (1917)

Max von Laue (1931)

the crystal as a periodic dielectric constant

→*Maxwell’s equation*

⇨ Dynamical theory by Laue

#1

Fundamental equation

Fundamental equation is derived

using **Maxwell's equations** and introducing **Bloch wave**

for 3-dimensional periodic medium (= perfect single crystal):

Maxwell's equations

→ $rot(rotE) = K^2(1+\chi)E$

$$K = 2\pi/\lambda$$

$$E = \cancel{\exp(-i\omega t)}\sum_g E_g \exp(ik_g \cdot r)$$

$$k_g = k_0 + h$$

$$\chi(r) = \sum_g \chi_g \exp(ig \cdot r)$$

$$\chi_g \propto F(g)$$

$$\frac{k_h{}^2 - K^2}{K^2} E_h = \sum_g \chi_{h-g} P \cdot E_g$$

Fundamental equation

Fundamental equation is derived

$$\frac{k_h{}^2 - K^2}{K^2} E_h = \sum_g \chi_{h-g} P \cdot E_g$$

$h, g, \ldots$: Reciprocal lattice points

E_h, E_g : Fourier components of electric field

$\boldsymbol{K}$: Incident wave vector in vacuum

$\boldsymbol{k}_\mathbf{h}$: Wave vectors in the crystal

$\chi_\mathbf{h}$: **Fourier components of the polarizability** **(Negative values, 10^{-6}~10^{-5})**

P : Polarization factor between ***h*** and ***g*** waves

$k_h = k_0 + h$: Momentum conservation

#2 When one wave E_0 in crystal

Fundamental equation

$$\frac{k_h{}^2 - K^2}{K^2} E_h = \sum_g \chi_{h-g} P \cdot E_g$$

Waves **E** *in the crystal*

$$E = \sum_g E_g \exp(ik_g \cdot r)$$

$$k_h = k_0 + h$$ ➔ Bloch wave

When one wave $\boldsymbol{E_0}$ *in the crystal*

$$\frac{k_0{}^2 - K^2}{K^2} E_0 = \chi_0 E_0 \quad \therefore \left\{(1+\chi_0)K^2 - k_0{}^2\right\} E_0 = 0$$

$$k_0 = K\sqrt{1+\chi_0} \equiv k$$

$$k \approx K(1+\chi_0/2)$$

k : <u>*Mean* </u>wave number in the crystal

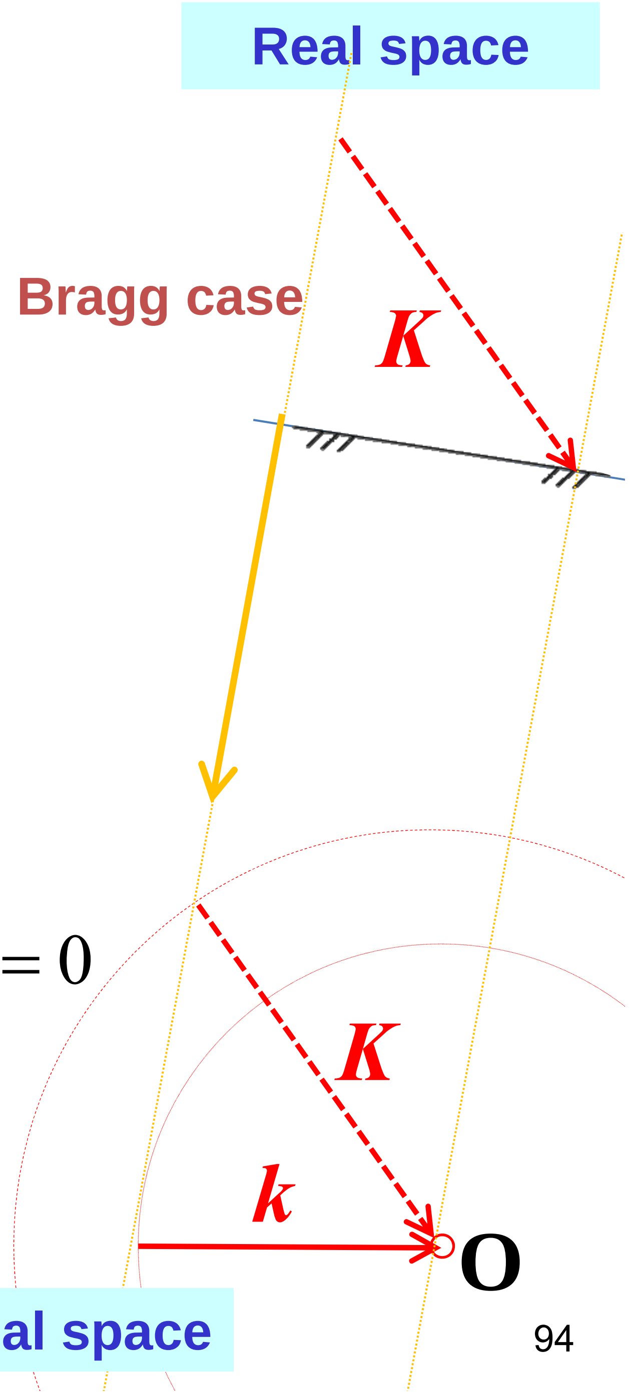

#3

Boundary condition of wave vector

We must consider connections of waves from vacuum into the crystal and from the crystal to vacuum, to solve the equations.

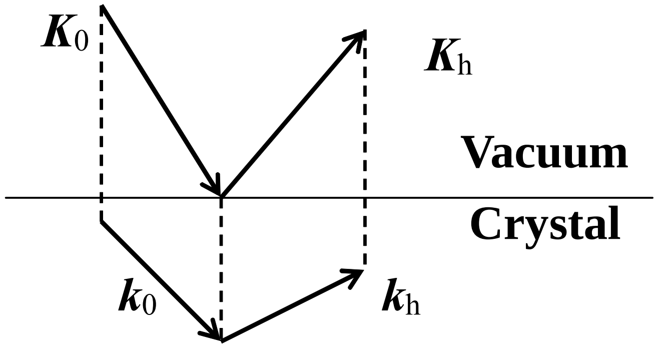

Incident wave in vacuum	K_0
→ Refracted wave in the crystal	k_0
→ Reflected wave in the crystal	k_h
→ Reflected wave in vacuum	K_h

Tangential component of wave vector must be continuous

#4

Two-beam approximation

Fundamental equation is reduced to the equation
for **two beams (waves)** of incidence E_0 and "one" intense diffraction E_h

$$\frac{k_h{}^2 - K^2}{K^2} E_h = \sum_g \chi_{h-g} P \cdot E_g \Rightarrow$$

$$\text{(A)} \quad \frac{k_0{}^2 - K^2}{K^2} E_0 = \chi_0 E_0 + P\chi_{-h} E_h$$

$$\text{(B)} \quad \frac{k_h{}^2 - K^2}{K^2} E_h = P\chi_h E_0 + \chi_0 E_h$$

$\chi_0, \chi_h, \chi_{-h}$ Fourier components of the polarizability

Negative values, 10^{-6}~10^{-5}

$\chi_h = \chi_{-h}$ for Si

P Polarization factor

$$\sigma : P = 1, \ \pi : P = \cos 2\theta_B$$

Two-beam approximation

Two beams (waves) of incidence E_0 and “one” intense diffraction E_h

$$\text{(A)} \quad \frac{k_0{}^2 - K_0{}^2}{K_0{}^2} E_0 = \chi_0 E_0 + P\chi_{-h} E_h$$

$$\text{(B)} \quad \frac{k_h{}^2 - K^2}{K^2} E_h = P\chi_h E_0 + \chi_0 E_h$$

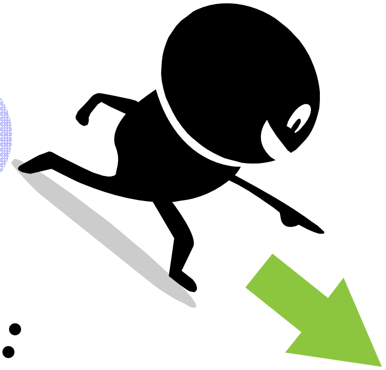

What means these equations:

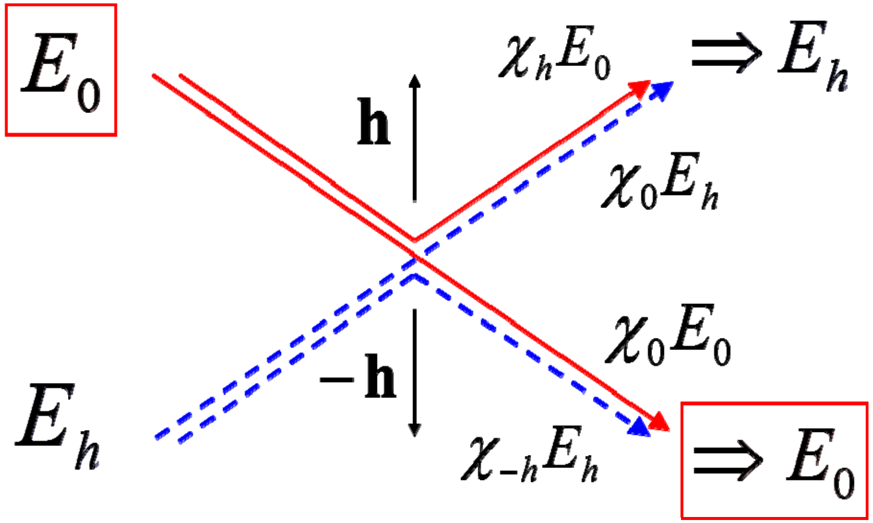

Scheme of **self-consistent wave field**

Goal

$$R = r^2 = \left(\frac{E_h}{E_0}\right)^2$$

$$FWHM = \Delta\theta_{\text{Darwin}}$$

Reflectivity curve

Effective band width

Dispersion surface

Using two equations, we obtain following secular equation:

(A) $$\frac{k_0^{\ 2} - K_0^{\ 2}}{K_0^{\ 2}} E_0 = \chi_0 E_0 + P\chi_{-h} E_h$$

(B) $$\frac{k_h^{\ 2} - K^2}{K^2} E_h = P\chi_h E_0 + \chi_0 E_h$$

Secular equation

$$\left(k_0^{\ 2} - k^2\right)\left(k_h^{\ 2} - k^2\right) = \chi_h \chi_{-h} P^2 K^4$$

$$k_h = k_0 + h$$

$$\chi_h = \chi_{-h} = 0$$

Not our goal!

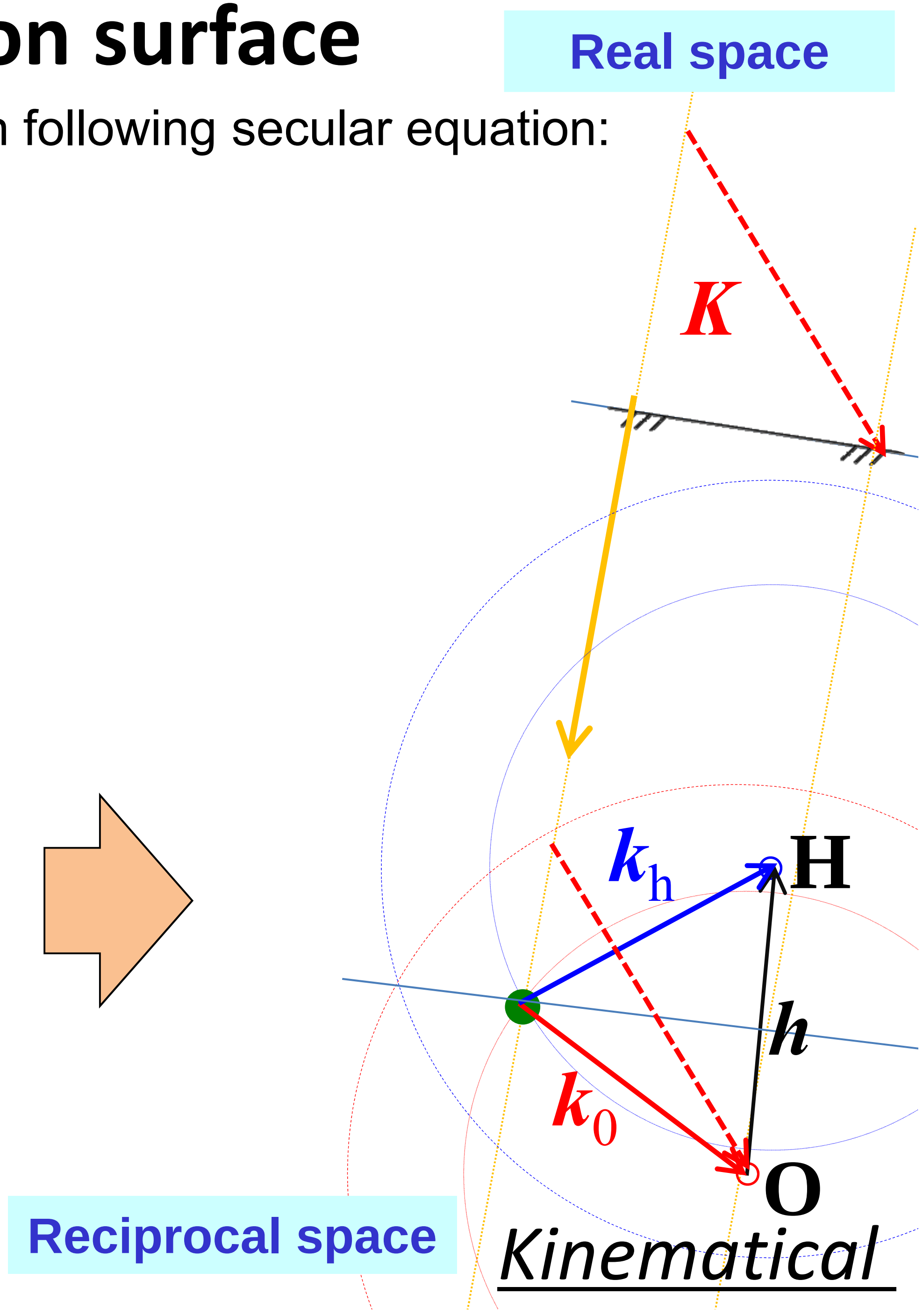

Dispersion surface

$$(A) \quad \frac{k_0^{\ 2} - K_0^{\ 2}}{K_0^{\ 2}} E_0 = \chi_0 E_0 + P\chi_{-h} E_h$$

$$(B) \quad \frac{k_h^{\ 2} - K^2}{K^2} E_h = P\chi_h E_0 + \chi_0 E_h$$

Secular equation

$$\left(k_0^{\ 2} - k^2\right)\left(k_h^{\ 2} - k^2\right) = \chi_h \chi_{-h} P^2 K^4$$

$$k_h = k_0 + h$$

$$\chi_h \neq 0 \neq \chi_{-h}$$

Secular equation can be reduced to quadratic equation near Brillouin zone boundary.

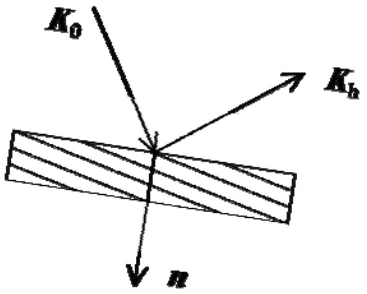

Bragg case

Real space

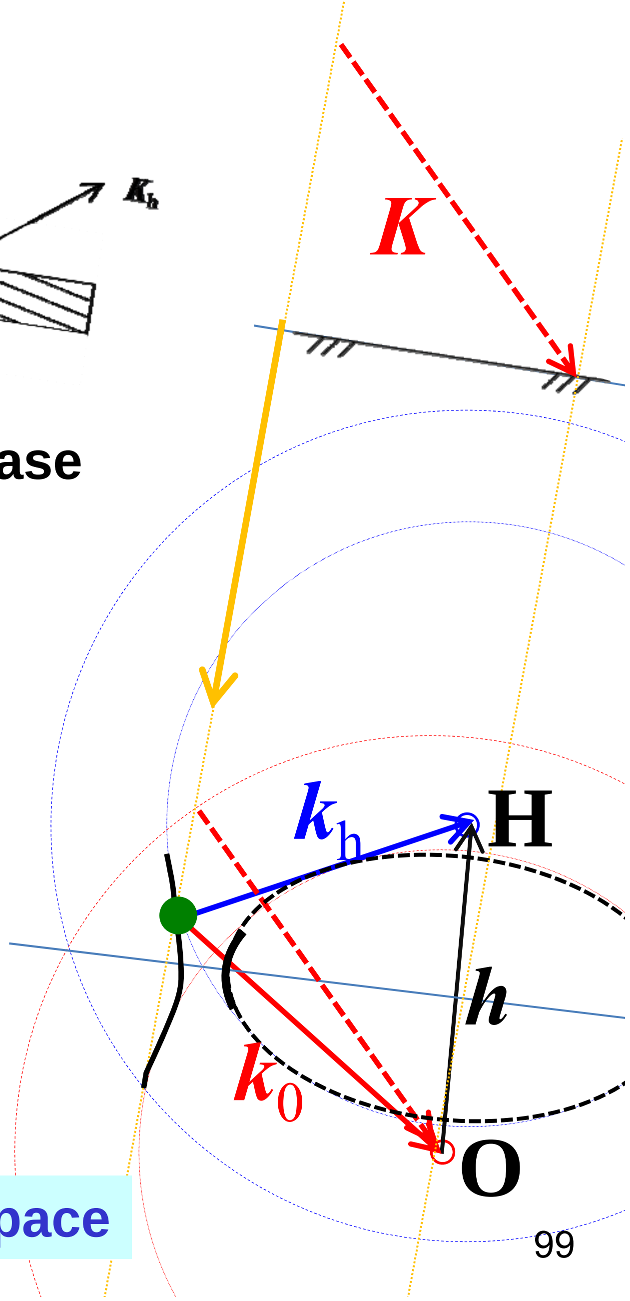

Reciprocal space

Dispersion surface

$$\text{(A)} \quad \frac{k_0{}^2 - K_0{}^2}{K_0{}^2} E_0 = \chi_0 E_0 + P\chi_{-h} E_h$$

$$\text{(B)} \quad \frac{k_h{}^2 - K^2}{K^2} E_h = P\chi_h E_0 + \chi_0 E_h$$

Secular equation

$$\left(k_0{}^2 - k^2\right)\left(k_h{}^2 - k^2\right) = \chi_h \chi_{-h} P^2 K^4$$

$$k_h = k_0 + h$$

$$\chi_h \neq 0 \neq \chi_{-h}$$

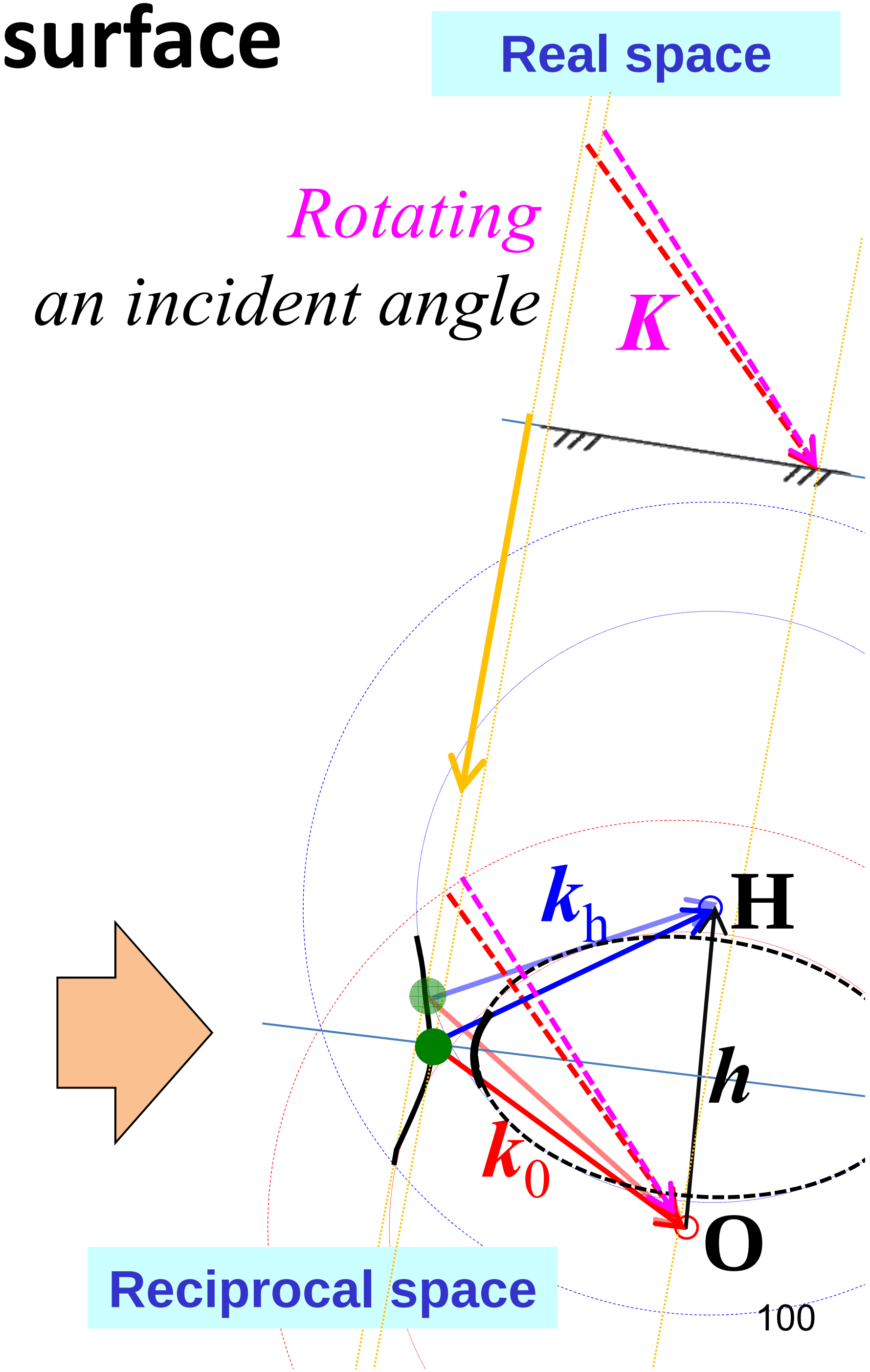

Dispersion surface

(A) $$\frac{k_0{}^2 - K_0{}^2}{K_0{}^2} E_0 = \chi_0 E_0 + P\chi_{-h} E_h$$

(B) $$\frac{k_h{}^2 - K^2}{K^2} E_h = P\chi_h E_0 + \chi_0 E_h$$

Secular equation

$$\left(k_0{}^2 - k^2\right)\left(k_h{}^2 - k^2\right) = \chi_h \chi_{-h} P^2 K^4$$

$$k_h = k_0 + h$$

$$\chi_h \neq 0 \neq \chi_{-h}$$

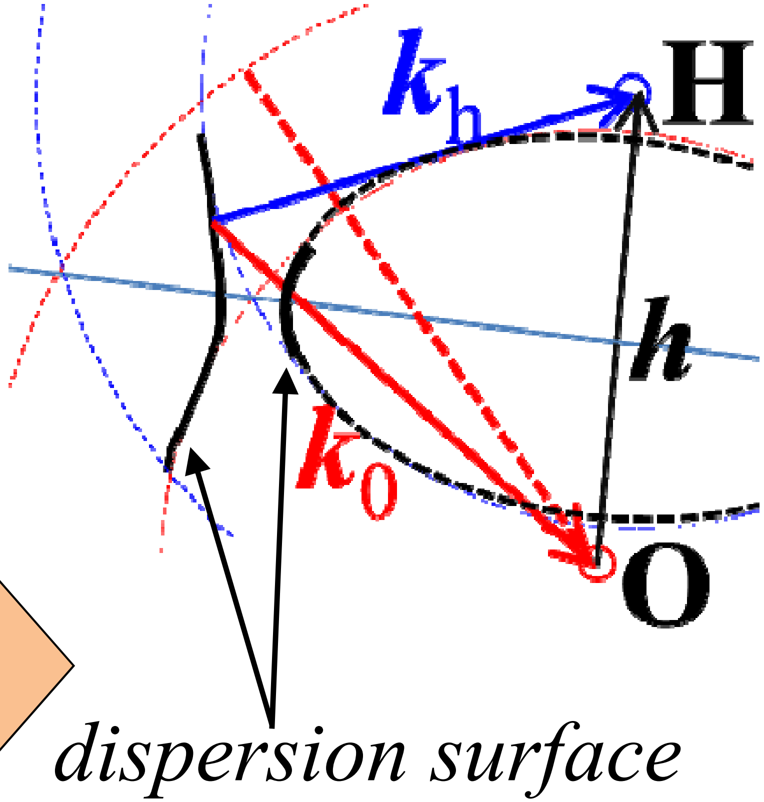

In the gap between two dispersion surfaces

total reflection *occurs for Bragg case.*

#6

Normalized deviation parameter *W*

Parameter *W* is related to **the gap between two dispersion surfaces**

and total reflection occurs at –1<*W*<1 for Bragg case.

$$W=-\frac{2\left(\mathbf{K}_0\cdot\mathbf{h}\right)+h^2}{2K_0{}^2}\sqrt{\frac{\gamma_0}{|\gamma_h|}}\frac{1}{|\chi_{hr}|\cdot|P|}+\frac{\chi_{0r}}{2|\chi_{hr}|\cdot|P|}\sqrt{\frac{\gamma_0}{|\gamma_h|}}\left(1-\frac{\gamma_h}{\gamma_0}\right)$$

$$\Downarrow$$

Δθ: Angle deviation for fixed photon energy,

Δ*E*: Energy deviation for fixed incident angle

$$W=\left\{\Delta\theta\sin 2\overline{\theta}_{BK}+2\frac{\Delta E}{E}\sin^2\overline{\theta}_{BK}+\frac{\chi_{0r}}{2}\left(1-\frac{\gamma_h}{\gamma_0}\right)\right\}\sqrt{\frac{\gamma_0}{|\gamma_h|}}\frac{1}{|\chi_{hr}|\cdot|P|}$$

For symmetric Bragg case, sigma polarization:

$$W=\left\{\Delta\theta\sin 2\overline{\theta}_{BK}+2\frac{\Delta E}{E}\sin^2\overline{\theta}_{BK}+\chi_{0r}\right\}\frac{1}{|\chi_{hr}|}$$

#7

Movement of tie point

Tie point moves by ***changing the incident angle***

at fixed photon energy (wavelength).

(1) Lower angle $W < -1$

(2) Near Bragg condition $-1 < W < 1$

(3) Higher angle $W > 1$

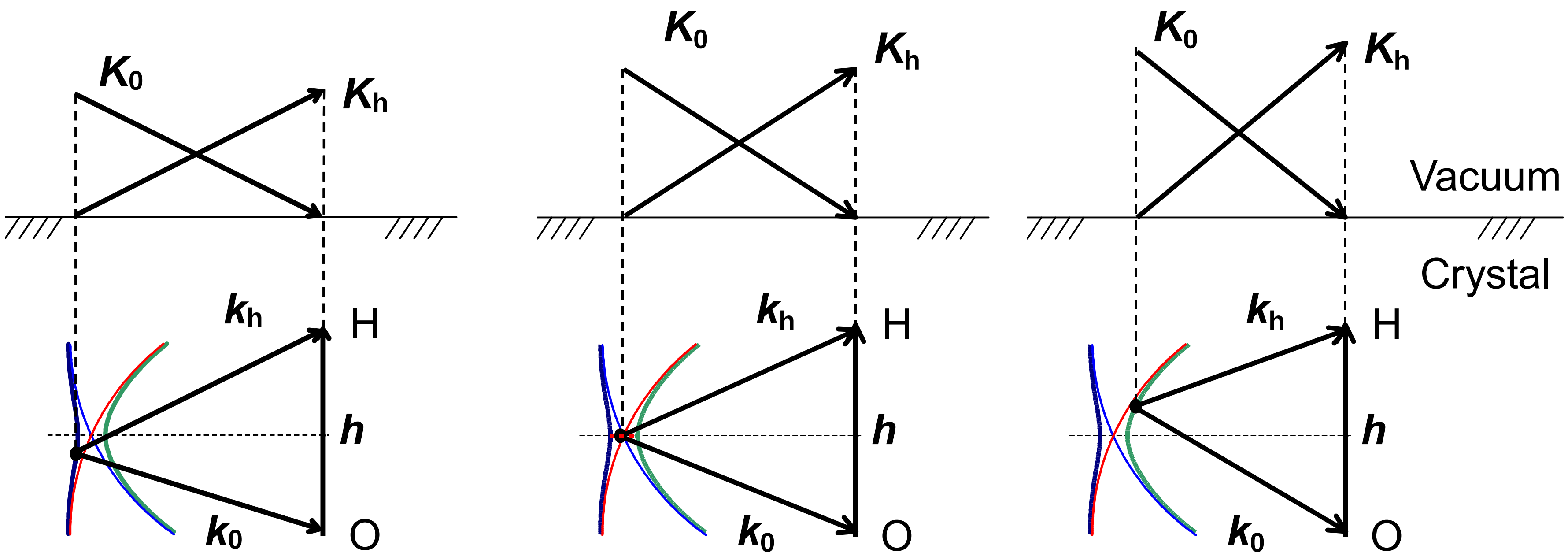

Total reflection

Dominant branch for thick Bragg-case crystal is close to O-sphere.

#8

Calculation of polarizability

χ_h: Fourier component of polarizability
→ proportional to the structure factor

$$\chi_h = -\frac{r_e\lambda^2}{\pi v_c} F(\mathbf{h}, E)$$

v_c: unit cell volume

$$\chi_h = \chi_{hr} + i\chi_{hi}$$

$$\chi_{hr} \Leftrightarrow f^0(\mathbf{h}) + f'(E)$$

Atomic form factor
+ real part of anomalous factor

$$\chi_{hi} \Leftrightarrow f''(E)$$

Imaginary part of
anomalous factor

For diamond structure

$\boxed{h+k+l=4m}$

$$\chi_{hr} = -\frac{r_e\lambda^2}{\pi v_c} 8\left(f^0 + f'\right)e^{-M}$$

$$\chi_{hi} = -\frac{r_e\lambda^2}{\pi v_c} 8 f'' e^{-M}$$

$\boxed{h+k+l=4m \pm 1}$

$$\chi_{hr} = -\frac{r_e\lambda^2}{\pi v_c} 4(1+i)\left(f^0 + f'\right)e^{-M}$$

$$\chi_{hi} = -\frac{r_e\lambda^2}{\pi v_c} 4(1+i) f'' e^{-M}$$

$\boxed{h=k=l=0}$

$$\chi_{0r} = -\frac{r_e\lambda^2}{\pi v_c} 8\left(Z + f'\right)$$

$$\chi_{0i} = -\frac{r_e\lambda^2}{\pi v_c} 8 f''$$

#9

Amplitude ratio

From **the solution** of the fundamental equations,
we obtain the ratio $r = E_h/E_0$ (← reflection coefficient)
as a function of parameter *W*.

For Bragg case, no absorption, and thick crystal:

$$\begin{cases} r = \dfrac{E_h}{E_0} = -\sqrt{\dfrac{\gamma_0}{|\gamma_h|}\dfrac{|\chi_{hr}|}{\chi_{-h}}}\dfrac{|P|}{P}\left(W + \sqrt{W^2 - 1}\right) \quad (W < -1) \\ r = \dfrac{E_h}{E_0} = -\sqrt{\dfrac{\gamma_0}{|\gamma_h|}\dfrac{|\chi_{hr}|}{\chi_{-h}}}\dfrac{|P|}{P}\left(W + i\sqrt{1 - W^2}\right) \quad (-1 \le W \le 1) \\ r = \dfrac{E_h}{E_0} = -\sqrt{\dfrac{\gamma_0}{|\gamma_h|}\dfrac{|\chi_{hr}|}{\chi_{-h}}}\dfrac{|P|}{P}\left(W - \sqrt{W^2 - 1}\right) \quad (W > 1) \end{cases}$$

← **Total reflection**

$$R = r^2$$

#10

Reflectivity (Darwin curve)

Darwin curve (intrinsic reflection curve for monochromatic plane wave)

for Bragg case, no absorption, and thick crystal:

$$\begin{cases} R=\left(W+\sqrt{W^2-1}\right)^2 & (W<-1) \\ R=1 & (-1\le W\le 1) \\ R=\left(W-\sqrt{W^2-1}\right)^2 & (W>1) \end{cases}$$

← Total reflection region

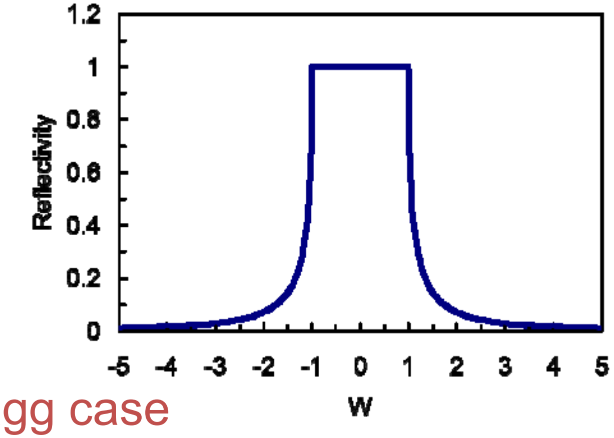

W: deviation parameter for s-polarization, symmetrical Bragg case

$$W=\left(\underline{\Delta\theta\sin 2\theta_B}+\underline{2\sin^2\theta_B\frac{\Delta E}{E}}+\underline{\chi_0}\right)\frac{1}{|\chi_h|}$$

Angular deviation

Energy deviation

Refraction

Geometry for symmetrical Bragg case

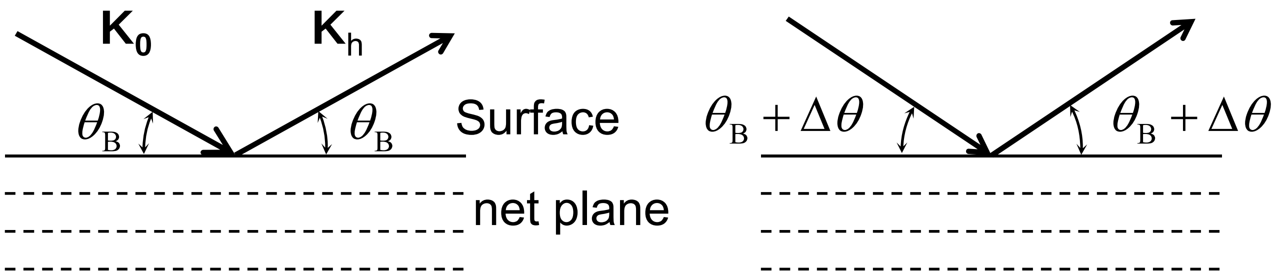

Darwin curve

For Bragg case, no absorption, and thick crystal:

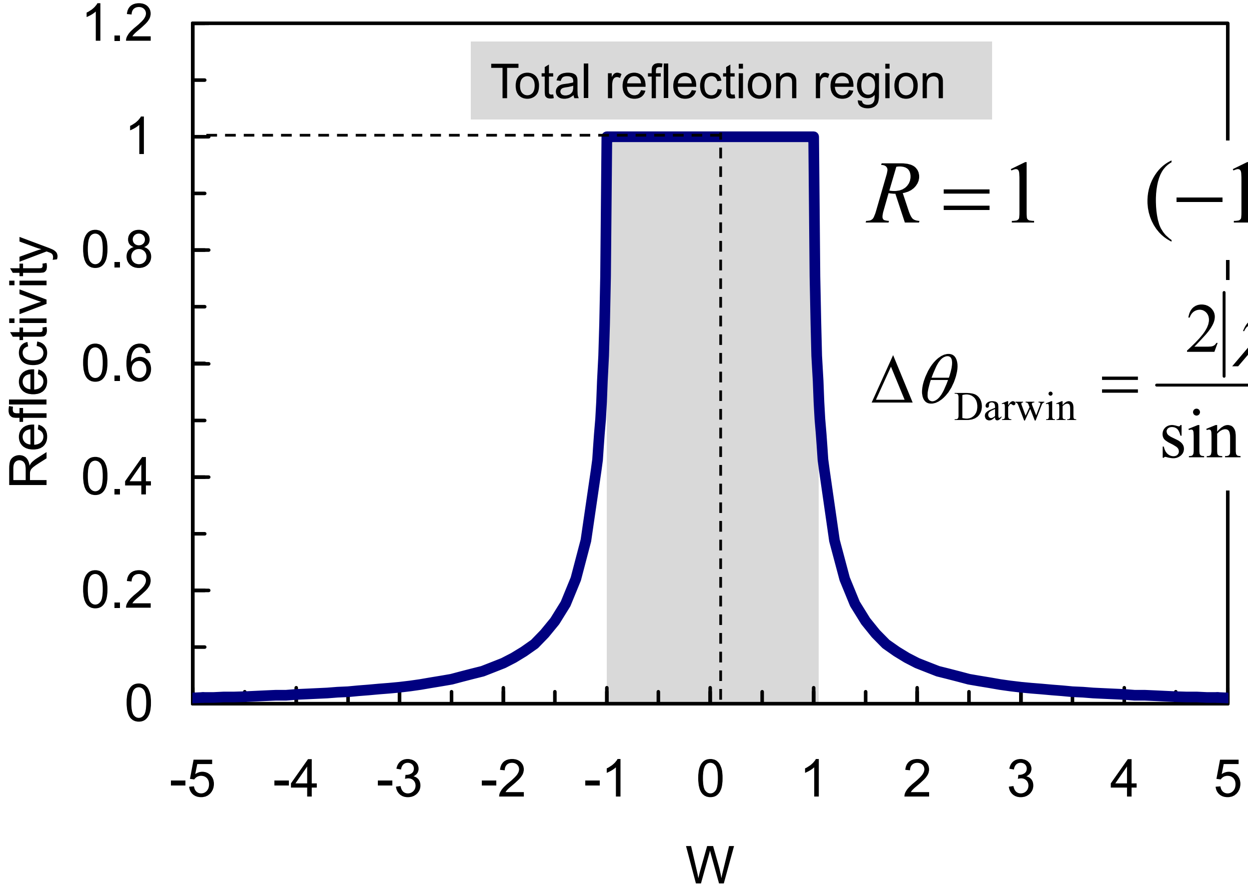

$$R = 1 \qquad (-1 \le W \le 1)$$

$$\Delta\theta_{\mathrm{Darwin}} = \frac{2|\chi_{hr}|}{\sin 2\theta_{\mathrm{B}}} \propto |F(\mathbf{h})|$$

Reflectivity with absorption

Reflectivity

- symmetrical Bragg case,
- s-polarization,
- thick crystal

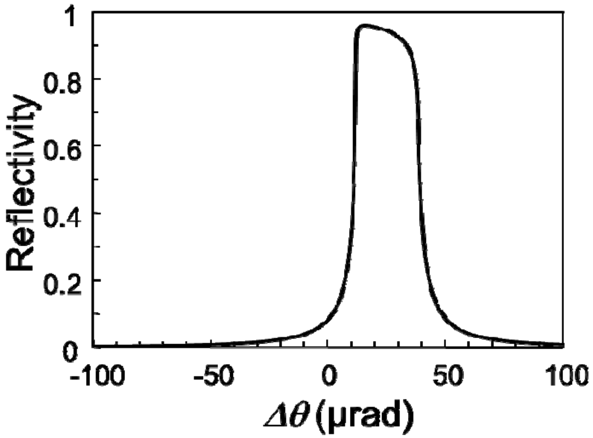

$$\boxed{R = L - \sqrt{L^2 - 1}}$$

$$L = \frac{\left\{W^2 + g^2 + \sqrt{\left(W^2 - g^2 - 1 + \kappa^2\right)^2 + 4\left(gW - \kappa\right)^2}\right\}}{1 + \kappa^2}$$

$$W = \left(\Delta\theta \sin 2\overline{\theta}_{\mathrm{B}} + 2\sin^2\overline{\theta}_{\mathrm{B}}\frac{\Delta E}{E} + \chi_{0r}\right)\frac{1}{\left|\chi_{hr}\right|}$$

$$g = \frac{\chi_{0i}}{\left|\chi_{hr}\right|}, \quad \kappa = \frac{\left|\chi_{hi}\right|}{\left|\chi_{hr}\right|}$$

Note: No absorption $g = 0, \kappa = 0 \;\; \Rightarrow \;\; R \to Darwin\ curve$

Reflectivity curve for silicon

Examples for symmetrical Bragg case, with absorption, s-polarization and thick crystal:

Si 111 refl., 10 keV

$$\chi_{0r} = -9.78\times10^{-6}$$

$$\chi_{0i} = -1.48\times10^{-7}$$

$$\chi_{111\_r} = -3.66\times10^{-6}(1+i)$$

$$\chi_{111\_i} = -7.30\times10^{-8}(1+i)$$

Si 333 refl., 30 keV

$$\chi_{0r} = -1.07\times10^{-6}$$

$$\chi_{0i} = -1.75\times10^{-9}$$

$$\chi_{333\_r} = -2.24\times10^{-7}(1+i)$$

$$\chi_{333\_i} = -7.87\times10^{-10}(1+i)$$

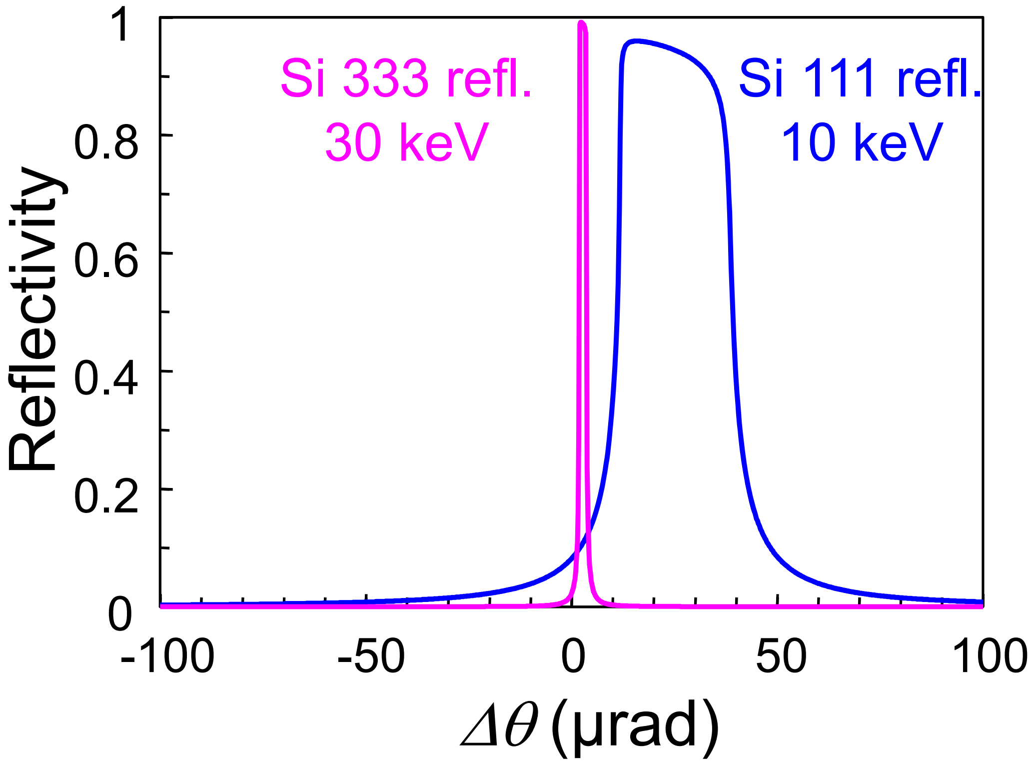

- Width of 0.1～100 μrad
- Peak ~1 with small absorption

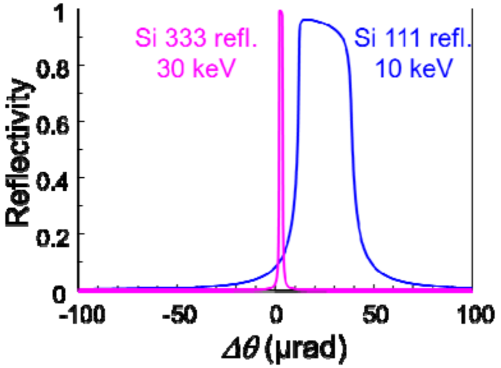

Tailoring x-rays to application

↓

X-ray monochromator

■ Principle

- ✓ Introduction of diffraction theory
- ✓ Dynamical theory
- ✓ DuMond diagram

■ Engineering

DuMond (angle-energy) diagram

The diagram helps to understand how we can extract x-rays from SR source.

Angular width (Darwin width)

$$\Delta\theta_{\mathrm{Darwin}} = \frac{2|\chi_{hr}|}{\sin 2\theta_{\mathrm{B}}} \propto |F(\mathbf{h})|$$

← ΔW= 2

Energy resolution

$$\frac{\Delta E}{E} = \cot\theta_{\mathrm{B}}\sqrt{\Omega^2 + \Delta\theta_{\mathrm{Darwin}}{}^2}$$

← Gaussian approximation for both light source and reflection curve

Effective band width

$$\frac{\Delta E}{E} \approx \frac{|\chi_{hr}|}{\sin^2\theta_{\mathrm{B}}}$$

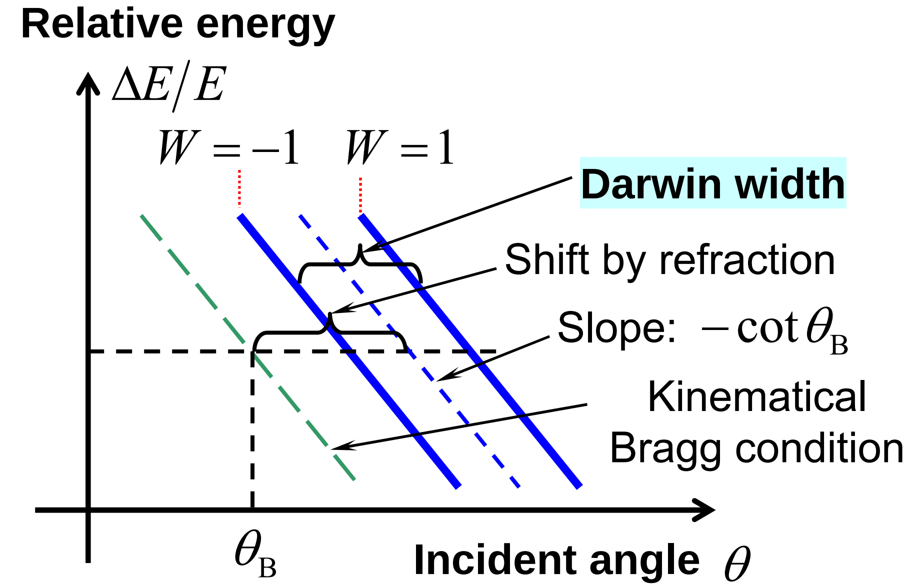

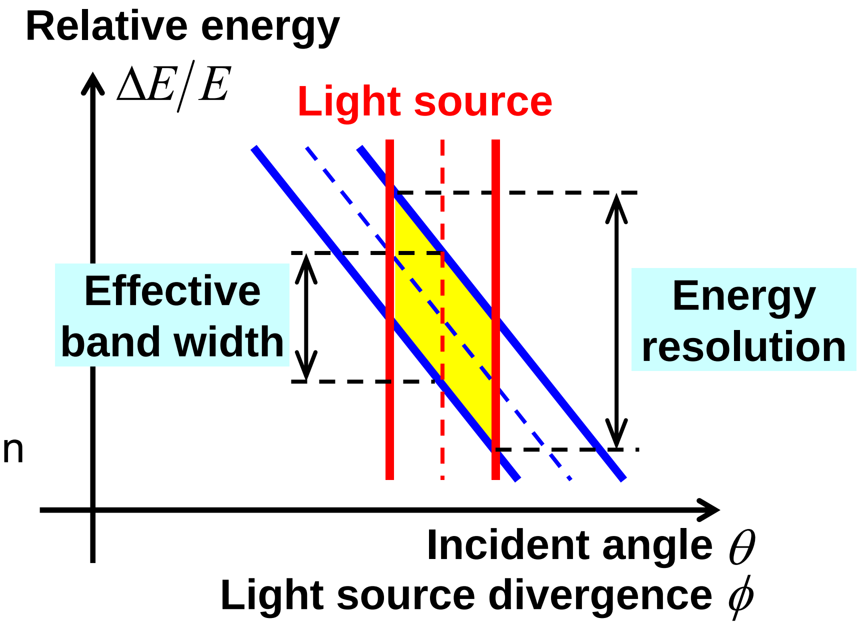

Source divergence and diffraction width

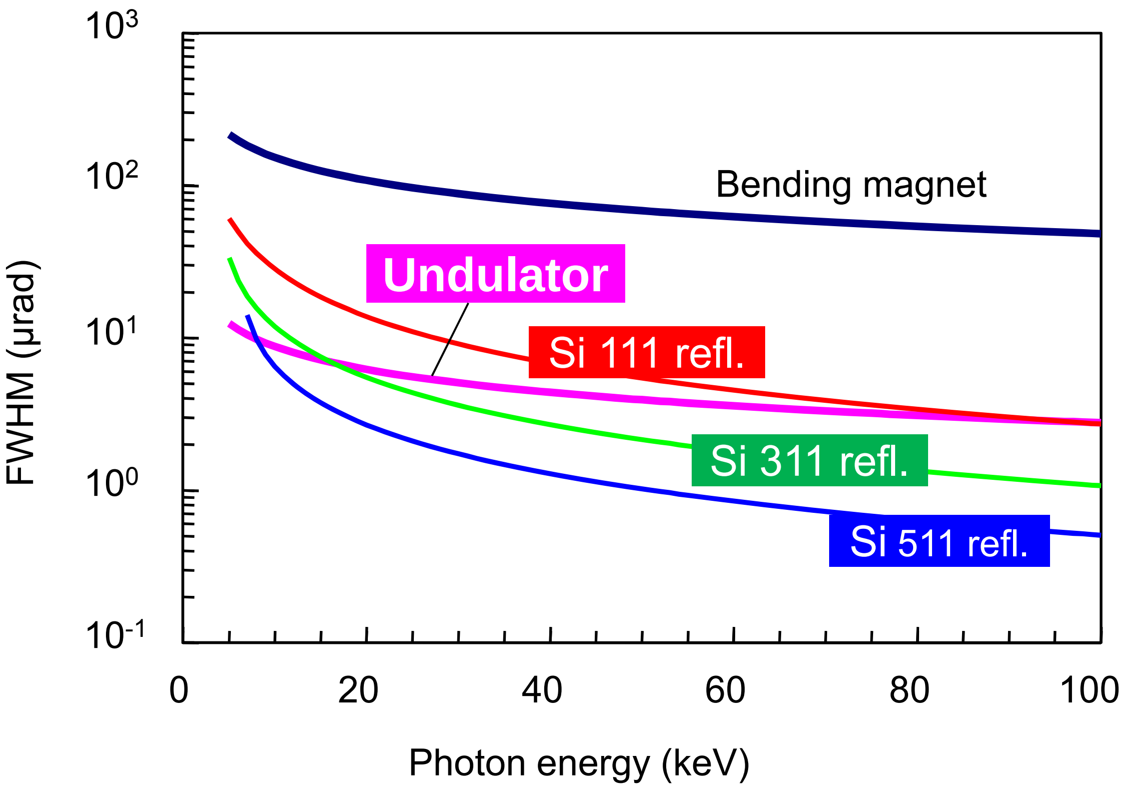

Natural divergence

- Bending magnet

$$\sigma_{r'} \approx 0.597 \frac{1}{\gamma}\sqrt{\frac{\lambda}{\lambda_c}} \propto \sqrt{\frac{1}{\hbar\omega}}$$

- Undulator

$$\sigma_{r'} \approx \sqrt{\frac{\lambda}{2N\lambda_u}} \propto \sqrt{\frac{1}{\hbar\omega}}$$

For SPring-8 case:

- Bending magnet

$$\sigma_{r'} \approx 60\,\mu\mathrm{rad}$$

- Undulator (*N*= 140)

$$\sigma_{r'} \approx 5\,\mu\mathrm{rad}$$

Divergence of undulator radiation ~ diffraction width

Energy resolution

$$\frac{\Delta E}{E} = \cot\theta_{\mathrm{B}} \sqrt{\Omega^2 + \omega^2}$$

Ω: source divergence,

ω: diffraction width

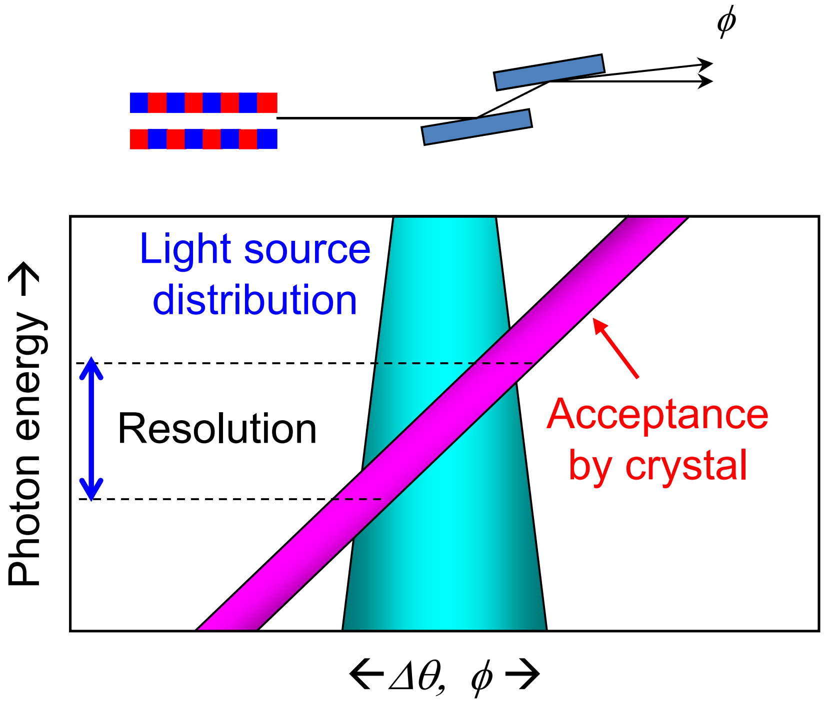

Angle-energy diagram
(DuMond diagram)

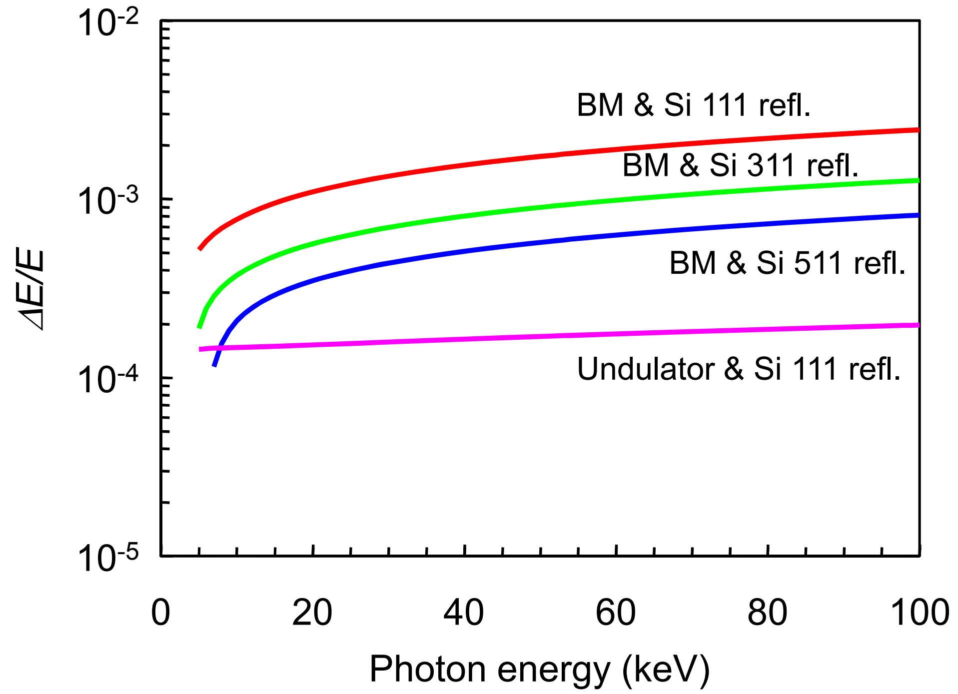

For usual beamline : $\Delta E/E$=10^{-5}～10^{-3}

DuMond diagram: undulator & DCM

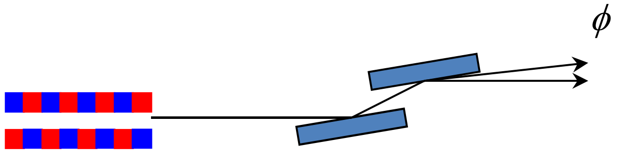

SPring-8 standard undulator

(λu= 32 mm, N= 140, K= 1.34, E_{1st}= 10 keV)

+ DCM (Si 111 refl.)

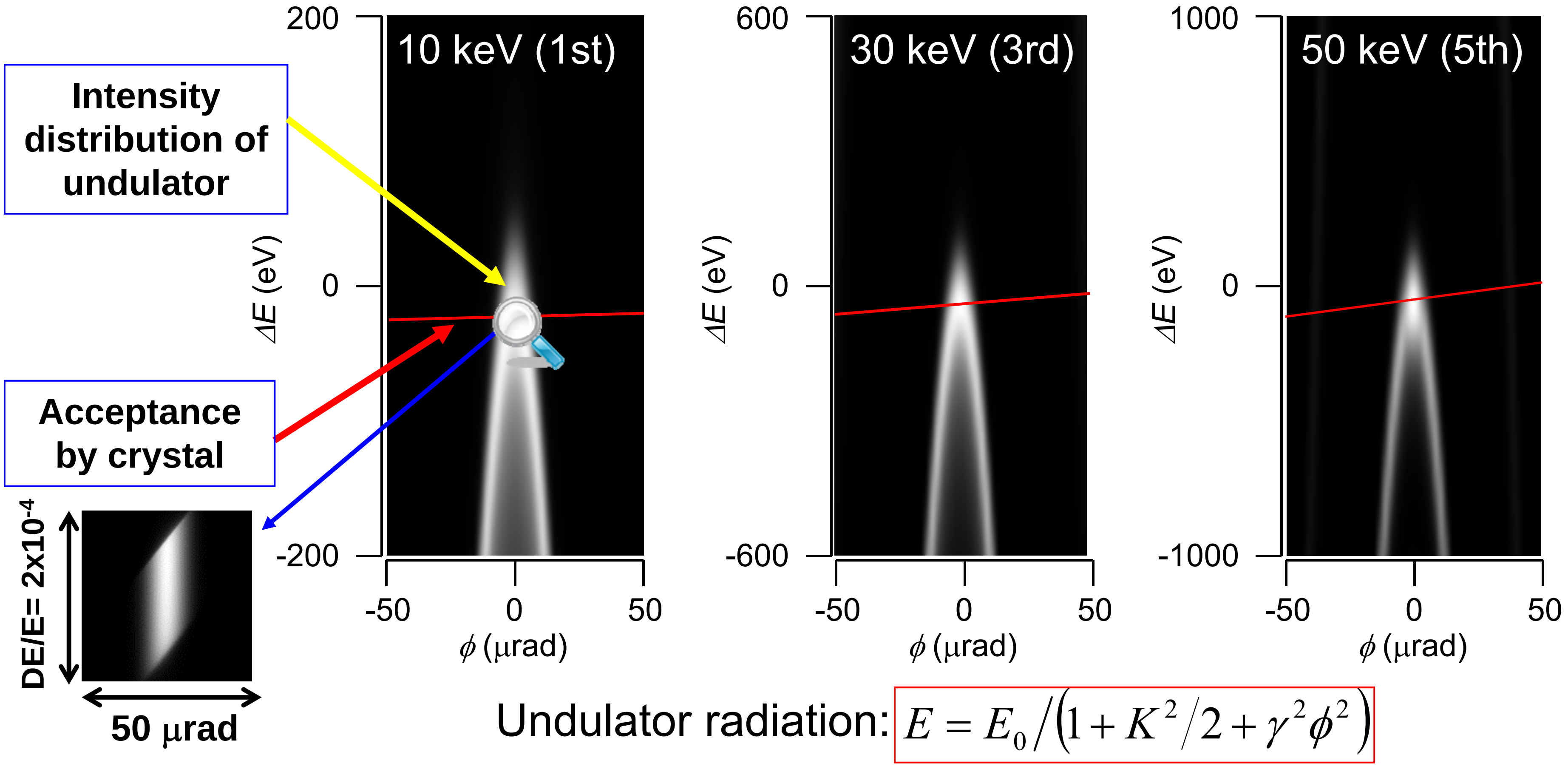

Intensity distribution of undulator

Acceptance by crystal

Undulator radiation: $\boxed{E = E_0 \big/ \left(1 + K^2/2 + \gamma^2\phi^2\right)}$

Wider slit increases unused photons (power) on the monochromator !

DuMond diagram: undulator & DCM

Undulator radiation

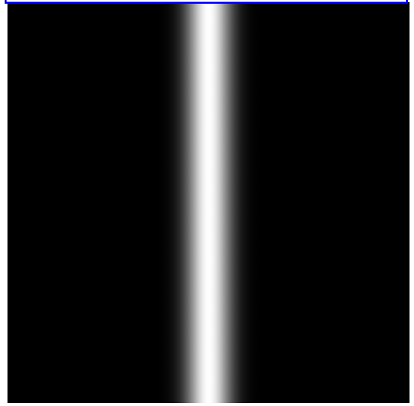

Acceptance by Si 111 DCM

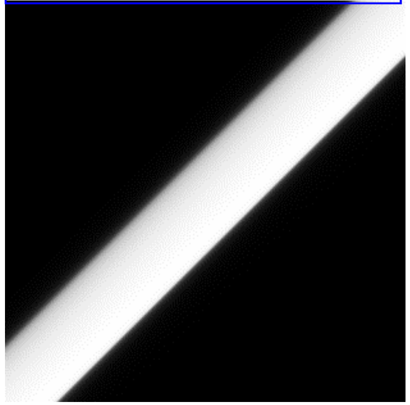

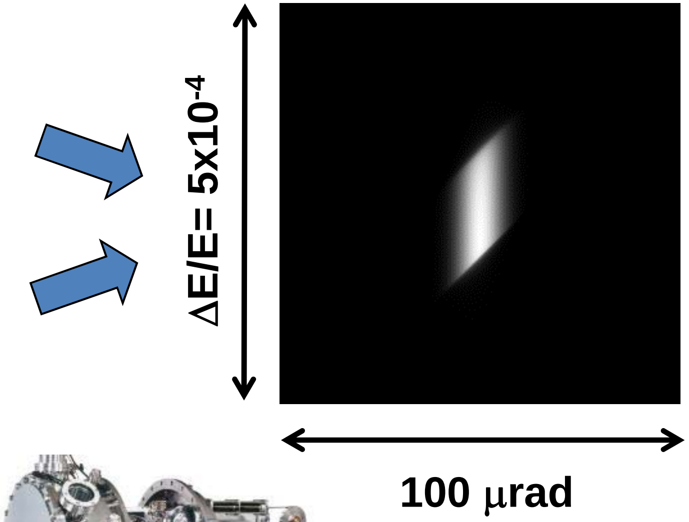

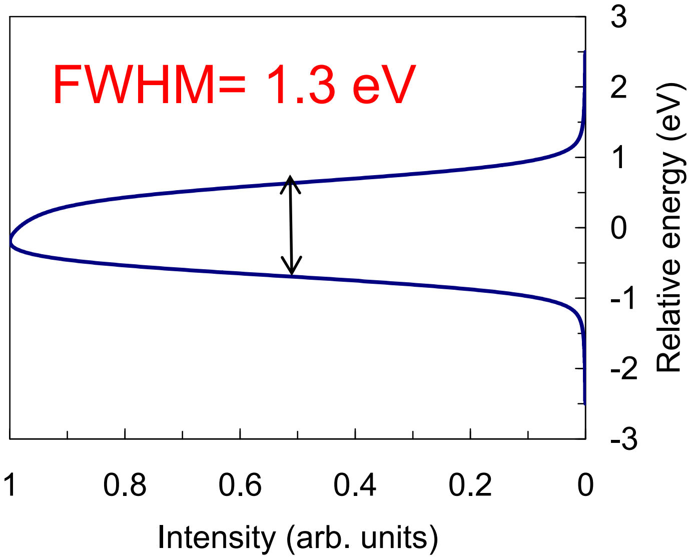

SPring-8 standard undulator + 20 μrad slit + Si 111 DCM

10-keV photons ➔ 1.3x10^{-4}

Improvement of **energy resolution**

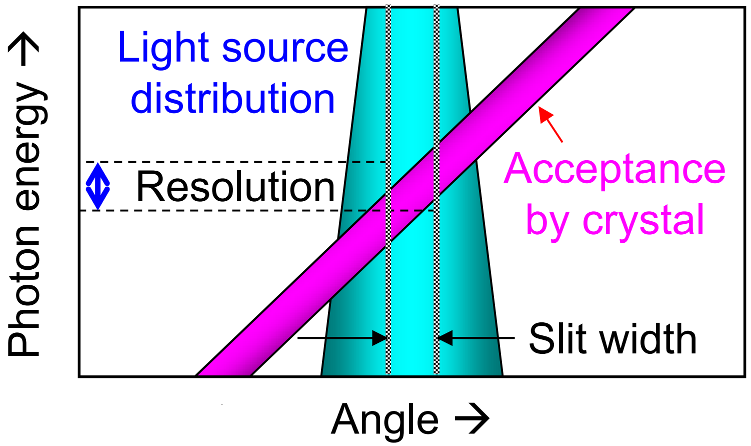

(A) Collimation using slit

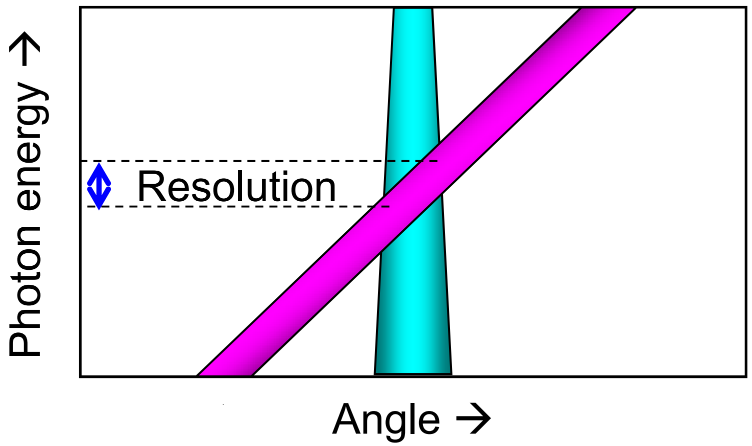

(B) Collimation using pre-optics w/ collimation mirror, CRL,..

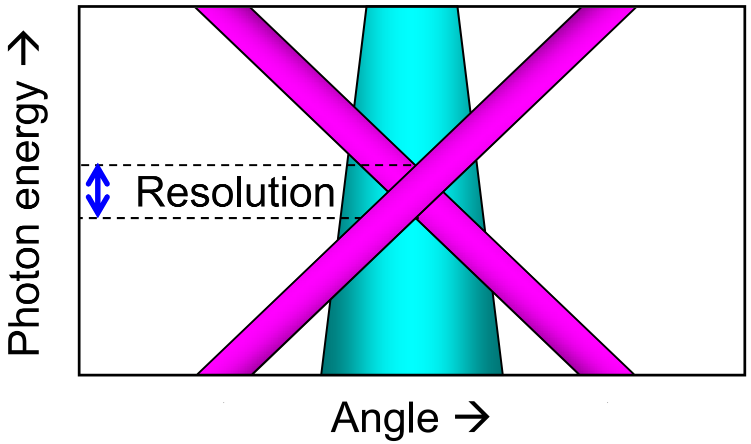

(C) Additional crystal w/ (+,+) setting

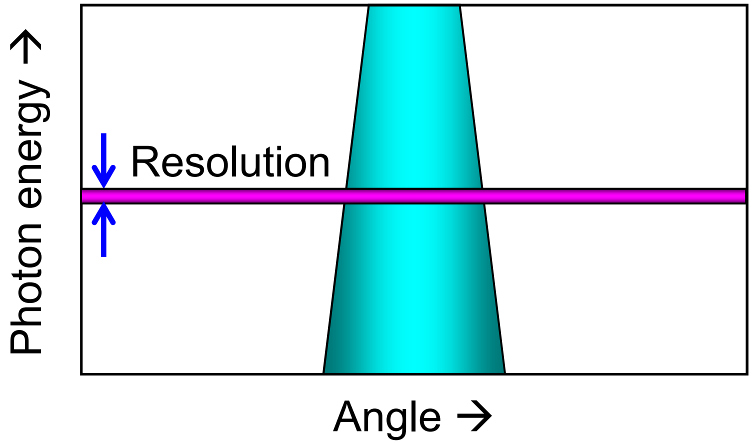

(D) HR monochromator of $\pi/2$ reflection (~meV)

(B)~(D): restriction on photon energy

Improvement of energy resolution

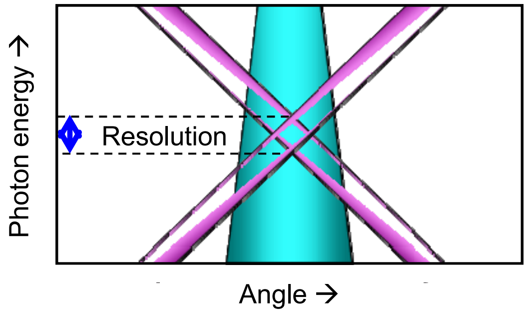

(C) Additional crystal w/ (+,+) setting

➔ HXPES

Si 111 DCM

Si *nnn* channel-cut mono.

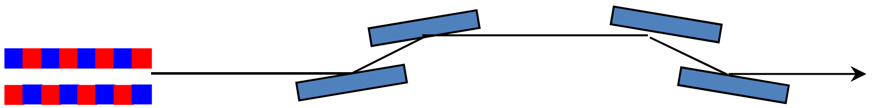

Si 333 refl. for 6 keV

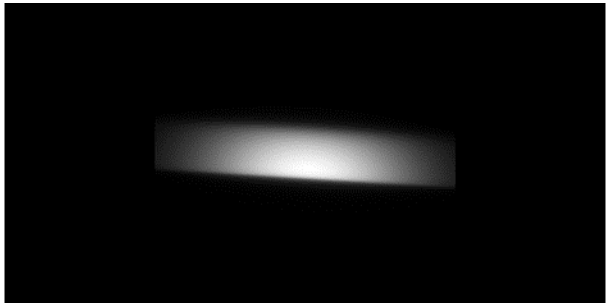

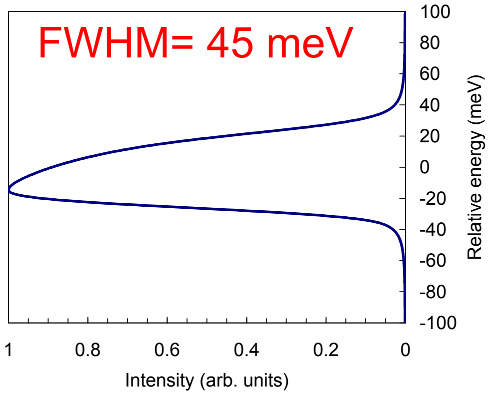

Si 555 refl. for 10 keV

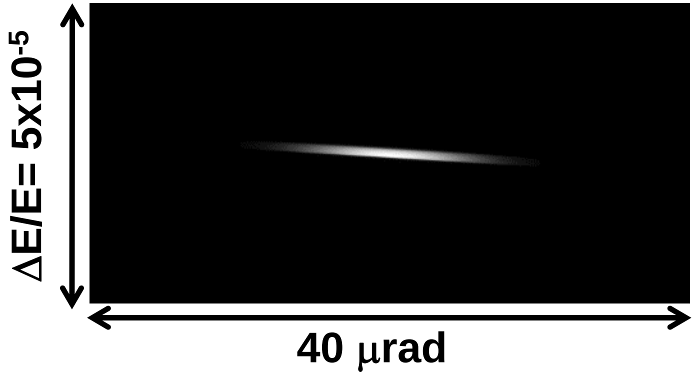

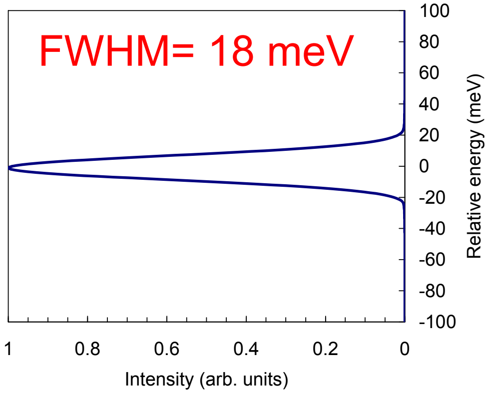

Improvement of energy resolution

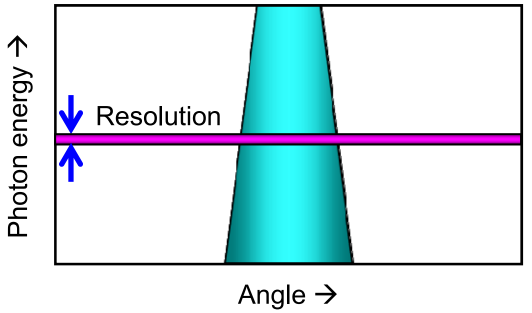

(D) HR monochromator of ~π/2 reflection (~meV)

➔ Inelastic scattering

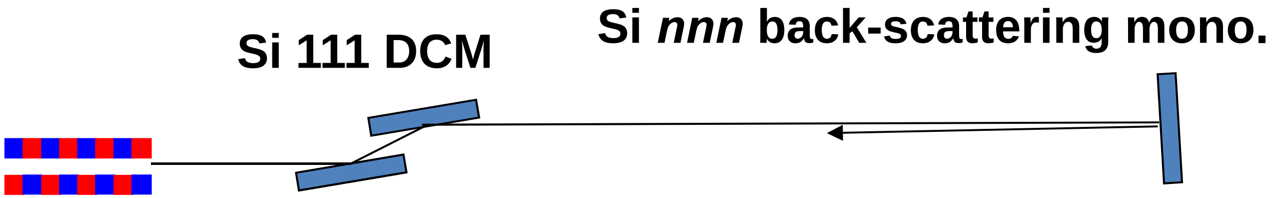

Si 111 DCM

Si *nnn* back-scattering mono.

Si 999 refl. for 17.8 keV

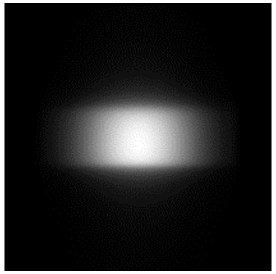

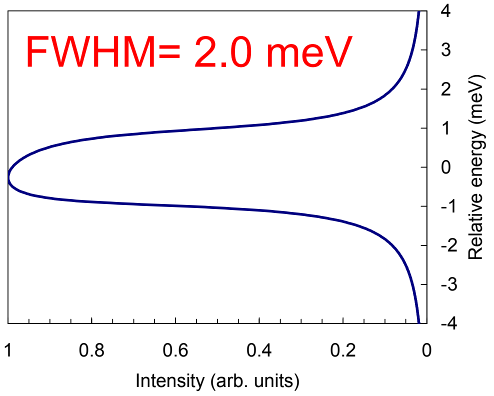

Si 11 11 11 refl. for 21.7 keV

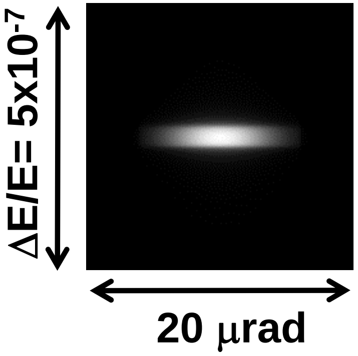

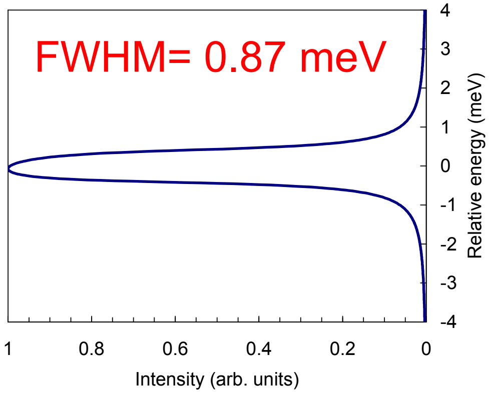

Photon flux after monochromator

Photon flux (throughput) after monochromator can be estimated using effective band width:

Photon flux (ph/s) =

Photon flux from light source (ph/s/0.1%bw)

x 1000

x Effective band width of monochromator

~~**Energy resolution**~~

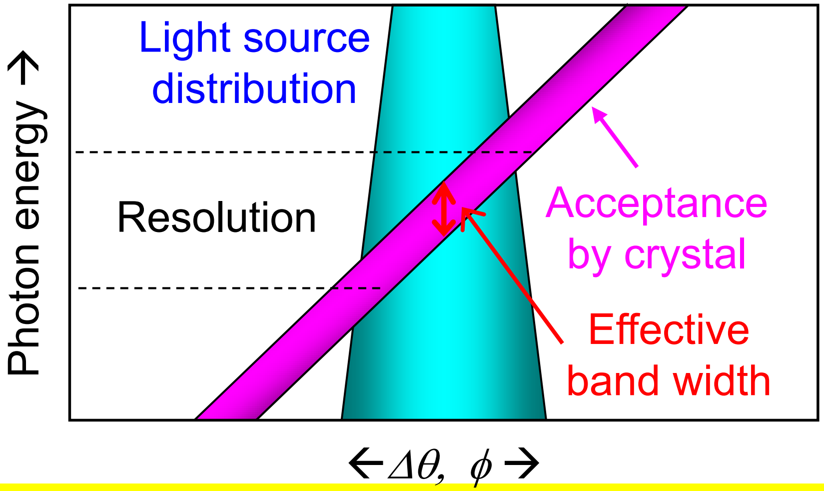

Throughput is estimated by overlapped area.

Note difference from energy resolution.

Effective band width

Starting with Darwin width in the energy axis

$$\frac{\Delta E}{E} \approx \frac{|\chi_{hr}|}{\sin^2\theta_\mathrm{B}}$$

$$\chi_{hr} \propto \lambda^2 \left\{ f^0(d_{hkl}) + f'(\lambda) \right\}$$

Neglecting anomalous scattering factor *f'*

$$\chi_{hr} \propto \lambda^2 f^0(d_{hkl})$$

$$\frac{\Delta E}{E} = -\frac{\Delta\lambda}{\lambda} \approx \frac{|\chi_{hr}|}{\sin^2\theta_\mathrm{B}}$$

$$= 4{d_{hkl}}^2 \frac{|\chi_{hr}|}{\lambda^2}$$

$$\frac{\Delta E}{E} = -\frac{\Delta\lambda}{\lambda} \propto {d_{hkl}}^2 f^0(d_{hkl})$$

Independent of photon energy

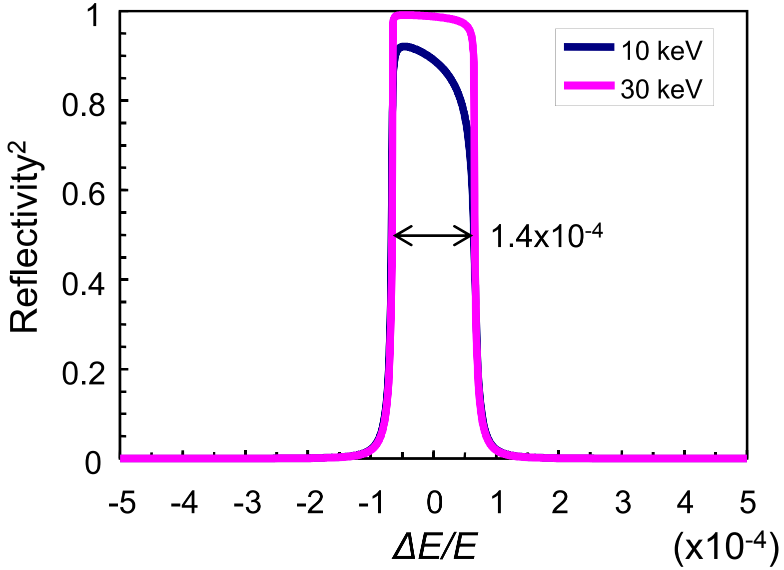

e.g. for Si 111 refl. DCM case

Note relative energy width is constant.

Effective band width (Integrated intensity)

For single-bounce monochromator

$$\frac{\Delta E}{E} = \frac{|\chi_{hr}|}{2\sin^2\theta_{\mathrm{B}}} \boxed{\int R(W)\, dW}$$

$$= \boxed{\frac{8}{3}} \cdot \frac{|\chi_{hr}|}{2\sin^2\theta_{\mathrm{B}}}$$

↑ For no absorption

For double-crystal monochromator

$$\frac{\Delta E}{E} = \frac{|\chi_{hr}|}{2\sin^2\theta_{\mathrm{B}}} \underline{\int R(W)^2\, dW}$$

= ~2

$$= \boxed{\frac{32}{15}} \cdot \frac{|\chi_{hr}|}{2\sin^2\theta_{\mathrm{B}}}$$

↑ For no absorption

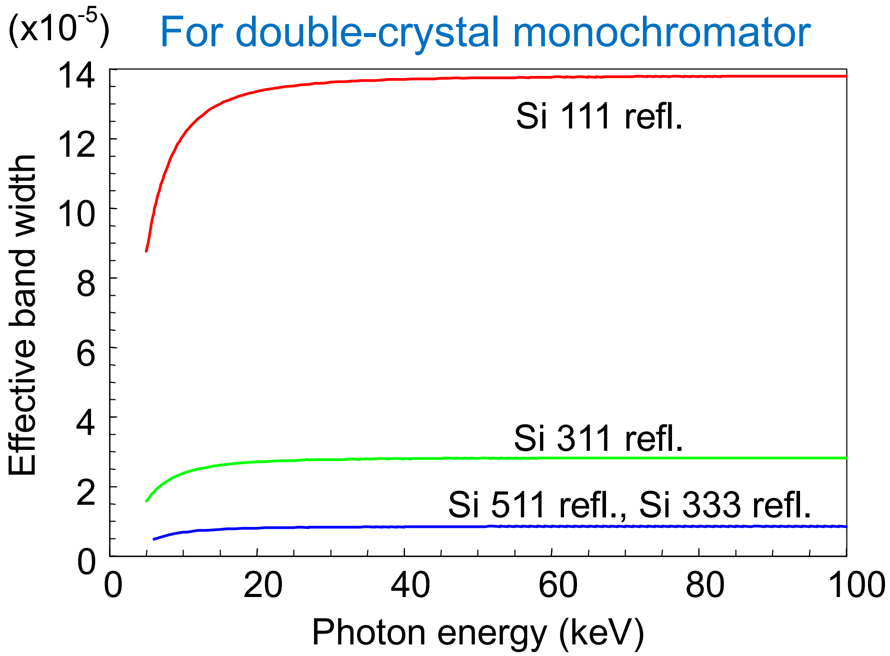

Effective band-width is obtained

by integration of reflection curve.

When you need flux → Lower order (Si 111 refl.,..)

When you need resolution → Higher order (Si 311, Si 511 refl,..)

Photon flux estimation

Effective band width

Reflection (nominal energy)	Effective band width
Si 111 DCM (6 keV)	1.0045×10^{-4}
Si 111 DCM (8 keV)	1.1399×10^{-4}
Si 111 DCM (10 keV)	1.2216×10^{-4}
Si 111 DCM (12 keV)	1.2710×10^{-4}
Si 111 DCM (14 keV)	1.3021×10^{-4}
Si 333 DCM (14 keV)	8.0996×10^{-6}

$$Flux = \int S(E,\phi)R(E,\phi)^2\, dE d\phi$$

Photon flux (ph/s/100mA/20 μrad(H))

(A) SPECTRA × Effective band width ⇔ (B) SPECTRA × DuMond

Reflection	Flux (A)	Flux (B)
Si 111 DCM (6 keV)	5.68×10^{13}	5.70×10^{13}
Si 111 DCM (8 keV)	6.14×10^{13}	6.15×10^{13}
Si 111 DCM (10 keV)	6.01×10^{13}	6.02×10^{13}
Si 111 DCM (12 keV)	5.28×10^{13}	5.29×10^{13}
Si 111 DCM (14 keV)	4.20×10^{13}	4.20×10^{13}
Si 333 DCM (14 keV)	2.62×10^{12}	2.61×10^{12}

Photon flux estimation

Effective band width

Reflection (nominal energy)	Effective band width
Si 111 DCM (6 keV)	$1.0045\text{x}10^{-4}$
Si 11	
Si 11	
Si 11	
Si 11	
Si 33	

$\phi)^{2}\, dEd\phi$

Photon fl

(A) uMond

Si 111 DCM (10 keV)	$6.01\text{x}10^{13}$	$6.02\text{x}10^{13}$
Si 111 DCM (12 keV)	$5.28\text{x}10^{13}$	$5.29\text{x}10^{13}$
Si 111 DCM (14 keV)	$4.20\text{x}10^{13}$	$4.20\text{x}10^{13}$
Si 333 DCM (14 keV)	$2.62\text{x}10^{12}$	$2.61\text{x}10^{12}$

Photon flux (throughput) after monochromator can be estimated using effective band width:

Photon flux (ph/s) =

Photon flux from light source (ph/s/0.1%bw)

x 1000

x Effective band width of monochromator

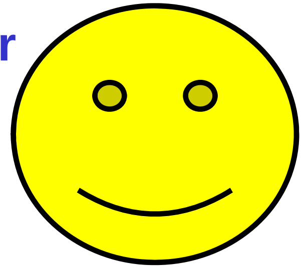

This approach is valid.

Photon flux at undulator beamline

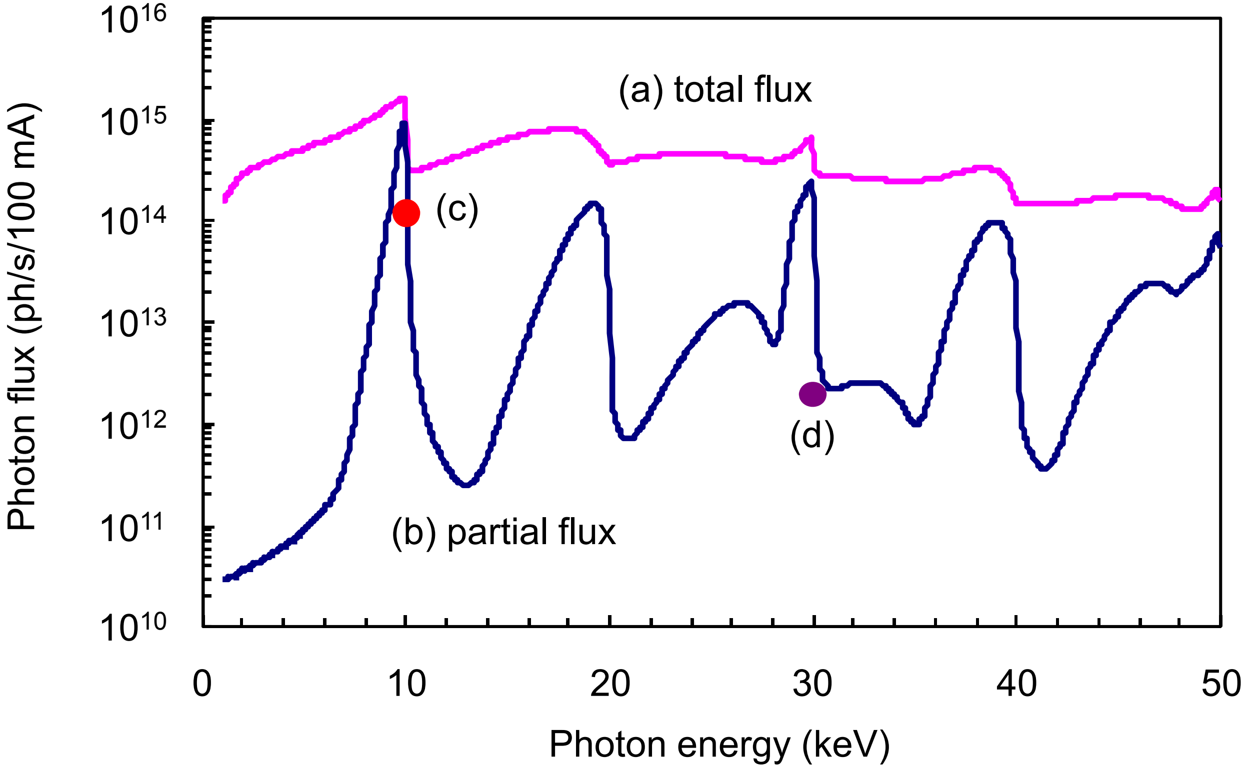

(a) Total flux @ 0.1% b.w.
(b) After frontend slit
1 × 1 mm^2 @30 m
(c) Si 111 refl. @10 keV
Effective b.w. = 1.3x10^{-4}
(d) 3rd harmonics @30 keV
Effective b.w. = 8.0x10^{-6}

Higher harmonics elimination more → mirror or detuning of DCM

We can obtain photon flux of 10^{13}~10^{14} ph/s/100 mA/mm^2 using standard undulator sources and Si 111 reflections at SPring-8 beamlines.

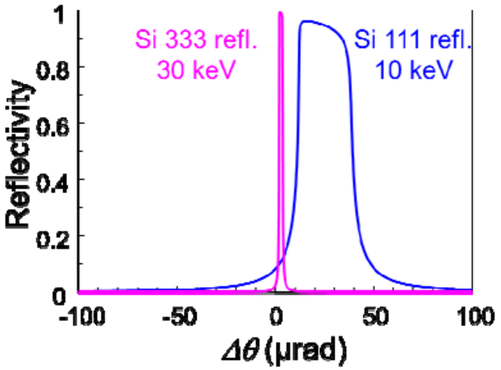

Tailoring x-rays to application

↓

X-ray monochromator

- ■ Principle
  - ✓ Introduction of diffraction theory
  - ✓ Dynamical theory
  - ✓ DuMond diagram
- ■ Engineering

Double-crystal monochromator

- ✓ Fixed-exit operation for usability at experimental station.
- ✓ Choose suitable mechanism for energy range
  (Bragg angle range).
- ✓ Precision, stability, rigidity,...

$$y = \mathrm{AB} = \frac{h}{2\sin\theta_B}$$

$$z = \mathrm{OB} = \frac{h}{2\cos\theta_B}$$

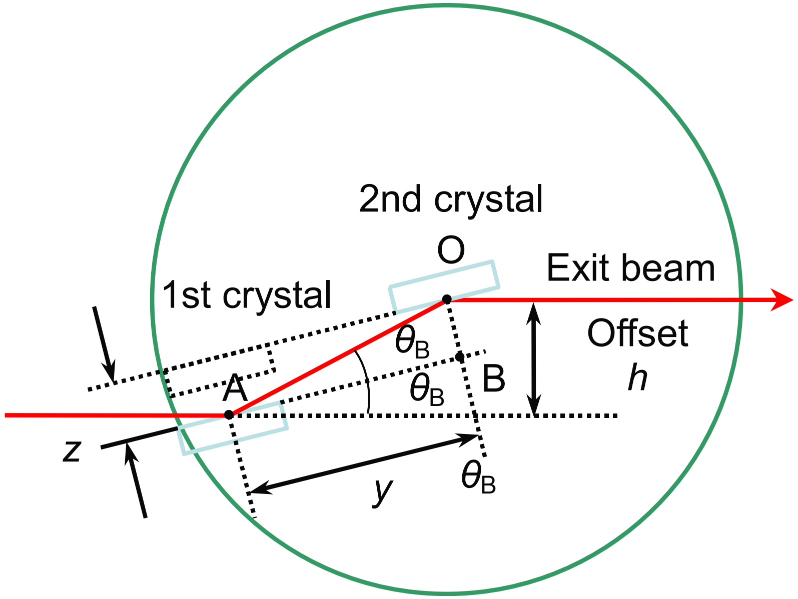

Fixed-exit operation using rotation (*θ*) + two translation mechanism

Double-crystal monochromator

θ1 + translation + θ2 computer link

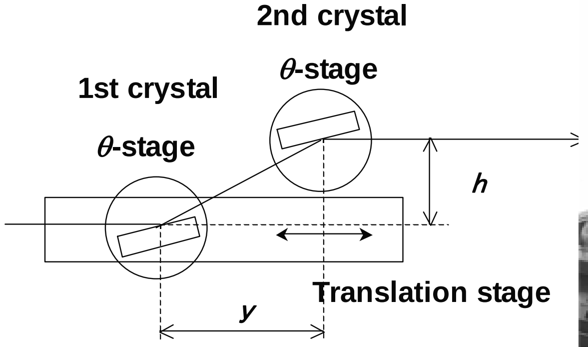

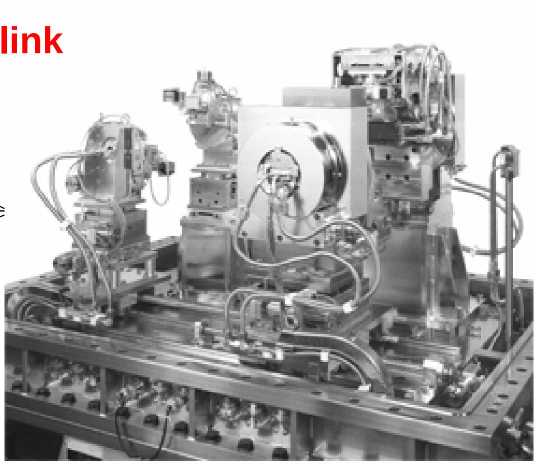

SPring-8 BL15XU

h= 100 mm,

θ_B= 5.7~72° (for lower energy range)

θ + two translation (2 cams)

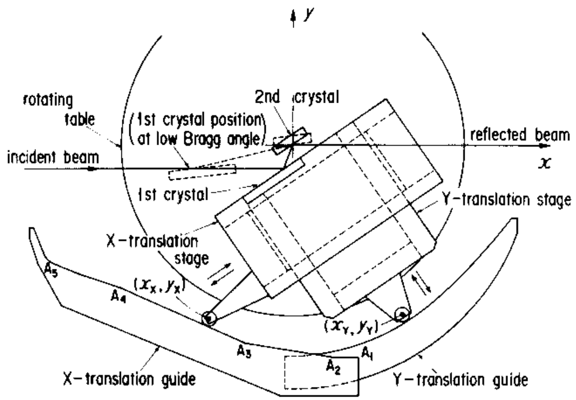

h= 25 mm, θ_B= 5~70°

KEK-PF BL-4C

Matsushita et al., NIM A246 (1986)

θ + two translation (1 cam)

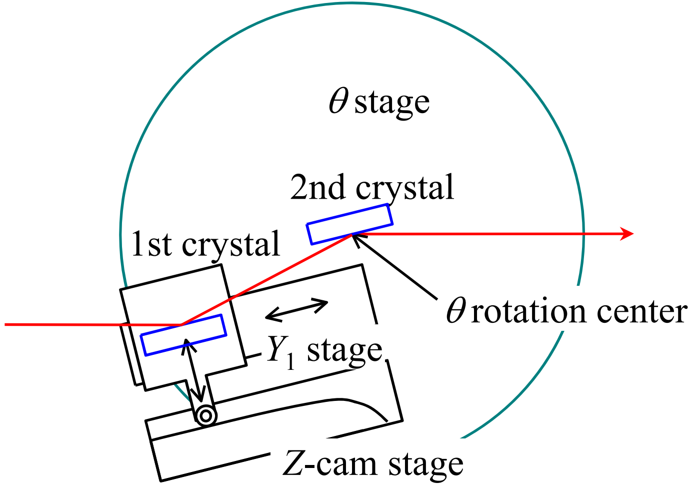

Offset h= 30 mm θ_B =3~27° for higher energy range

SPring-8 std. DCM

Yabashi et al., Proc. SPIE 3773, 2 (1999)

Crystal cooling

Why crystal cooling？

Qin (Heat load by SR) = Qout (Cooling + Radiation,..)

→ with temperature rise ΔT

→ $\alpha\Delta T = \Delta d$ (d-spacing change)

α: thermal expansion coefficient

or → $\Delta\theta$ (bump of lattice due to heat load)

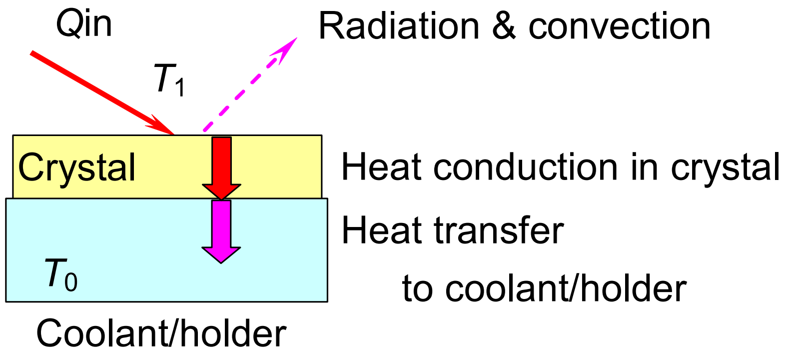

Qin

Radiation & convection

T_1

Crystal

Heat conduction in crystal

Heat transfer to coolant/holder

T_0

Coolant/holder

Miss-matching between 1st and 2nd crystals occurs:

→ Thermal drift, loss of intensity, broadening of beam, loss of brightness

→ Melting or limit of thermal strain → Broken !

We must consider:

- Thermal expansion of crystal: α,
- Thermal conductivity in crystal: κ,
- Heat transfer to coolant and crystal holder.

Solutions:

(S-1) κ/α → Larger

(S-2) Contact area between crystal and coolant/holder → larger

(S-3) Irradiation area → Larger, and power density → smaller

Figure of merit

	Silicon	Silicon	Diamond
	300 K	80 K	300 K
κ (W/m/K)	150	1000	2000
α (1/K)	$2.5\text{x}10^{-6}$	$-5\text{x}10^{-7}$	$1\text{x}10^{-6}$
κ/α $\text{x}10^{6}$	60	2000	2000

Figure of merit of cooling:
Good for silicon (80 k)
and diamond (300 K)

Crystal cooling at SPring-8

<Bending magnet beamline>

Power & power density:

~100 W, ~1 W/mm^2

Fin crystal direct-cooling - (S2)

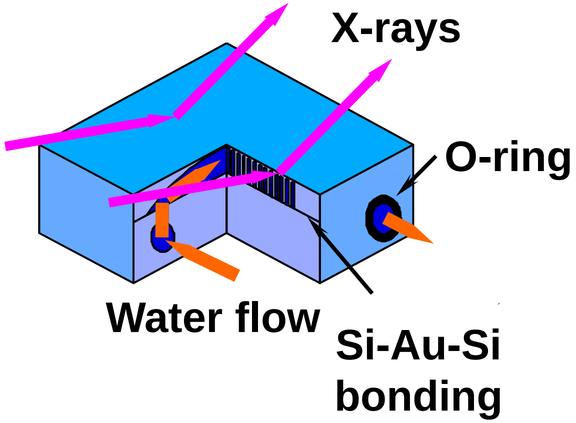

<Undulator beamline>

Linear undulator, N= 140, λu= 32 mm

Power & power density: 300~500 W ,

300~500 W/mm^2

a) Direct cooling of silicon pin-post crystal – (S2) & (S3)

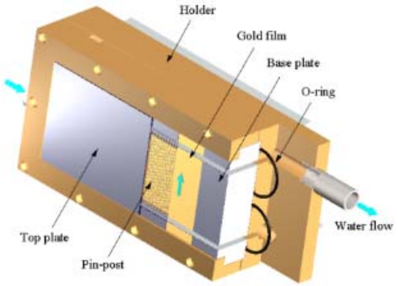

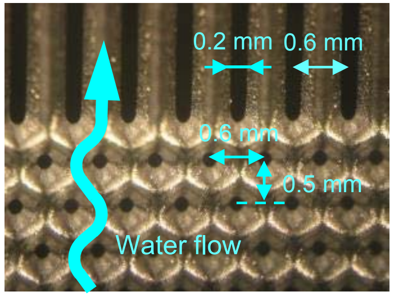

b) Silicon cryogenic cooling - (S1)

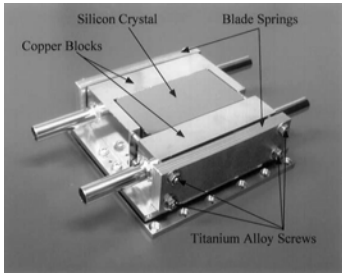

c) IIa diamond with indirect water cooling - (S1)

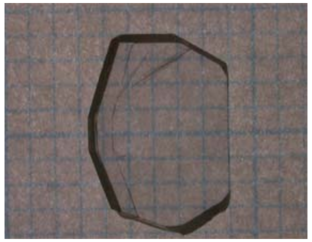

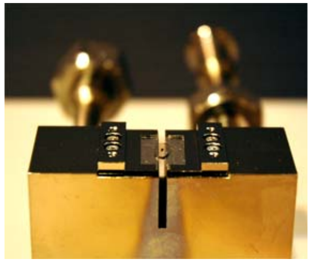

Improvement of stability of DCM

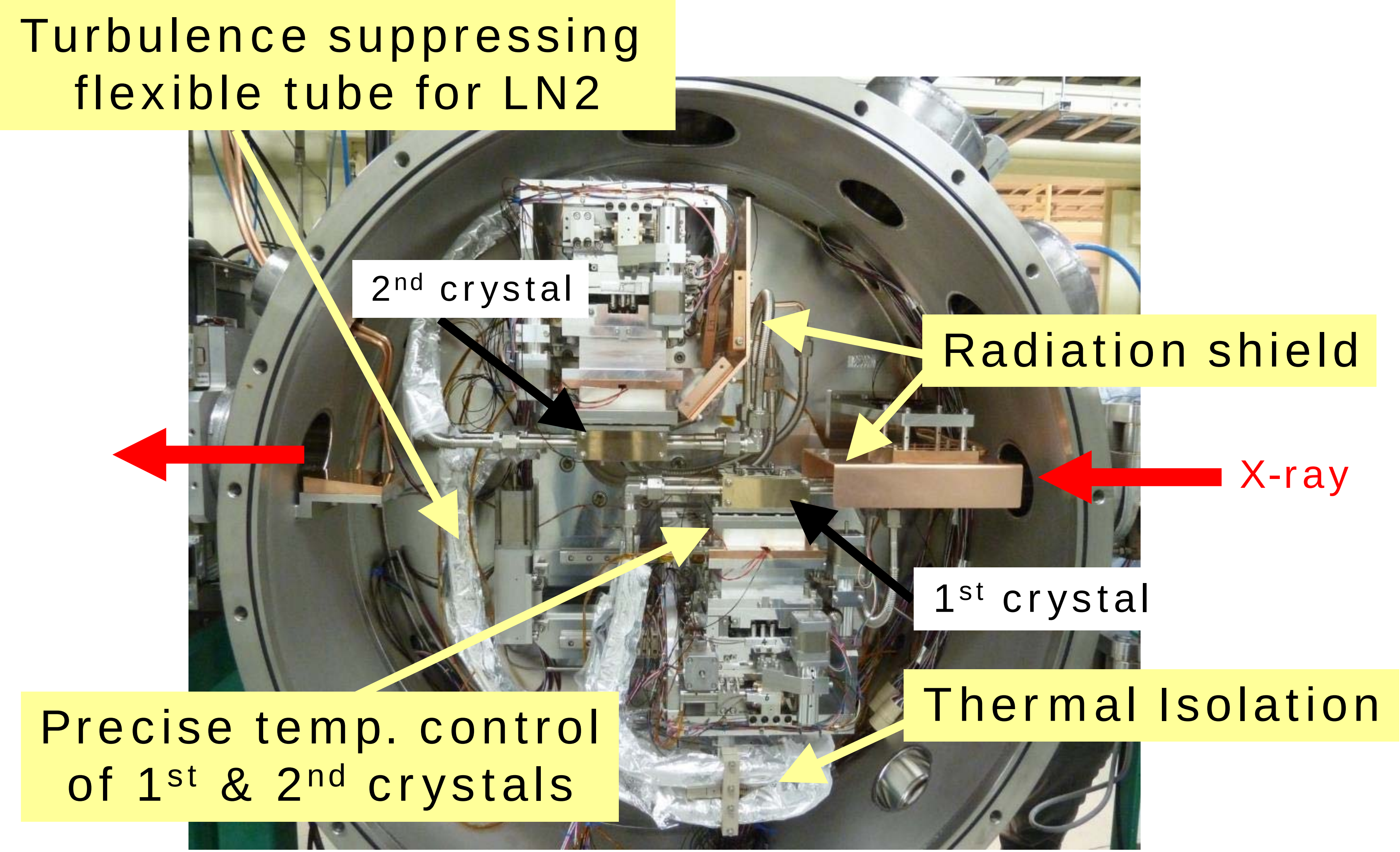

Turbulence suppressing flexible tube for LN2

2nd crystal

Radiation shield

X-ray

1st crystal

Thermal Isolation

Precise temp. control of 1st & 2nd crystals

Improvement of stability of DCM

Measured Intensity fluctuation of 1 Å x-rays at BL13XU

Average time : 1 ms ･･･ very sensitive

Measurement frequency : 1 kHz

Δθ1 stage : 0.2″ stepping at a time interval of 5 s

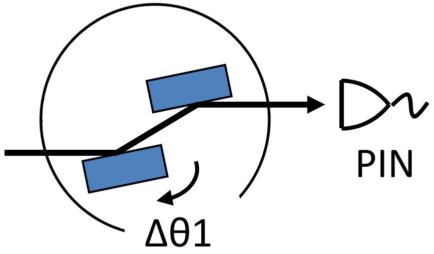

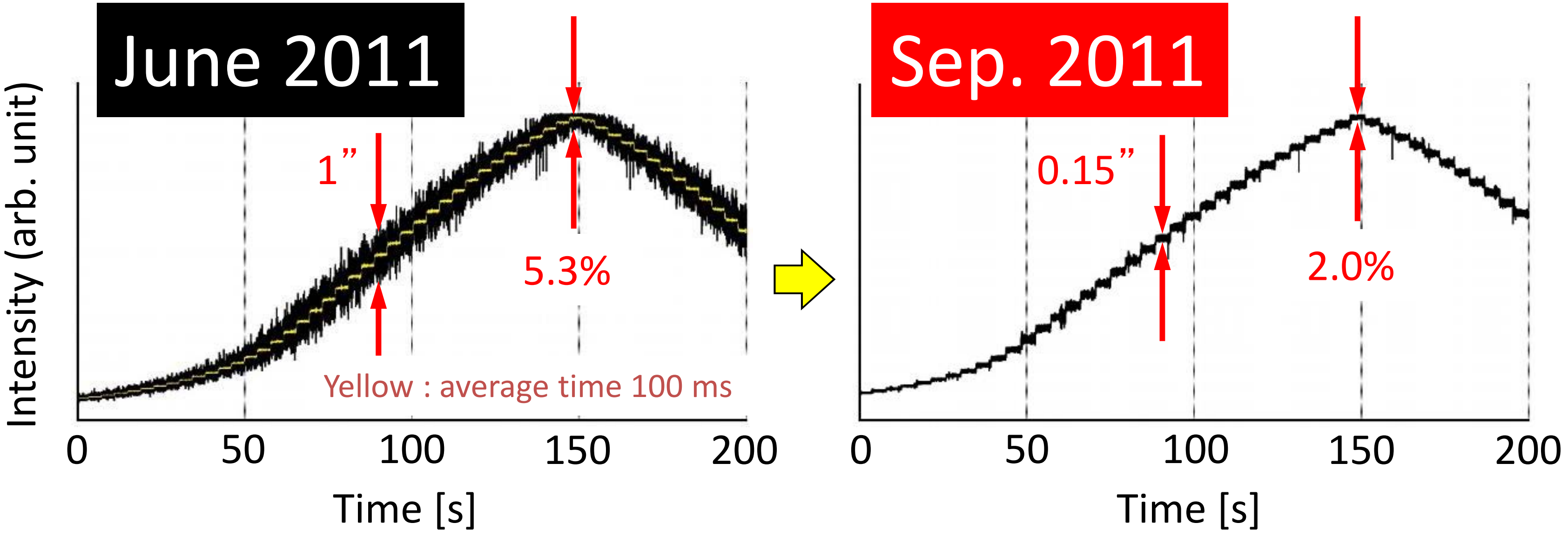

Angular fluctuation between the crystals : 1″ → 0.15″

Intensity fluctuation of 1 Å x-rays : 5% → 2%

Key issues of X-ray monochromator

Introducing the dynamical x-ray diffraction for large & perfect crystal,
w/ several important points:

1) Total reflection occurs at the gap between dispersion surfaces.
2) Normalized deviation parameter *W* is related to the gap.
3) W is parameter of angular deviation and energy (wavelength) deviation.
It gives DuMond diagram as a band of $|W|<1$.
4) By combination of light source and monochromator crystals,
photon energy, energy resolution, photon flux,･･･ can be controlled / tuned.

Double-crystal monochromator w/ crystal cooling is needed for practical use at the SR beamline.

By understanding these, you will be approaching to good design/use of the beamline for your SR science.

Text books following Laue's dynamical theory

Ergebnisse der Exakt Naturwiss.

10 (1931) 133-158.

Die dynamische Theorie der Röntgenstrahlinterferenzen in neuer Form.

Von **M. v. LAUE**, Berlin.

Mit 4 Abbildungen.

Inhaltsverzeichnis.

	Seite
§ 1. Die dynamische Grundgleichung	137
§ 2. Annäherungen in der Lösung der Grundgleichung (I)	141
§ 3. Die einfachsten Beispiele für nichtabsorbierende Kristalle	144
§ 4. Untersuchung über die Realität der Dispersionsfläche	149
§ 5. Die Reflexion von Röntgenstrahlen an der Grenze nichtabsorbierender Kristalle	153

EWALDs dynamische Theorie der Röntgenstrahlinterferenzen[1] gehört nach unserer Ansicht auf alle Zeiten zu den Meisterwerken der mathematischen Physik. Sie bewältigte mit glänzenden Methoden ein zunächst schier unlösbares Problem, rechtfertigte eigentlich erst die elementare, rein auf Phasenzusammensetzung beruhende Theorie,
Unzulänglichkeiten quantitativ abzuschätzen lehrte,
Verbundenheit mit der optischen Dispersionstheorie
Abweichungen von den Ergebnissen der älteren The
wenige Jahre später für die vollständige Deutung der
HJALMARs sowie für eine exakte Messung der Wellenl
lich wurden. Aber wir glauben aussprechen zu dürfen,
denen, die ihre Resultate oft benutzen, nicht allzu
durchgearbeitet haben. Denn jene glänzenden mathe
thoden waren nicht nur schwierig zu finden, sie bereiten in manchen Teilen auch dem Leser Schwierigkeiten. Daran hat auch die Neubearbeitung durch WALLER[2] nicht viel geändert, welche im übrigen das Verdienst besitzt, zuerst Gitter mit Basis in die Rechnung einbezogen zu haben. Der Zweck der folgenden Seiten ist, der Theorie eine leichter verständliche Form zu geben. Daß wir trotz weitgehenden Verzichtes auf neue Ergebnisse die neue Form veröffentlichen, scheint uns durch die Wichtigkeit der Sache gerechtfertigt; ebenso, daß wir, um dem Leser das Zurückgreifen auf die genannten Arbeiten zu erleichtern, die geometrische Diskussion EWALDs nochmals zum Abdruck bringen, obwohl wir an ihr fast nichts zu ändern brauchen.

---

[1] EWALD, P. P.: Ann. Physik 54, 519, 557 (1917); Z. Physik 2, 332 (1920); 30, 1 (1924).

[2] WALLER, J.: Uppsala Universitets Arsskrift 1925.

Dover (1945)

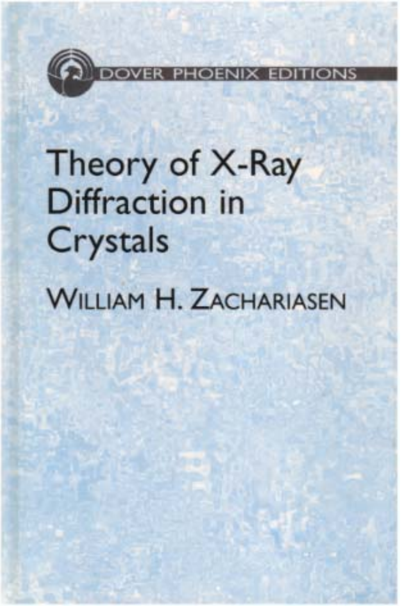

R. W. James

"The Dynamical Theory of X-Ray Diffraction"

Solod State Physics **15**, (1963) 53-220.

B. W. Batterman & H. Cole

"Dynamical Diffraction of X-Rays by Perfect Crystals"

Rev. Modern Phys. **36**,

(1964) 681-717.

Oxford (2001)

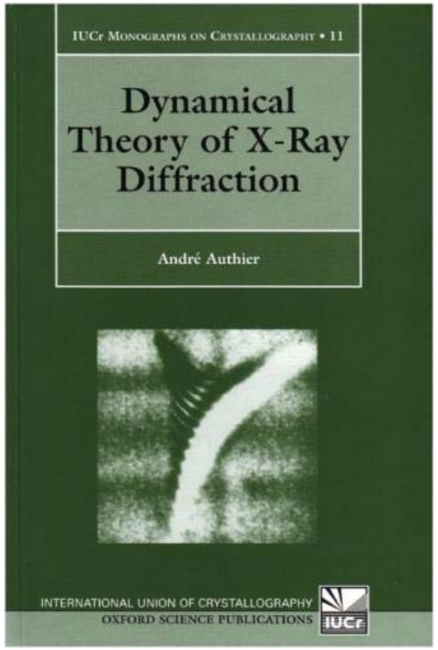

Springer (2004)

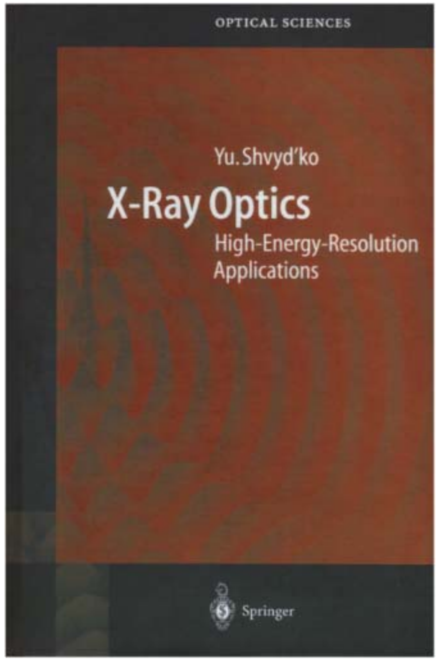

S. Kikuta

"X-ray scattering and Synchrotron Radiation Science – Fundamentals"

Univ. of Tokyo Press. 2011
ISBN 978-4-13-062831-0

in Japanese

References

For X-ray physics

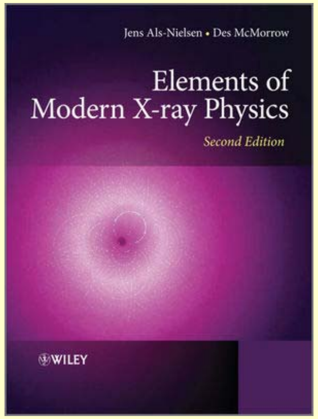

[0] J. Als-Nielsen, D. McMorrow,
Elements of mMdern X-ray Physics, 2nd Ed.
Wiley & Sons (2011).

For monochromator

[1] T. Matsushita & H. Hashizume,
Handbook on Synchrotron Radiation Vol. 1,
North-Holland (1983).

[2] Y. Shvyd'ko, Springer (2004), *for high energy resolution*

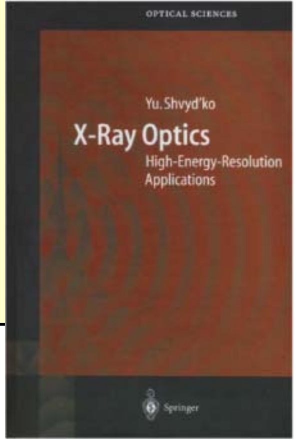

References

For atomic scattering factor

- For f^0

[3] International Tables for X-ray Crystallography (IUCr).
[4] Hubbell et al.: J. Phys. Chem. Ref. Data Vol. 4, No. 3, 1975.

- For anomalous scattering factor f', f''

[5] S. Sasaki, KEK report 88-14 (1989),
[6] Tables of LBNL (B. L. Henke et al.),
http://henke.lbl.gov/optical_constants/index.html,
[7] Tables of NIST,
http://physics.nist.gov/PhysRefData/FFast/html/form.htm

Acknowledgment

S. Takahashi (front end), *T. Matsushita* (interlock),
H. Takano, Y. Kohmura, T. Koyama (focusing devices)
T. Uruga, Y. Senba (mirrors),
S. Matsuyama, H. Yumoto, H. Mimura, K. Yamauchi
(ultimate focusing mirror, alignment),
S. Goto, H. Yamazaki, S. Kikuta and T. Ishikawa

Thank you for your kind attention.

Enjoy Cheiron school

Enjoy SPring-8

and

Enjoy Japan!